“Sapienza” Università di Roma

PhD in “Chimica Analitica e dei Sistemi Reali”

- *XXVI Cycle* –

PhD thesis title:

IDENTIFICATION AND ANALYSIS OF ALLERGENIC SUBSTANCES IN ATMOSPHERIC PARTICULATE MATTER ACTING AS A CARRIER OF TOXIC-HARMFUL COMPOUNDS INTO HUMAN RESPIRATORY TRACT

PhD Student

Dr Patrizia Di Filippo

Supervisor

Dr Francesca Buiarelli

1. INTRODUCTION

1.1. Atmospheric Particulate Matter (PM) composition

Atmospheric Particulate Matter (PM) is a pollutant essentially constituted by inorganic salts, crustal siliceous minerals, carbonaceous matter including organic (OC) and elemental (EC) carbon, and water. Chemical characterization of inorganic salts, mainly metal sulphates (about 30% of PM), nitrates and carbonates and crustal siliceous minerals (10–15% of PM) is easily achieved, while carbonaceous matter poses analytical problems due to its complexity [Seinfeld and Pankow, 2003].

Besides their chemical composition, the particles are identified according to their aerodynamic diameter (da), which is the diameter of a sphere with unit density that has aerodynamic behavior identical to that of the particle in question. In atmosphere, particles having the same aerodynamic diameter may have different dimensions and shapes.

1.2. Carbonaceous matter

The carbonaceous matter is a significant part of the atmospheric particulate matter, accounting for about 30–50% of total PM, depending on meteorological conditions during the sampling period and PM collection sites [Heal, 2011; Na, 2004; Ye, 2003]. Natural sources, as vegetative waxes, biomass combustion or anthropogenic sources, as fuel oil combustions, contribute to carbonaceous component of atmospheric aerosol, that is, therefore, extremely complex, being composed of thousand of organic compounds. Hence, information is extremely incomplete. The organic matter that is extractable from aerosol is about 25%; of this 25% only 5% is elutable in GC column; the identifiable portion of the elutable organics is 78%, that is only 1% of the total fine particle mass [Pio et al., 2001].

Identifiable compounds are hopanes, organic acids (fatty acids), alkanes and alkylcycloalkanes, n-alkanones, n-alkanols, pristine, phytane, and steranes, polycyclic aromatic hydrocarbons (PAHs and derivatives), terpenoids, or their derivatives, including phytosterols; triterpenols and triterpenoid acids sesquiterpenoids and diterpenoids, polars (nonanal, levoglucosan) [Pio et al., 2001; Fraser et al., 2002].

Up to now, source apportionment, atmospheric effects and toxicity in terms of carcinogenicity, teratogenicity, and mutagenicity, have prompted the study of different classes of compounds, and scientific community can now convey valuable information about a series of atmospheric organics.

The chemical composition of the emissions from individual sources (cooking operations, paved road dust, fireplaces, vehicles, forest fires, organic chemical processes, brake lining and tire wear debris, industrial point sources, natural gas combustion, primary and secondary metallurgical processes, residual oil stationary sources, refinery gas combustion, mineral industrial processes, jet aircraft, coal burning, wood processing, vegetative detritus) can be used to estimate source contributions to atmospheric samples taken at receptor air monitoring sites [Schauer et al., 1996]. Among the organic compound classes to be used as markers of those sources we can find: n-alkanes, iso- and anteiso-alkanes, hopanes and steranes, cis-9-n-octadecenoic acid as n-alkenoic acids, aldehydes, n-akanoic acids, dicarboxylic acids, aromatic carboxylic acids, polycyclic aromatic hydrocarbons, PAH ketones and quinines, steroids, N-containing compounds.

Besides contributing to alteration of cloud coverage [Sun and Ariya, 2006] and hence to the global climate [Kanakidou et al., 2005], some organic compounds can induce genotoxicity, cardiovascular effects, and allergic, toxic, and infectious responses in exposed individuals.

Polycyclic aromatic hydrocarbons (PAHs) constitute one of the few classes established for regulatory purposes, based largely on their hazard as carcinogens.

In general, we can have reasonable confidence that environmental exposures to the organic components have adversely affected public health, even though we have no direct confirmatory evidence, and a definitive link between particulate chemical composition and respiratory health effects has not been established.

1.3. Bioaerosol and its allergenic effects

The most direct evidence for the adverse health effects of environmental organic aerosols is provided by bioaerosols, airborne particles that are living (bacteria, biofilms, viruses and fungi) or originate from living organisms (pollens, cellular debris, acres and insect fragments) [Deguillaume et al., 2008; Mauderly & Chow, 2008; Zhang et al., 2010].

Bioaerosols are also called PBAPs (Primary Biological Aerosol Particles). Though the two terms are more or less equivalent, PBAPs is used to define biological organisms, fragments of biological materials, and any kind of organic substances deriving from biomolecules [Jaenicke, 2005; Deguillaume et al., 2008; Despres et al.,

2012]. In contrast, 'bioaerosol' is not very clearly defined and is frequently used with different meanings [Despres et al., 2012].

While generally PBAPs are used to define the biogenic particles that play an important role in atmospheric processes and in formation of secondary organic aerosols [Deguillaume et al., 2008], bioaerosols are known to cause adverse respiratory health effects in a large percentage of the population [Womiloju et al., 2003; Srikanth et al.,2008; Deguillaume et al., 2009].

Although it is recognized that exposures to complex mixtures of toxins and allergens cause high prevalence of respiratory symptoms and airway inflammation with major public health impact, a knowledge of the total amount of bioaerosols in a parcel of air is still a challenge. Therefore, risk assessment is seriously hampered by the lack of valid quantitative exposure assessment methods.

Bioaerosols are associated with a wide range of common health effects: mucous membrane irritation, bronchitis and obstructive pulmonary disease, allergic rhinitis and asthma, allergic alveolitis (granulomatous pneumonitis) or organic dust toxic syndrome (inhalation fever or toxic pneumonitis) [Sorenson and Lewis, 1996], regardless of their indoor and outdoor different composition, concentrations and sources. For example, in the spring and summer, outdoor pollens and fungal spores begin to increase as temperatures rise, causing allergic reactions in millions of people worldwide. Allergic reactions also occur due to exposures to bioaerosols in particular occupational environments, including sewage plants, the waste recycling industry, occupations in which stored products are handled or where aerosols are created as a result of leaks from equipment intentionally or accidentally contaminated with microorganisms or during particular operations as, for instance, in laboratories and during post-mortem or surgical procedures [Lacey and Dutkiewicz, 1994; Bünger et al., 2000]. Occupational asthma can be a serious condition in such work activities, as handling animals, the manufacture of detergents, the logging or furniture sectors, the production of highly purified biological substances such as microbial enzymes that are used particularly in the food processing industry and detergent industry. Pathogenic agents include viruses; bacteria; actinomycete, fungal, moss and fern spores; algal and plant cells; insects and mites and their fragments and excreta; proteins from plant and animal sources; enzymes, antibiotics and other products from biotechnological processes; endotoxins from Gram-negative bacteria, and mycotoxins and glucans from fungi [Douwes et al., 2003].

As described above, bioaerosol speciation is a central unresolved problem, nevertheless some researchers have identified the presence of pollen, bacteria and fungal spores in atmosphere, through the detection of chemical biomarkers or through traps or viable microorganism sampling, growing and count, or molecular biology techniques [Ong et al., 1995; Bauer et al., 2002; Womiloju et al., 2003; Bauer et al., Ho et al., 2005; Lee et al., 2006a,b; 2008a,b; Di Filippo et al., 2013].

1.3.1. Fungal spores

Fungal spores, ubiquitous in outdoor air [O'Gorman and Fuller, 2008], are the dominant biological component of air and contribute to 4 and 10% of OC and to 2 and 5% of particulate matter with aerodynamic diameters of 10 μm or less (PM_{10} particles) [Bauer, 2008b]. Their main source is vegetation and their growth is favored by temperature of 18–32 °C, relative humidity above 65% and conditions of calm winds. Their presence in indoor air is also confirmed, at concentrations generally lower than those detected in outdoor samples [Codina et al., 2008; Fairs et al., 2010]. Airborne fungal spores induce hypersensitivity (allergic) respiratory reactions in sensitized atopic subjects, causing rhinitis and/or asthma. Fungal spore sizes range from 2 to 50 μm, and the most allergenic ones are in the range 3–10 μm [Deguillaume et al., 2009]. Few data on their presence in PM are available, because it is not possible to recognize them by conventional analysis. One possible approach is their determination by signature biochemicals.

In the late 1970s the steroid ergosterol was first considered as a marker for fungal abundance in environmental samples [Seitz et al., 1977; Seitz et al., 1979; Lee et al., 1980], and it is still considered a reliable biomarker for fungi [Miller & Young, 1997; Volker et al, 2000; Mille-Lindblom et al., 2004; Lau et al., 2006; Zhao et al., 2008].

In addition, sugar alcohols, especially arabitol and mannitol, constitute an important fraction of the dry weight of fungi, and in particular mannitol can contribute between 20–50% of the mycelium dry weight [Vélëz et al., 2007]. Although other natural sources of these two polyols (lower plants, bacteria, insects and algae) [Graham et al., 2003; Vélëz et al., 2007; Zhang et al., 2010] are also known to exist, arabitol and mannitol in airborne particulate matter can be associated to fungal spores, as biomarkers [Carvalho et al., 2003].

Although a number of factors, including age, growth rate, carbon and nutrient availability, temperature, and oxygen, have been identified as affecting ergosterol,

arabitol, and mannitol contents in airborne fungal biomass, their use as biomarkers still remains reasonable.

Also, a number of conversion factors can be found in literature to correlate ergosterol, arabitol, and mannitol concentrations to the number of spores [Gessner and Chauvet, 1993; Miller & Young, 1997; Pasanen et al., 1999; Hippelein & Rügamer, 2004; Bauer et al., 2008a,b; Cheng et al., 2008a,b].

Furthermore, since Elbert assigned to each spore an average mass of 65 pg [Elbert, 2007], from the number of airborne spores, obtained through atmospheric ergosterol, arabitol, and mannitol concentrations, and their respective conversion factors, it is reasonably possible to determine the fungal mass in air.

1.3.2. Mycotoxins

Epidemiological studies have shown that molds are associated with increased prevalence and exacerbation of respiratory symptoms and asthma and mycotoxins may contribute to these effects. Filamentous fungi can produce mycotoxins, as secondary metabolites, in favorable conditions of pH, humidity, temperature, presence of substrates. All mycotoxins are low-molecular-weight (MW~700 u.m.a) natural products and constitute a toxigenically and chemically heterogeneous assemblage, causing disease and death in human beings and other vertebrates. Many mycotoxins also display overlapping toxicities to invertebrates, plants, and microorganisms [Bennett, 1987].

Once produced, mycotoxins can withstand longer than the producer fungus, since they are photo- and thermally (up to 150°C) stable molecules, insoluble in water [Turner et al., 2009].

The majority of mycotoxicoses results from eating contaminated foods, since they can occur in a variety of food commodities of which cereals and cereal products, coffee, beer and wine are the most important sources of intake. Anyway skin contact with mold-infested substrates and inhalation of spore-borne toxins are also important sources of exposure.

As for air mycotoxin contamination, studies by Hintikka [Hintikka et al., 2009] and Sudakin [Sudakin and Fallah, 2008], relating to the determination of the possible presence of such substances in indoor and outdoor environments, appear to be particularly interesting. In the first article, aflatoxin B1 and sterigmatocystin were

found in the ventilation system of some schools in Finland. In the second case, it has been proven the presence of toxigenic fungal species in dusts from surfaces of a public park. A screening assessment was also conducted to assess for trichothecene mycotoxins in the same outdoor samples.

Aflatoxin B1, ochratoxin A, T-2 toxin, zearalenone and sterigmatocystin are among the most studied mycotoxins in real matrices.

Aflatoxins are the most studied and widely known mycotoxins, and have been recognized as significant contaminants within agriculture since the 1960s. Figure 1.3.2.a. shows the structure of some aflatoxins.

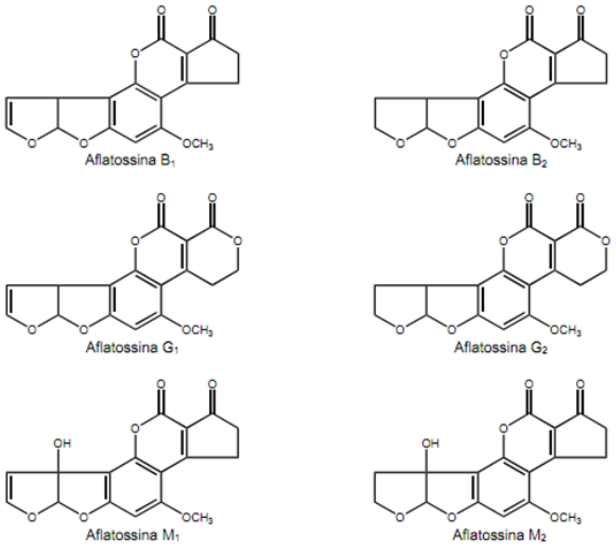

Figure 1.3.2.a.: Structures of some aflatoxins

Ochratoxins (Fig. 1.3.2.b.) are mycotoxins produced by several species of the most common fungal species: Aspergillus and Penicillium.

Ochratoxin A (OTA) is carcinogenic to humans and is nephrotoxic, hepatotoxic, teratogenic, and immunotoxic and is assumed to cause Balkan Endemic Nephropathy (BEN), a chronic kidney disease in humans when it is digested in combination with mycotoxin citrinin.

Ochratoxin B, a dihydroisocoumarin derivative, is the non-chlorinated analogue of the much more extensively studied Ochratoxin A.

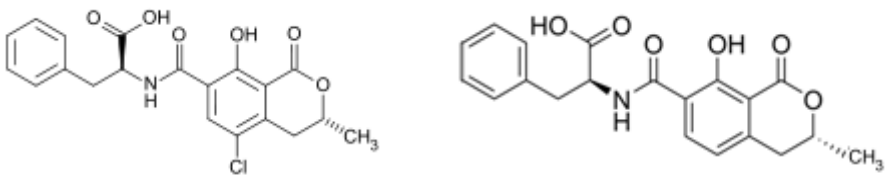

A *B*

Figure 1.3.2.b.: Structures of Ochratoxin A and B

The trichothecenes are a group consisting of at least 170 metabolites produced by different kinds of fungi, such as Fusarium, Myrothecium, Stachybotrys, Cephalosporium, and Tricothecium Verticimonosporium, and have a basic structure of sesquiterpenoide tetracyclic with an epoxy group between the C12 and the C13 carbons which causes the toxicity (Fig. *1.3.2.c.*).

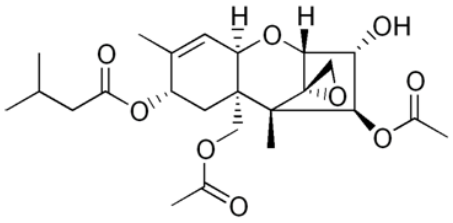

Figure 1.3.2.c.: Structure of T-2 toxin

Zearalenone (*1.3.2.d.*) and its derivatives (α-zearalenol, β-zearalenol and zearalanone) are phenolic compounds produced by several species of Fusarium, in particular Fusarium graminearum, Fusarium and Fusarium Gulmorum Esquiseti.

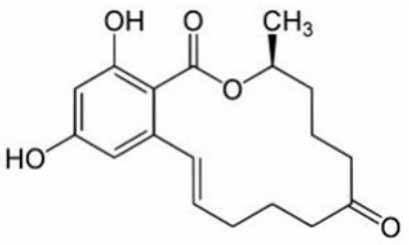

Figure 1.3.2.d.: Structure of zearalenone

The sterigmatocystin (Fig. 1.3.2.e.) is a toxic polyphenolic steroid, produced by various species of Aspergillus.

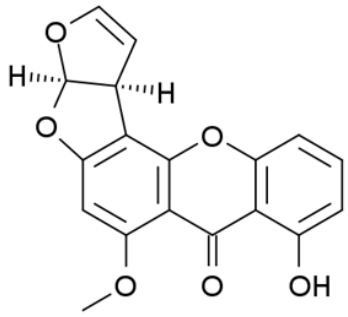

Figure 1.3.2.e.: Structure of sterigmatocystin

There are different types of chromatographic methods suitable for the analysis of mycotoxins, many of which include, in relation to the matrix on which it works, a pretreatment of the sample by liquid-liquid extraction or by solid phase extraction [Romero-Gonzalez et al., 2009]. Analysis of mycotoxins by capillary electrophoresis, by immunoassays, by both gas and liquid chromatography (coupled to detection systems such as FID, FTIR or, more commonly, MS) are fairly routine [Van Egmond et al., 1986; Cavaliere et al., 2005; Peña et al., 2002; Rahmani et al., 2011]. The derivatization is sometimes required [Scott, 1995], for the fluorometric or UV detection.

1.3.3. Amino acids and proteins as bioaerosol markers

Amino acids and proteins appear to be more generic biomarkers of bioaerosol. Both important constituents of bioaerosol, they can be an index of its occurrence in atmosphere [Poruthoor et al., 1998; Czerwieniec et al., 2005].

Free amino acid contribution to ambient inhalable airborne is due to direct emission from plants and animals and from biomass burning, or may be issued by peptides and proteins through enzymatic or photo-catalytic reactions in atmosphere (for example, degradation of organic litter) [Melillo et al., 1989; Gorzelska et al., 1992; Lobert and Warnatz, 1993; Milne and Zika, 1993].

Specific outdoor and indoor airborne proteins deriving from bacteria, fungi, house dust mites, multiple pollens, animal dander, and molds, are implicated in severe lung diseases, causing respiratory disorders, asthma and chronic obstructive pulmonary disease to exposed individuals [Miguel et al., 1996; Douwes et al., 2003; Adhikari et al., 2006; Georgakopoulos et al., 2009].

There are few studies reported in literature concerning free and combined amino acid occurrence in atmosphere.

In 1996, Saxena and Hildemann [Saxena and Hildemann, 1996, Turpin et al., 2000] reported a list of water-soluble atmospheric organic compounds; among them amino acids emerged as likely to contribute to the water soluble fraction. In particular free amino acids together with combined amino acids are about 10% of atmospheric water soluble organic nitrogen (WSON), that corresponds to about 18% of the total fine aerosol mass [Chan et al., 2005].

In 2003, Zhang showed that the average concentrations of free amino compounds (amino acids and alkyl amines) were generally 4–5 times lower than those of combined amino compounds (proteins and peptides); and in 2005, Jaenicke reported that cellular protein-containing particles were a major fraction of atmospheric aerosols [Zhang and Anastasio, 2003; Jaenicke, 2005].

The study of peptides and proteins is particularly complex, for the presence in atmosphere of composite mixtures, with each protein at low concentrations, and with the possibility of being modified by chemical and physical processes in the atmosphere [Milne and Zika, 1993; McGregor and Anastasio, 2001; Franze et al., 2005; Haan et al., 2009]. Therefore some authors only studied the total protein contribution through bicinchoninic acid assay (Micro BCA Protein Assay Kit) for the 'colorimetric detection and quantitation' of the total proteins [Chen and Hildemann, 2009; Kang et al., 2012]; or using the Nano-Orange Protein Quantification Kit (Molecular Probes, Eugene, OR) [Menetrez et al., 2007; Menetrez et al., 2009; Mandalakis et al., 2011] or through water-soluble organic nitrogen analysis [Zhang et al., 2002].

To sum up: the study of amino compounds in atmosphere represents both a way to amply the knowledge about water soluble organic compounds in atmosphere and also represents a concrete way to give an index of bioaerosol occurrence.

In addition, atmospheric proteins can cause adverse health effects, mostly allergic diseases of the human respiratory tract, and pulmonary inflammatory response, so that airborne concentration can be related to the allergenic content of the atmosphere.

In 1998, Mondal studied free amino acids in crushed and homogenized pollen from four plants that had been shown to play a significant role in causing various allergic disorders in sensitive patients and he found a percentage higher than 6% in weight [Mondal et al., 1998].

Significant amounts of free amino acids were found in the marine aerosol [Matsumoto and Uematsu, 2005; Mandalakis et al., 2011], in the continental aerosol [Zhang and Anastasio, 2003; Barbaro et al., 2011], as well as in the rain [Gorzelska et al., 1992] and in the fog [Zhang and Anastasio, 2001; Zhang and Anastasio, 2003]. As for their analytical determination, the high polarity of these compounds, their low volatility and the lack of strong chromophore groups make their separation and determination difficult. In order to solve these problems, pre- and post-column derivatization reactions have been developed, for either increasing the volatility of the analytes for analysis by gas chromatography [Mandalakis et al., 2010; Mandalakis et al., 2011], or introducing chromophore/fluorophores groups in their structure for analysis by liquid chromatography with UV or fluorescence.

In most studies [Gorzelska et al., 1992; Zhang and Anastasio, 2001; Zhang et al., 2002; Zhang and Anastasio, 2003; Matsumoto and Uematsu, 2005], the identification and quantitation of amino acids in particulate matter were performed by HPLC analysis with a fluorescence detector, after derivatization of compounds with o-phthalaldehyde/mercaptoethanol (OPA).

In addition, in the same studies, the extraction of amino acids from aerosols was performed in an ultrasonic bath by hydroalcoholic solutions, and, after centrifugation and filtration, the samples were directly analyzed [Barbaro et al., 2011; Zhang and Anastasio, 2003] by chromatography.

All of the existing derivatization methods present various analytical problems: derivative instability, reagent interference, long preparation times, inability to derivatize the secondary amino groups and difficulties in derivatization toward specific amino acids [Petritis et al., 2002]. Therefore the ability to investigate amino acids, without derivatization, by liquid chromatography-tandem mass spectrometry (HPLC/MS-MS), reduces sample preparation times and eliminates reagent associated interferences and the possible side reactions that may occur by performing derivatization in complex sample matrix [Samy et al, 2011].

1.4. Atmospheric particle sizes

Since toxic compounds adsorbed on particles can reach the systemic circulation, across the pulmonary alveoli, on the basis of particle size, their distribution into different size fractions of airborne particulate matter is an interesting approach to

assess atmospheric toxicity [Busse et al., 1972; Penn et al., 2005; Shimada et al., 2006].

Figure 1.4.a. represents the efficiency with which aerosol particles, based on their dimension, penetrate and deposit in the regions of the human respiratory system.

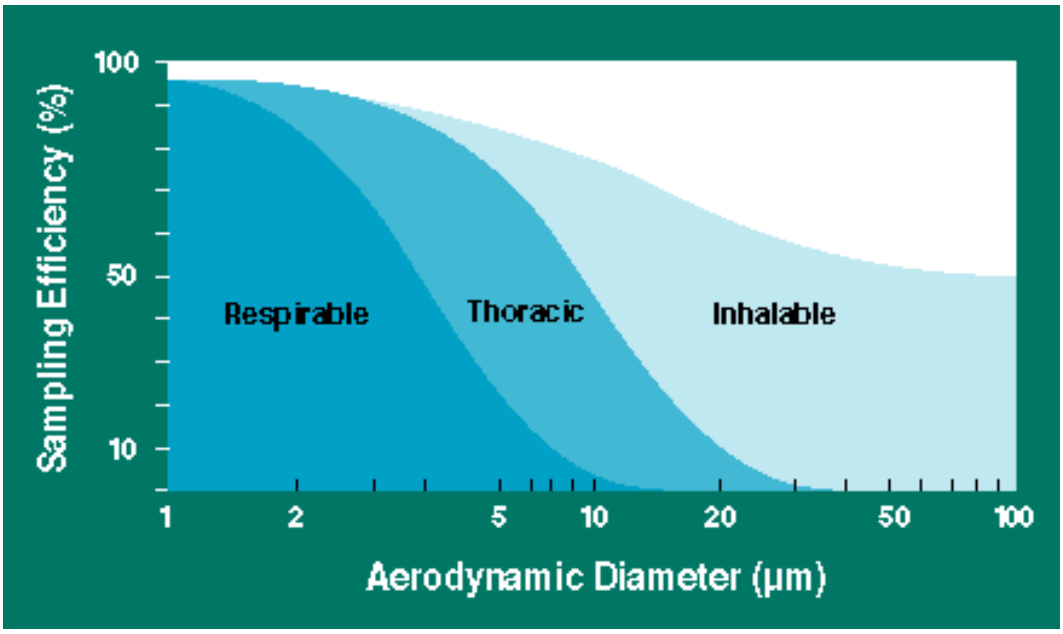

Figure 1.4.a. Graphic showing the ability of the particle to penetrate and deposit at different sites of the respiratory tract based on their aerodynamic diameter (APPLICATION NOTE ITI-050 TSI)

Inhalable particles are those capable of entering the respiratory system via the nose or mouth with 50% sampling efficiency. They have particle diameter corresponding to 100 µm.

Thoracic particles are that portion of the inhalable particles that pass the larynx and penetrate into the conducting airways (trachea, bifurcations) and the bronchial region of the lung with 50% efficiency. They have particle diameter corresponding to 10 µm.

Respirable particles are that portion of the thoracic particles that pass the deepest part of the lung, the nonciliated alveoli with 50% efficiency. They have particle diameter corresponding to 4 µm.

Such definitions are internationally accepted since developed by the Organization for Standardization (ISO), the American Conference of Governmental Industrial Hygienists (ACGIH), and the Comit Europen de Normalisation (CEN).

Relating to environmental criteria in the definition of particles, EPA (US Environmental Protection Agency) groups particle pollution into two categories: the

inhalable coarse particles are larger than 2.5 micrometers and smaller than 10 micrometers in diameter; the fine particles are 2.5 micrometers in diameter and smaller.

1.4.1. Coarse particles

Thoracic particulate matter (PM_{10}) defined as airborne particles ≤10 μm aerodynamic equivalent diameter, relates to that fraction of particulate matter which can primarily deposit in the conducting airways and the gas-exchange areas of the human respiratory system during mouth breathing. Sources of coarse particles include crushing or grinding operations, and dust from paved or unpaved roads.

1.4.2. Fine particles

Fine particulate ($PM_{2.5}$) matter is a second particle size cut-point of ≤2.5 μm diameter; it is demonstrated a predominant penetration of $PM_{2.5}$ into the gas-exchange region of the respiratory tract, and their major responsibility for adverse health effects. They are found in smoke and haze, and can be directly emitted from sources such as forest fires, or they can form when gases emitted from power plants, industries and automobiles react in the air.

1.4.3. Ultrafine particles

More recent scientific advances in PM-related health led now to focus on nano-sized particles. Ultrafine particles (UFPs, size cut-point of ≤0.1 μm diameter) contribute very little to the overall mass, but are very high in number, which in episodic events can reach several hundred thousand cm^{-3} in the urban air. As the size of a particle decreases, its surface area increases and also allows a greater proportion of its atoms or molecules to be displayed on the surface rather than the interior of the material. The biological impacts of nanoparticles and their biokinetics are dependent on size, chemical composition, surface structure, solubility, shape, and aggregation. These parameters can modify cellular uptake, protein binding, translocation from portal of entry to the target site, and the possibility of causing tissue injury. In fact, these particles largely escape alveolar macrophage surveillance and gain access to the pulmonary interstitium [Oberdörster, 2001; Oberdörster et al., 2005; Nel et al., 2006]. Hence they and their components have the potential to translocate to the brain and also the blood, and thereby reach other targets such as the cardiovascular system, spleen and liver [Li et al., 2003; Donaldson et al., 2005].

As for chemical composition, evidence now supports the view that UFPs carry considerable amounts of air toxics [Sioutas et al., 2005], and some authors have found that a large proportion of UFPs are made up of organic carbon [Kim et al. 2002; Chow & Watson, 2007; Mauderly & Chow, 2008]. In order to support this point, figure 1.4.3.a. [by Mauderly & Chow, 2008] shows the chemical composition of aerosol samples in nine size fractions using Micro Orifice Uniform Deposit Impactor (MOUDI) samplers for particles sizes from <0.056 μm to 10 μm at the Fresno Supersite in urban central California. As it is clearly illustrated, particles in the submicron PM are dominated by OC.

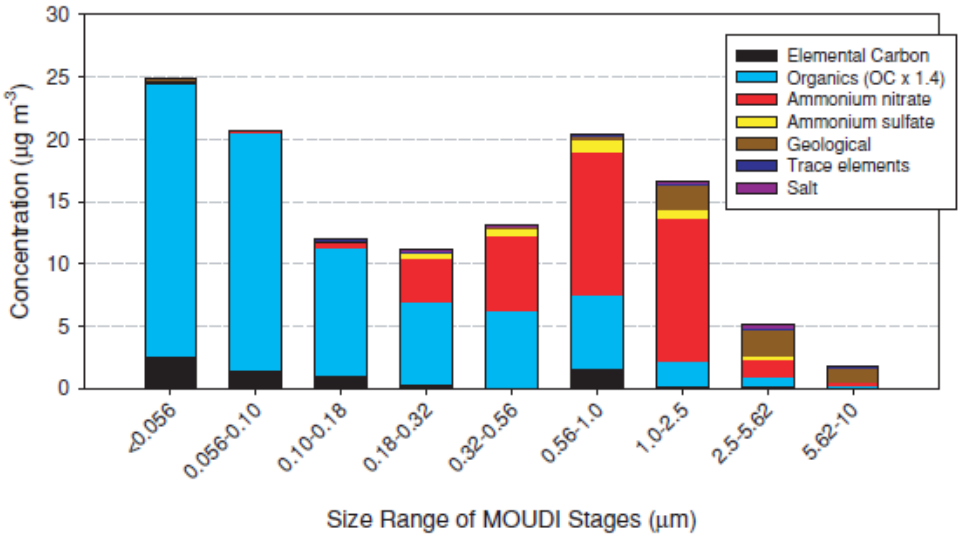

Figure 1.4.3.a.: An example of PM chemical composition as a function of particle size [Mauderly & Chow, 2008].

1.5 Particulate matter sampling

Atmospheric particulate matter sampling is based on removing particles from an air stream, drawing the air flow through a filter by a pump located downstream (inertial impactors). An inertial impactor consists of three main parts: sampling inlet, filtering system and pump. The sampling inlet, also defined "cutting head", is located upstream of the sampler both to discriminate particles according to their aerodynamic diameter, and to protect the filter by atmospheric agents. The most common cut-offs are 10, 2.5 and 1 μm for PM_{10}, $PM_{2.5}$ and PM_1 sampling. Particles successfully passing through the sampling inlet and having large enough inertia will impact upon a collection plate while the other particles, having lowest aerodynamic diameter, will

follow the airflow out of the impact region. The fraction of particles of a certain size that are collected at the impaction plate depends on the collection efficiency curve.
This curve should have a sharp division between the size of particles that are collected and those which are not. In practice, this curve has a sigmoid shape, in which the inflection point corresponds to 50% efficiency and represents the nominal cut-sizes of the impactor stage (Fig. 1.5.a.).

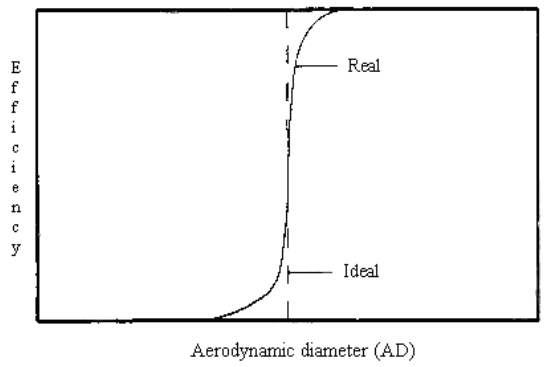

Figure 1.5.a.: Collection efficiency curve of single stage impactor: comparison between theoretical and real cutting

The inertial impactors can be at single stage or multiple stage (also called "cascade impactors").

1.5.1. Single stage impactor: dual channel sampler

Among the single stage impactors, the dual channel samplers are automatic and sequential PM_x sampling systems, simultaneously collecting particulate matter on two independent filter membranes. These instruments can work with any sampling inlet (PM_{10}, $PM_{2.5}$, PM_1) within the operating flow rate range 0.8 ÷ 2.5 $m^3\ h^{-1}$, on two distinct independent channels.

1.5.2. Multistage impactor sampler

Multiple stage impactors (or "cascade impactors") belong to the low volume inertial impactors and work at low pressure, about 100 mbar, and at a constant flow of about 10–30 L min^{-1} (0.6–1.8 $m^3\ h^{-1}$). Each stage of an inertial impactor consists of single or multiple nozzles and a collection plate. The nozzle diameter gets smaller and smaller from one stage to another and hence the aerosol velocities get higher and higher (Fig. 1.5.2.a.).

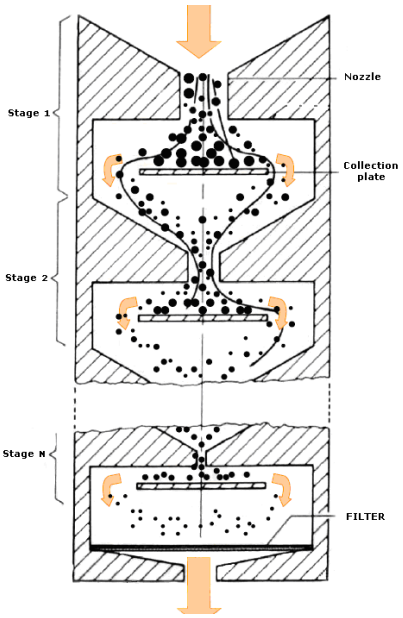

Figure 1.5.2.a:. Scheme of operation multistage impactor

At each stage a discrete range of particle size is collected, according to the aerodynamic cut-off of the collecting plate considered. For each stage an efficiency curve is defined (Fig. 1.5.2.b.). In order to maintain the efficiency curves and the cutting of each plate of impact, pressure and flow must be kept constant at the value declared by the manufacturer. A reduction of flow could result in an increase in the diameter of cut off of each impactor stage.

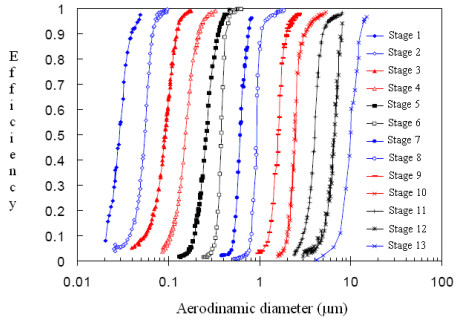

Figure 1.5.2.b.: Collection efficiency curves of a 13-stage impactor (Dekati LPI)

1.6. Particulate matter measurement

Particulate matter concentration is mainly determined by gravimetric method.
Filters must be conditioned in a controlled environment for a minimum of 24 hours prior to pre- and post-sampling weighing, in order to reduce errors occurring during the weighting phase caused by temperature variation, changes in humidity and static charges on the filters.

The volume of gas sampled must be accurately measured and corrected to standard conditions of temperature and pressure.

To calculate the concentration, the mass of particulate matter collected during sampling (μg) is divided by the volume of air sampled, so that the concentration of PM is expressed in μg Nm^{-3}.

2. AIM AND DESCRIPTION OF THE THESIS

As discussed above, exposures to airborne biological agents in both the occupational and residential indoor environment and in the outdoors are associated with adverse health effects, including allergies. Indoor and outdoor allergenic bioaerosol can have different sources and consequently different composition and concentrations. Identifying which specific allergenic agents are responsible for adverse effects on human health is essential to establish exposure assessment tools.

The main objective of this project is the identification and quantitation of allergens and toxics to human health, or markers of them, such as fungal spores, mycotoxins, amino acids and proteins in the atmospheric particulate matter, including the ultrafine fraction, both in indoor and outdoor environments. To achieve this purpose, methods of extraction and analysis of different classes of compounds from particulate matter of different particle size, sampled in the course of appropriate measurement campaigns, have been developed.

In particular, we studied the fungal component of aerosol in outdoor environment, through ergosterol, arabitol, and mannitol as biomarkers. Sterol and sugar polyols content in airborne particulate matter even at different sizes was studied, to verify the common source of these three biomarkers. The "US National Bureau of Standards" air particulate sample, Urban Dust SRM 1649a, was used as a complex matrix for evaluation of the method for the quantitative analysis of target compounds, and the matrix effect was studied.

In addition, an analytical method aimed at the determination of mycotoxins, as fungal secondary metabolites, in trace amounts in samples of atmospheric particulate matter was developed and applied to samples collected indoor and outdoor.

For this study, five mycotoxins have been taken into account: aflatoxin B1, ochratoxin A, T-2 toxin, zearalenone, and fumonisin B1, chosen on the basis of studies previously carried out in food matrices.

Next, this paper describes a method for the detection of underivatized amino acids, as biogenic components, by high resolution liquid chromatography coupled to tandem mass spectrometry (HPLC-MS/MS) in multiple reaction monitoring (MRM) mode on a triple quadrupole. In particular, we focused on the application of this method to the detection of these compounds on the particulate matter of different sizes, including the ultrafine fraction.

As there are no urban dusts, with certified and reference values for amino acids, we optimized their extraction, purification and analysis in a standard reference material (SRM) from National Institute of Standards and Technology (NIST), SRM 1649a-Urban Dust.

We gave great importance to the step of purification in order to guarantee the analysis of trace amounts of compounds, in case of small available quantities of particulate matter. Thanks to the purification steps and MS-MS detection, we obtained an interference-free determination and an increase in signal-to-noise ratios (S/N) [Buiarelli et al., 2013b].

At the same time, proteins were studied, through the Nano-Orange Protein Quantification Kit, on the urban dust samples, in order to compare amino acid and protein content and determine a possible match.

Finally, analyses were performed on size segregated airborne particulate matter, to know in particular about chemical composition of ultrafine particles, which, penetrating into the circulatory system, convey allergenic substances through the vascular systems to sites where adverse chemical reaction takes place.

EXPERIMENTAL

3. INSTRUMENTS AND MATERIALS

3.1. Sampling instruments

The following samplers were used to collect particulate matter: a low volume dual channel sampler, a low volume multistage impactor and a low volume Universal XR Pump.

3.1.1. Low volume dual channel sampler

Low volume dual channel sampler, HYDRA Dual Sampler FAI Instrument srl (Rome, Italy) (Fig. 3.1.1.a.), equipped with two size selective inlets, was used to collect PM_{10} on PTFE (polytetrafluoroethylene) filters (diameter: 47 mm, porosity: 2-3 µm, PALL Gelman Laboratory). Operational flow rate was set at 38.3 l min^{-1} (2.3 m^3 h^{-1}).

The maximum pressure drop in the sampler was 0.40 atm, and temperature was conditioned at 20° C.

Figure 3.1.1.a.: HYDRA Dual Sampler; FAI Instruments

3.1.2. Low volume multistage impactor sampler

A thirteen-stage cascade impactor, DLPI Dekati Ltd (Tampere, Finland) (Fig. 3.1.2.a.), was used to collect particles in the diameter range of 0.03-10 µm on PTFE filters (diameter: 37 mm, porosity: 0.45 µm, ALBET). Operational flow rate was 10 l min^{-1} and pressure was set at 100 mbar.

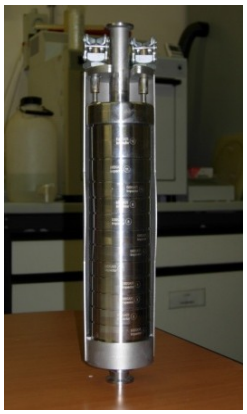

Figure 3.1.2.a.: Multistage Impactor sampler; DLPI, Dekati

The cascade low-pressure impactor classifies airborne particles into 13 size fractions. The 50% cut-off diameters of DLPI Dekati are 0.03, 0.06, 0.10, 0.17, 0.26, 0.40, 0.65, 1.0, 1.6, 2.5, 4.4, 6.8, and 10 µm. Therefore the fraction of particles collected on impactor-stages 1–3 (Dp < 0.1 µm) is referred to as the ultrafine fraction, while the portions on impactor-stages 4–8 (0.17 µm < Dp < 1.0 µm) and on impactor-stages 9–13 (Dp > 1.0 mm) are respectively referred to as the fine and the coarse fractions.

3.1.3. Low volume Universal XR Pump

The air sampling pump, SKC Ltd, Universal XR Pump Model PCXR8 (Fig. 3.1.3.a.) is a constant flow air sampling pump suited for personal sampling because of its compact dimensions and low weight. Its flow range is 5 to 5000 mL min^{-1}. PTFE filters (diameter: 37 mm, porosity: 2 µm, PALL Gelman Laboratory) were used to collect particles in indoor environment. Operational flow rate was 2.5 l min^{-1}.

Figure 3.1.3.a.: Universal XR Pump Model PCXR8

3.2. Climatic cabinet

Activa Climatic cabinet (Aquaria s.r.l., Lacchiarella, Milan, Italy) (Figure 3.2.a.) allows the conditioning filters at T = 20 ± 1 °C and 50 ± 5% RH (Relative

Humidity), before and after use (as indicated by the European Standard EN 12341 of 1998, by the method UNICHIM n ° 285/2003 and the Ministerial Decree No. 60 of 2 April 2002). The internal dimensions of the hood allow permanent housing as an analytical balance and a reasonable number of filters.

Figure 3.2.a.: Climatic cabinet

3.3. Microbalance

For the weighing operations an analytical balance Sartorius Mod MC-5 used (Fig. 3.3.a.) was able to appreciate up to ± 0.001 mg. The microbalance, housed inside the climatic cabinet, is provided with a shield glass supplied with a special coating in order to eliminate any interference factors, such as the electrostatic charges of the samples to be weighed. In addition, thanks to the stabilization time of only ten seconds, you can save your precious time with each weigh.

Figure 3.3.a.: Analytical balance

3.4. Extraction instrument

For the determination of target analytes, filters were extracted with Dionex ASE200 Accelerated Solvent Extractor (ThermoFisher, Sunnyvale, CA) (Fig. 3.4.a.) operating at high pressure and temperature with suitable solvents or solvent mixtures.

Figure 3.4.a.: Accelerated Solvent Extractor, Dionex ASE-200

3.5. Evaporation instrument

Evaporation of extracts was carried out with SE500s solvent evaporator system (Fig. 3.5.a.; Glas-Col, Terre Haute, IN, USA) under nitrogen stream. This instrument greatly reduces evaporation time since it allows programming of both gas and solution heating and vial stirring rate.

Figure 3.5.a.: SE500s solvent evaporator system

3.6. SPE vacuum manifold

Sample clean-up was carried out on solid phase extraction (SPE) cartridges with an Alltech SPE Vacuum manifold, 12-Port model (Alltech – Grace, Deerfield, IL - USA), (Fig. 3.6.a.).

The manifold consists of a rectangular glass cabinet with a vacuum gauge and a polypropylene cover which can hold the cartridges. The instrument can simultaneously elute twelve samples.

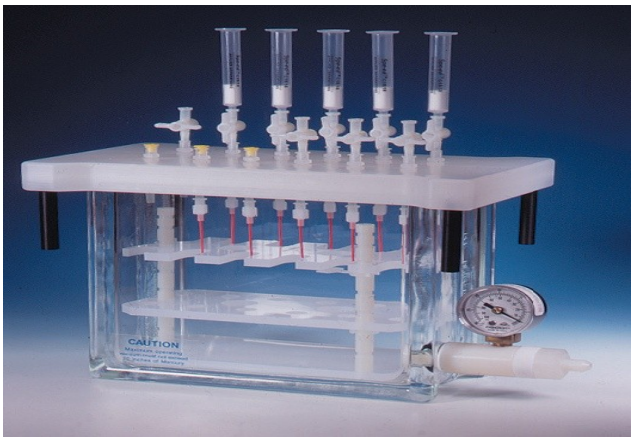

Figure 3.6.a.: Alltech SPE vacuum manifold

3.7. Analytical instrumentations

3.7.1. Gas chromatograph –Mass Spectrometer (GC/MS)

Gas-chromatographic analyses were performed on a gas-chromatograph (Agilent HP6890) equipped with an autosampler (Agilent 7693), and coupled to a single quadrupole mass spectrometer (HP5973, Agilent Technologies, Palo Alto, CA), operating with an electron-impact ionization source (EI) (Fig. 3.7.1.a.).

The quadrupole consists of four parallel metal rods. Each opposing rod pair is connected together electrically. A radio frequency (RF) voltage and a direct current (DC) voltage is applied between one pair of rods and the other. Ions travel down the quadrupole between the rods. Only ions of a certain mass-to-charge (m/z) ratio will reach the detector for a given ratio of voltages: other ions having unstable trajectories will collide with the rods. This permits selection of ions with a particular m/z or allows to scan a range of m/z-values by continuously varying the applied voltage. The electron-impact source emits electrons from a tungsten filament heated to 230 °C. These electrons are accelerated by a potential of 70eV and made to collide with gaseous atoms or molecules of the sample causing their ionization. The ionization efficiency and production of fragment ions depends strongly on the chemistry of the analyte and the energy of the electrons. At around 70 eV, energy transferred to organic molecules is maximized, leading to the strongest possible ionization and fragmentation. Depending on the compound, the molecular ion peak does not always appear or can be weak.

Figure 3.7.1.a.: GC/MS

3.7.2. High-performance liquid chromatograph – Tandem Mass Spectrometer (HPLC/MS-MS)

HPLC-MS/MS analyses were carried out with a HPLC (Agilent 1100 series HPLC) including a quaternary pump and an autosampler (Agilent G1313A) (Agilent Technologies, Santa Clara CA, USA). The chromatograph is coupled to a mass spectrometer API2000 (Applied Biosystem, Foster City, CA, USA) with ElectroSpray Ionization (ESI) (Fig. 3.7.2.a.).

A triple quadrupole mass spectrometer is a tandem mass spectrometer consisting of three quadrupole in series. The first (Q1) and third (Q3) quadrupoles are used as mass filters, whereas the middle (Q2) quadrupole serves as a collision cell. This collision cell is a quadrupole (non-mass filtering) using an inert gas (N2) to provide collision-induced dissociation of a precursor ion that is selected in Q1. Subsequent fragments are passed through Q3, where they may be filtered or fully scanned.

In this study, mass parameter optimization is carried out in the precursor ion scan mode. Q1 parameters are optimized to maximize signal intensity for the precursor ion which is fragmented in Q2. Fragment ions are transferred to Q3 that is set to scan the entire m/z range giving information on their intensities. Then both Q1 and Q3 are set to a selected mass, allowing only a distinct fragment ion from a certain precursor ion to be detected. This configuration is called multiple reaction monitoring (MRM) and is characterized by high specificity and sensitivity, with high ratio S/N.

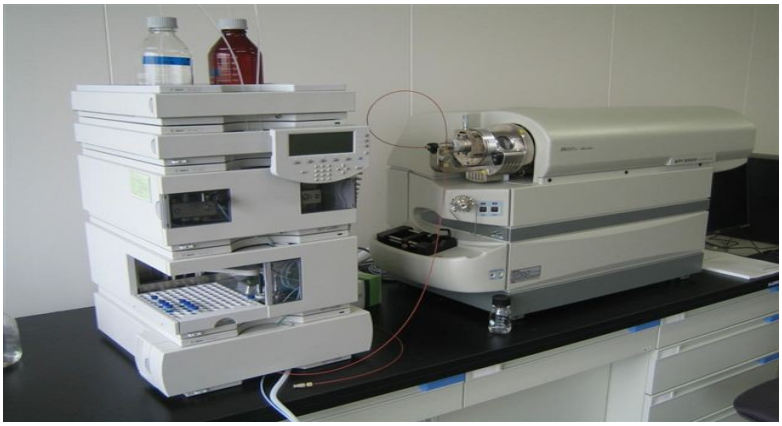

Figure 3.7.2.a.: HPLC/MS-MS

3.7.3. Fluorescence Spectrometer

In order to use the NanoOrange® Protein Quantitation Kit a Perkin-Elmer LS 5 Fluorescence Spectrometer was utilized. The monochromator uses a high energy pulsed Xenon source for excitation. The pulsed Xenon source minimizes photo bleaching of samples and provide a long-lived excitation source. The LS 5 includes a single cell thermostatted sample holder that can accommodate 1 cm pathlength cells.

Figure 3.7.3.a.: Perkin-Elmer LS 50 Fluorescence Spectrometer

3.8. Materials

3.8.1. Chemicals and reagents

- Acetonitrile, Ultra Gradient, Super Purity Solvent (Romil, Cambridge, UK);
- Ethanol anhydrous, Ultra Gradient, Super Purity Solvent (Romil, Cambridge, UK);
- Ethyl acetate anhydrous, Ultra Gradient, Super Purity Solvent (Romil, Cambridge, UK);
- n-Hexane, Ultra Gradient, Super Purity Solvent (Romil, Cambridge, UK);
- Methanol, Ultra Gradient, Super Purity Solvent (Romil, Cambridge, UK);

- Toluene, Ultra Gradient, Super Purity Solvent (Romil, Cambridge, UK);
- Water, Ultra Gradient HPLC Grade (Romil, Cambridge, UK);
- Ultrapure Water produced with Pure Lab System (USF Elga Ransbac-Baumbach. Germany);
- Hydrochloric acid (Carlo Erba Reagenti S.p.A. Arese, MI, Italia);
- Propan-1-ol (Carlo Erba Reagenti S.p.A. Arese, MI, Italia);
- Formic Acid 99% (Carlo Erba Reagenti S.p.A. Arese, MI, Italia);
- Glacial acetic acid (Carlo Erba Reagenti S.p.A. Arese, MI, Italia);
- Ammonia solution 30% (Carlo Erba Reagenti S.p.A. Arese, MI, Italia);
- Ammonium formate (Fluka - Sigma-Aldrich, St. Louis, MO, USA);
- Ammonium acetate, (Carlo Erba Reagenti S.p.A. Arese, MI, Italia);
- N,O-bis (trimethylsilyl) trifluoroacetamide (BSTFA) (Sigma-Aldrich, St. Louis, MO, USA);
- Pyridine, (Sigma-Aldrich, St. Louis, MO, USA);
- Timethylchlorosilane (TMCS) (Sigma-Aldrich, St. Louis, MO, USA);
- Mannitol (Sigma-Aldrich, St. Louis, MO, USA);
- Arabitol (Sigma-Aldrich, St. Louis, MO, USA);
- Mannitol-^{13}C (Sigma-Aldrich, St. Louis, MO, USA);
- Xylitool-^{13}C (Sigma-Aldrich, St. Louis, MO, USA);
- Ergosterol (Sigma-Aldrich, St. Louis, MO, USA);
- Dehydrocholesterol (Sigma-Aldrich, St. Louis, MO, USA);
- N-methyl-glucamine (Sigma-Aldrich, St. Louis, MO, USA);
- N-methyl-N(-trimethylsilyl)trifluoroacetamide/ammonium iodide/ethanethiol (mixture MSTFA/NH4/ethanethiol) (Sigma-Aldrich, St. Louis, MO, USA);
- Sodium chloride, (Carlo Erba Reagenti S.p.A. Arese, MI, Italia);
- Dithiothreitol (DTT) 99%, (Sigma-Aldrich, St. Louis, MO, USA);
- Sodium dodecylsulfate (SDS) (Fluka - Sigma-Aldrich, St. Louis, MO, USA);
- Tris(hydroxymethyl)aminomethane, (Carlo Erba Reagenti S.p.A. Arese, MI, Italia);
- LD- proline (Pro) (Fluka - Sigma-Aldrich, St. Louis, MO, USA);
- LD- tryptophan (Trp) (Fluka - Sigma-Aldrich, St. Louis, MO, USA);
- LD-phenylalanine (Phe) (Fluka - Sigma-Aldrich, St. Louis, MO, USA);
- LD-alanine (Ala) (Fluka - Sigma-Aldrich, St. Louis, MO, USA);

. LD-glycine (Gly) (Fluka - Sigma-Aldrich, St. Louis, MO, USA);
. LD-glutamine (Gln) (Fluka - Sigma-Aldrich, St. Louis, MO, USA);
. LD-asparagine (Asn) (Fluka - Sigma-Aldrich, St. Louis, MO, USA);
. LD-valine (Val) (Fluka - Sigma-Aldrich, St. Louis, MO, USA);
. LD-leucine (Leu) (Fluka - Sigma-Aldrich, St. Louis, MO, USA);
. LD-isoleucine (Ile) (Fluka - Sigma-Aldrich, St. Louis, MO, USA);
. LD-tyrosine (Tyr) (Fluka - Sigma-Aldrich, St. Louis, MO, USA);
. L-serine (Ser) (Sigma-Aldrich, St. Louis, MO, USA);
. L-methionine (Met) (Sigma-Aldrich, St. Louis, MO, USA);
. L-threonine (Thr) (Sigma-Aldrich, St. Louis, MO, USA);
. DL-proline (2,3,3,4,4,5,5 - D7, 97-98%) ($^2H_7$-Pro) (Cambridge Isotope Laboratories Inc Tewksbury, MA - USA);
. L-tryptophan (D8, 98%) ($^2H_8$-Trp) (Cambridge Isotope Laboratories Inc Tewksbury, MA - USA);
. L-isoleucine-2-D1 (98.9%) ($^2H_1$-Ile) (CDN ISOTOPES C/D/N Isotopes Inc. Pointe-Claire, Quebec – Canada);
. DL-serine-2,3,3-D3 (99.3%) ($^2H_3$-Ser) (CDN ISOTOPES C/D/N Isotopes Inc. Pointe-Claire, Quebec – Canada);
. L-treonina-2,3-D2 (98.8%) ($^2H_2$-Thr) (CDN ISOTOPES C/D/N Isotopes Inc. Pointe-Claire, Quebec – Canada);
. Bovine serum albumin (BSA) (Sigma-Aldrich, St. Louis, MO, USA);
. Standard Reference Material (SRM) Urban Dust 1649a (National Institute of Standards and Technology - NIST - Gaithersburg, MD USA);
. Standard Reference Material (SRM) Urban Dust 1649b (National Institute of Standards and Technology - NIST - Gaithersburg, MD USA);
. Aflatoxin B1, STD 5 mg, (Sigma-Aldrich, St. Louis, MO, USA);
. Ochratoxin A, STD 5 mg, (Sigma-Aldrich, St. Louis, MO, USA);
. Sterigmatocystin, STD 5 mg, (Sigma-Aldrich, St. Louis, MO, USA);
. T-2Toxin, STD 5 mg, (Sigma-Aldrich, St. Louis, MO, USA);
. Zearalenone, STD 5 mg, (Sigma-Aldrich, St. Louis, MO, USA);
. Fumonisin B1, 5 mg, (Sigma-Aldrich, St. Louis, MO, USA);
. Deuterated zearalenone, STD 10 µg, (Sigma-Aldrich, St. Louis, MO, USA);
. Potassium Chloride (Carlo Erba Reagenti S.p.A. Arese, MI, Italia);

- Potassium dihydrogen phosphate, (Fluka - Sigma-Aldrich, St. Louis, MO, USA);
- Disodium phosphate dodeca-hydrate (Carlo Erba Reagenti S.p.A. Arese, MI, Italia);
- Hydromatrix Dionex (ThermoFisher Scientific, Sunnyvale, CA).

3.8.2. Chromatographic columns and SPE cartridges

- Amino SPE cartridge (55 μm, 70 A), Strata- NH_2 (Phenomenex, Torrance, CA, USA);
- J&W Scientific DB-5MS (5%phenyl-95%dimethylpolysiloxane) 30 m x 0.25 mm diameter, 0.25 μm film thickness (Agilent Technologies, Palo Alto, CA);
- NH_2 column Restek (5 μm particle size and 50 mm length, 2.1 mm I.D.) (Restek Corporation, Bellefonte, PA – USA);
- Supelco C18 column (5 μ m particle size and 30 mm length, 2.1 mm I.D.) (Supelco - Sigma-Aldrich, St. Louis, MO, USA);
- Strata X cartridge (200mg/6mL), (Phenomenex, Torrance, CA, USA);
- Extract Clean SCX cartridges (500mg/4mL), (ALLTECH – Grace, Deerfield, IL - USA);
- Strata-XC PCX cartridges (30mg/1mL) (Phenomenex, Torrance, CA, USA);
- Strata SCX cartridges (500mg/6mL), (Phenomenex, Torrance, CA, USA);
- Dionex Acclaim® TrinityTM Analytical P1 (2.1 x 100 mm, 3μm) column (ThermoFisher Scientific, Sunnyvale, CA);
- LUNA HILIC (50 x 2.0 mm, 3 μm) column (Phenomenex, Torrance, CA, USA);
- C18 (250 mm x 2,1 mm) spherisorb 5 μm C18 column (packed in our laboratory);
- Polytetrafluoroethylene Membrane Disc Filters, (47 mm, 2.0 μm) (Pall Corporation - Port Washington, NY USA);
- Polytetrafluoroethylene Membrane Disc Filters (25 mm, 0.45 μm) (ALBET-Hahnemuehle S.L., Barcelona - Spain);
- NanoOrange® Protein Quantitation Kit (Life Technologies LTD, Paisley, UK);

. Polytetrafluoroethylene Membrane Disc Filters (37 mm, 2.0 μm) (Pall Corporation - Port Washington, NY USA);
. C18 Zorbax Eclipse XDB (25 cm, 4.6 mm) column (Agilent Technologies, Palo Alto, CA);
. Supelco Discovery C18 Column (5 cm, 2.1 mm, 5 μm), (Supelco - Sigma-Aldrich, St. Louis, MO, USA);
. Strata C18-M cartridges (500mg/3mL), (Phenomenex, Torrance, CA, USA);
. Strata C18-E cartridges (End-Capped, 500mg/3mL), (Phenomenex, Torrance, CA, USA);
. Strata X (200mg /6mL) cartridges, (Phenomenex, Torrance, CA, USA);
. Oasis HLB (3 mL) cartridges (Waters Corporation Milford, MA – USA).

RESULTS

4. RESULTS AND DISCUSSION

4.1. Fungal component of aerosol

4.1.1. Aerosol analysis

Optimization of the analytical method for the simultaneous analysis of levoglucosan, xylitol, arabitol, mannitol, and ergosterol has been the subject of the PhD thesis Pomata D., 2012, and results were published in Buiarelli et al., 2013a. Figure 4.1.1.a. shows the flowsheet of the whole analytical procedure.

Briefly, marker extraction from sampled filters was performed with ASE-200 Dionex, using pure ethanol, after spiking samples with levoglucosan-^{13}C, xylitol-^{13}C, mannitol-^{13}C and dehydrocholesterol as internal standards. The extract was then passed through an amino cartridge and divided into two parts: the apolar fraction was immediately released from the cartridge in ethanol, while polar compounds, retained by the cartridge, were eluted with a mixture of methanol-water (80:20). The two fractions were separately derivatized by BSTFA containing 1% of TMCS and pyridine at 70 °C for 1 h, evaporated and analyzed in GC-MS. GC separation was achieved in 12 minutes on a DB-5MS capillary column. The temperature program was: 100°C initial temperature, ramped at 25°C/min to 180°C, then ramped at 40°C/min to 300°C and held for 8 min. Samples (1μL) were injected in splitless mode. The injector temperature was set at 280°C. The helium carrier gas was maintained at a constant flow of 1.0 ml min^{-1}. The quadrupole and ion source temperatures were set at 150°C and 230°C, respectively.

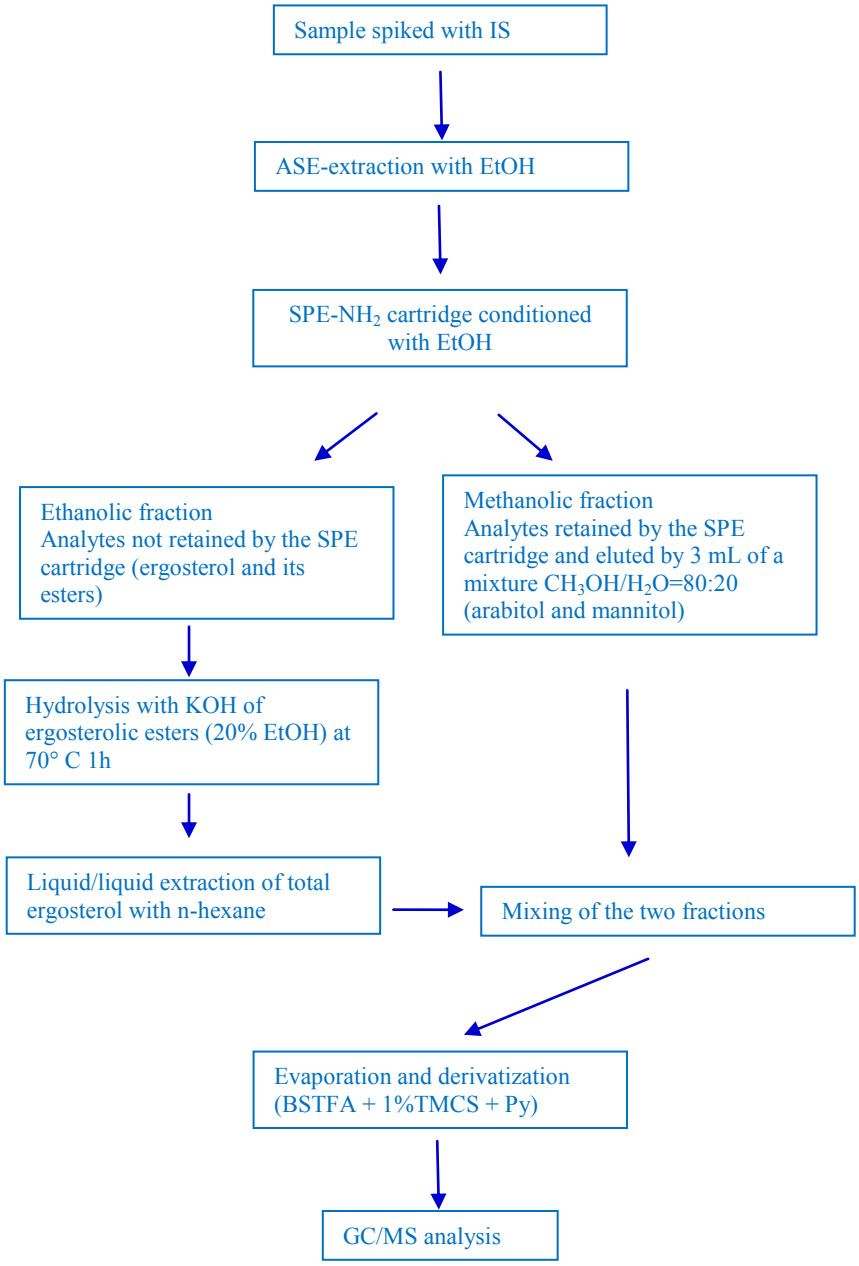

Figure 4.1.1.a.: Flowsheet of the whole analytical procedure for fungal biomarkers

Acquisitions were performed in selected ion monitoring (SIM) mode. The mass spectrometer was operated in EI mode at 70 eV.

Table 4.1.1.α. shows silanized -arabitol, -mannitol, -ergosterol, -levoglucosan, -xylitol target and qualifier ions.

	target ions (m/z)	qualifier ions (m/z)
Silanized-arabitol	217 (M-295)	307 (M-205); 319 (M-193)
Silanized-mannitol	319 (M-295)	217 (M-397); 205 (M-409)
Silanized-ergosterol	363 (M-105)	337 (M-131); 468 (M)
Silanized-levoglucosan	204 (M-174)	217 (M-161); 333 (M-45)
Silanized-xylitol	217 (M-295)	307 (M-205); 319 (M-193)

Table 4.1.1.α.: Silanized -arabitol, -mannitol, -ergosterol, -levoglucosan, -xylitol target and qualifier ions

4.1.2. Optimization of the quantitative analysis for the determination of levoglucosan, sugar polyols and ergosterol in airborne particulate matter

Currently, standard reference materials (SRM) with certified values for arabitol, mannitol, ergosterol, levoglucosan, xylitol are not available. Only a reference value for levoglucosan concentration is expressed as mass fraction in "SRM 1649a Certificate of Analysis". In the present work, the NIST air particulate sample, Urban Dust SRM 1649a was used as a complex matrix for evaluation of the optimized method of analysis, and the matrix effect was studied [Pomata et al., in press].

The quantitative analysis of target analytes in SRM 1649a was carried out using both internal standard calibration curves and standard addition method.

4.1.2.1. Quantitative analysis of target analytes in SRM 1649a using standard calibration curves

Standard calibration curves were constructed by adding increasing volumes of the multi-standard solution and a constant volume of the internal standard solution, for six calibration levels, on clean Teflon filters, in a concentration range from 28 to 300 μg L^{-1} for levoglucosan, from 28 to 1480 μg L^{-1} for arabitol, from 14 to 1500 μg L^{-1} for xylitol, from 14 to 860 μg L^{-1} for mannitol, and from 30 to 830 μg L^{-1} for ergosterol.

The thus prepared samples were processed following the whole procedure of figure 4.1.1.a. to take account of any losses during sample treatment, and injected three times in the GC-MS system. The standard calibration plots were constructed by plotting area ratios of analyte/internal standard vs. concentration ratios of analyte/internal standard.

For the analysis of SRM 1649a, the standard material was weighed using an analytical electronic balance (Sartorius MC-5, Δm ± 0.001 mg) after conditioning in a climatic chamber (Activa 114 Climatic Cabinet, Aquaria MI, according to UNI EN 12341/2001; UNI CHIM 285/2003 and D.M. 115 60/2002) for 24h, at T = 20 ± 1 °C and at 50 ± 5 relative humidity and deposited on clean Teflon filters.
Such samples were subjected to the analytical procedure shown in figure 4.1.1.a. and the concentrations were determined by interpolation of the calibration curves.

4.1.2.2. Quantitative analysis of target analytes in SRM 1649a using the standard addition method

Two samples of 1.47 and 10.43 mg of urban dust SRM 1649a, deposited on two clean Teflon filters, were extracted. Both extracts were divided into seven aliquots, each corresponding to the extract of respectively 0.21 and 1.49 mg of urban dust. The extract corresponding to 0.21 mg was chosen to simulate a sample coming from a multistage impactor whose filters collect an amount of particulate matter ranging from about 0.05 to 0.7 mg if the sampling period is two weeks [Di Filippo et al., 2010]. The extract corresponding to 1.49 mg was chosen based on the quantity of particulate matter averagely collected with a sampler sampling at a flow rate of 2.3 m^3 h^{-1}, for 24 h.
From 10 to 100 µl of the methanolic standard solutions were then added to the extracts, so as to obtain final concentrations of ^{13}C-labelled and unlabelled analytes consistent with those of standard calibration curve points in a concentration range from 10 to 300 µg L^{-1} for levoglucosan, arabitol and mannitol, from 70 to 460 µg L^{-1} for xylitol and from 30 to 250 µg L^{-1} for ergosterol. The resulting solutions were processed following the procedure of figure 4.1.1.a. starting from the clean-up step, and then injected three times in the GC-MS system. For each analyte two standard addition plots (PLOT1 and PLOT2 respectively for 0.21 and 1.49 mg of urban dust), were obtained by plotting area ratios of analyte/internal standard vs. concentration ratios of analyte/internal standard.
The concentrations (Cx) of analytes in the SRM 1649a were obtained as x-intercept of the regression lines. Small contributes due to blank filters and protocol of extraction, clean-up, and derivatization were subtracted by the chromatographic signals obtained. Concentration values obtained for each analyte were also corrected for the recovery of the ASE extraction.

4.1.2.3. Results for arabitol, mannitol, ergosterol, levoglucosan, xylitol concentrations in SRM 1649a

Good linearities with correlation coefficients (R^2) not lower than 0.993, for both internal standard calibration curves (Tab. 4.1.2.3.α.) and standard addition plots (Tab. 4.1.2.3.β.), were obtained for all analytes of interest.

Compounds	Concentration ranges (µg L^{-1})	Equation of calibration curves	R^2
^{13}C-Levoglucosan	220		
Levoglucosan	28-300	y = (0.625 ± 0.029) x + (0.099 ± 0.022)	0.993
^{13}C-Xylitol	200		
Xylitol	28-1480	y = (4.456 ± 0.019) x + (0.139 ± 0.062)	0.999
Arabitol	14-1500	y = (3.177 ± 0.048)x + (0.198 ± 0.016)	0.997
^{13}C-Mannitol	190		
Mannitol	14-860	y = (0.794 ± 0.029) x + (0.057 ± 0.017)	0.996
Deidrocholesterol	400		
Ergosterol	30-830	y = (0.792 ± 0.013) x - (0.014 ± 0.004)	0.995

Table 4.1.2.2.α.: Concentration ranges, equations and correlation coefficients of standard calibration curves for target analytes

Compounds	Concentration ranges (µg L^{-1})	Equation of standard addition plots	R^2
^{13}C-Levoglucosan	220		
Levoglucosan (PLOT1)	7-300	y = (0.679 ± 0.008) x + (0.129 ± 0.005)	0.997
Levoglucosan (PLOT2)	7-300	y = (0.524 ± 0.001) x + (0.545 ± 0.007)	0.995
^{13}C-Xylitol	200		
Xylitol (PLOT1)	70-460	y = (3.313 ± 0.030) x + (0.216 ± 0.022)	0.999
Xylitol (PLOT2)	70-460	y = (2.639 ± 0.108) x + (0.231 ± 0.140)	0.995
Arabitol (PLOT1)	8-300	y = (2.157 ± 0.036) x + (0.115 ± 0.027)	0.996
Arabitol (PLOT2)	8-300	y = (3.681 ± 0.012) x + (0.217 ± 0.009)	0.999
^{13}C-Mannitol	190		
Mannitol (PLOT1)	6-260	y = (1.184 ± 0.004) x + (0.035 ± 0.003)	0.999
Mannitol (PLOT2)	6-260	y = (1.811 ± 0.008) x + (0.171 ± 0.005)	0.999
Deidrocholesterol	400		
Ergosterol (PLOT1)	30-250	y = (0.668 ± 0.048) x + (0.016 ± 0.030)	0.993
Ergosterol (PLOT2)	30-250	y = (0.563 ± 0.010) x + (0.040 ± 0.003)	0.999

Table 4.1.2.2.β.: Concentration ranges, equations and correlation coefficients of standard addition plots for target analytes

As for quantitative analysis of urban dust SRM 1649a carried out with standard calibration curves, concentrations (µg g^{-1}) of levoglucosan, polyols and ergosterol (expressed as mean ± standard deviation of three repeated tests) obtained from the extraction of three samples of about 0.6-2 mg are shown in table 4.1.2.2.γ. Table

4.1.2.2.γ. also shows the concentrations (μg g^{-1}) of the target analytes extrapolated with standard addition plots (expressed as extrapolated values ± their standard deviations (S_{XE})).

Standard deviation of extrapolated value (S_{XE}) was calculated according to the following formula:

$$s_{x_E}^2 = \frac{s_{y/x}^2}{b^2}\left[\frac{1}{n} + \frac{\bar{y}^2}{b^2\sum(x_i - \bar{x})^2}\right]$$

where b is the slope of standard addition plot; and are the centroids of the points x_i, y_i: n is the number of standard addition points and $s_{y/x}$ is the standard deviation of y/x.

Analytes	Calibration curves	Standard addition PLOT1	Standard addition PLOT2
		Concentration [μg g^{-1}]	
Levoglucosan	148.54 ± 18.39	173.23 ± 27.68	160.3 ± 16.22
Xylitol	107.86 ± 23.46	130.96 ± 12.44	86.07 ± 18.85
Arabitol	16.58 ± 3.91	n.d.	12.40 ± 0.96
Mannitol	15.63 ± 0.86	n.d.	19.81 ± 0.98
Ergosterol	0.61 ± 0.14	n.d.	0.41 ± 0.06

n.d.: not detected

Table 4.1.2.2.γ.: Mean values (μg/g) ± standard deviation and extrapolated values (μg/g) ± standard deviations (S_{XE}) of target analyte concentrations in SRM 1649a measured with both internal standard calibration method and standard addition method

As seen from table 4.1.2.2.γ., for quantitative analysis of levoglucosan, both standard addition plots were used and the results obtained with two extrapolations were 173.3 ± 27.7 μg g^{-1} (PLOT1) and 160.3 ± 16.2 μg g^{-1} (PLOT2) with a mean of 166.78 and percentage differences of 7.51%.

Arabitol, mannitol and ergosterol concentrations in SRM 1649a were only extrapolated with PLOT2 since the concentration of these compounds in 0.21 mg of SRM 1649a was lower or equal to the analytical LOD, as expected given their low atmospheric concentrations.

On the contrary only PLOT1 was used to extrapolate xylitol concentration in SRM 1649a since the concentration obtained with PLOT2 showed a very high percentage standard deviation (see table 4.1.2.2.γ.) probably due to the higher number of

interferents present in 1.49 mg of SRM 1649a and the high amount of xylitol, as expected for its averagely higher atmospheric concentration [Di Filippo et al., 2013].

4.1.2.4. Evaluation of the matrix effect

Matrix effect can both reduce and enhance the detector response when compared to response of the standards in neat solvent. The matrix effect depends on the instrument (mainly GC-injection system), the type and amount of matrix (grams of matrix per milliliter of extract), the sample pretreatment procedure (derivatization), the analytes and their concentration [Pizzuti et al. 2012].

Matrix-induced signal suppression in GC typically occurs when coextracted matrix components, accumulated into the gas chromatographic system generate new active sites which cause the analyte to be adsorbed and/or degraded [Pizzuti et al. 2012].

In the case of matrix-induced signal enhancement, coextracted matrix components are competitively adsorbed to the active sites of the gas chromatography system (inlet and column), instead of target analytes [Pizzuti et al. 2012; Poole, 2007].

In this study, the matrix effect was calculated as the slope ratios between standard calibration curves and standard addition plots. For compounds showing slope ratios between 0.9 and 1.1, matrix effect was considered to be negligible.

Figures 4.1.2.4.a. and 4.1.2.4.b. show the comparison between standard calibration curves and standard addition plots (for arabitol, ergosterol and mannitol the plot shown is PLOT2, for xylitol PLOT1), the latter shifted to the origin by subtracting the marker concentrations present in the SRM 1649a (Standard addition plot – C_x).

For arabitol (Fig. 4.1.2.4.a.) and levoglucosan (Fig. 4.1.2.4.b.) in PLOT1, a negligible matrix effect, with slopes ratio of 0.9, was obtained. The slope ratio of 1.2, obtained for levoglucosan in PLOT2 (Fig. 4.1.2.4.b.), indicates the presence of a small matrix effect, probably due to ion suppressions caused by the higher number of interferents present in 1.49 mg of SRM 1649a.

A negative matrix effect (slope ratio > 1) was found for xylitol and ergosterol (respectively ratios = 1.3 and 1.4), while a positive matrix effect (slope ratio < 1) was found for mannitol (ratio = 0.4) (Fig. 4.1.2.4.a.). Negative matrix effect observed for xylitol and ergosterol may originate from the competition between the analytes and the presence of coeluting, undetected matrix components, as also demonstrated by higher slopes of PLOT1 on respect PLOT2. For ergosterol the

measured matrix effect may also be due to the use of a homologue rather than the stable isotope-labeled analyte as internal standard.

Positive matrix effect observed for mannitol may be due to the presence of interferences that compete with the ionization and ion evaporation processes, effectively increasing (ion enhancement) the formation efficiency of the desired mannitol ions, as also demonstrated by higher slope of PLOT2 on respect PLOT1.

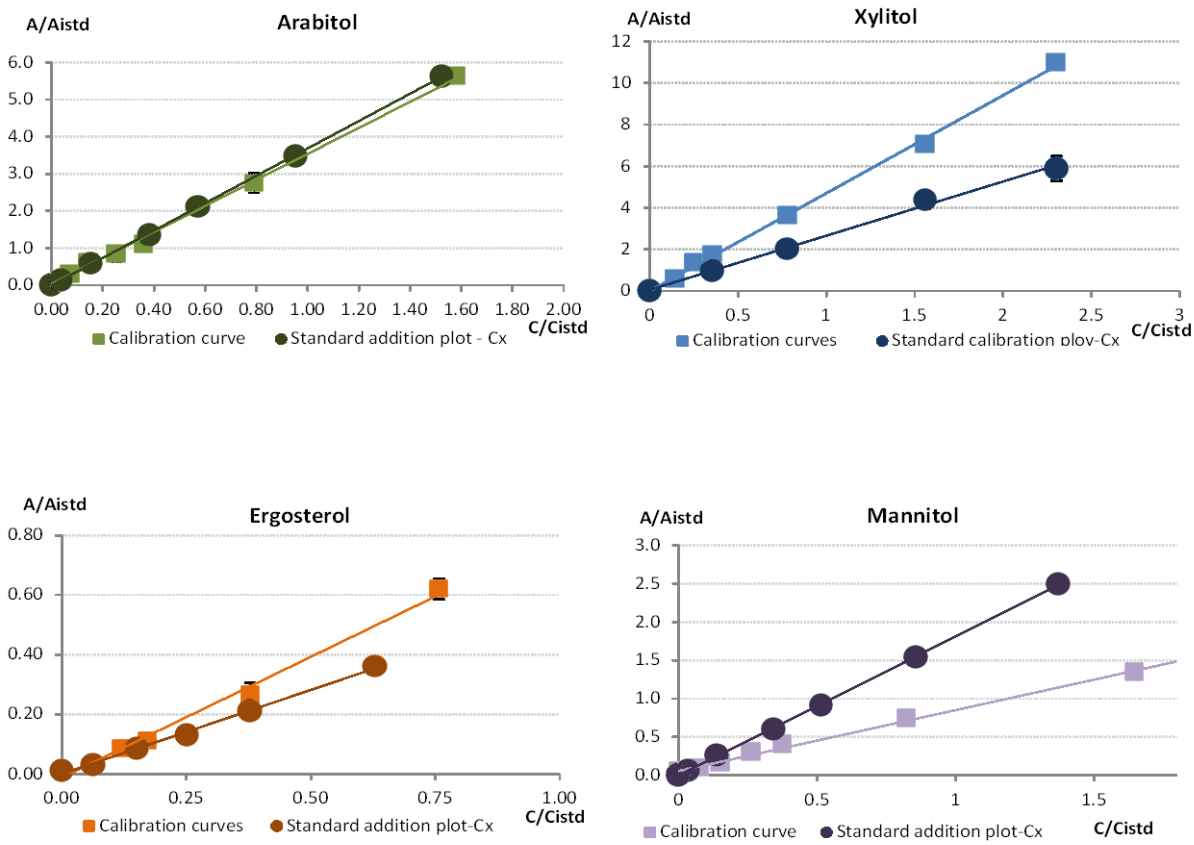

Figure 4.1.2.4.a.: Comparison of the calibration curves and the standard addition plots-Cx of arabitol (PLOT2), xylitol (PLOT1), ergosterol (PLOT2) and mannitol (PLOT2). A/Aistd is the ratio of the areas of the analyte to that of the internal standard; C/Cistd is the ratio of their concentrations.

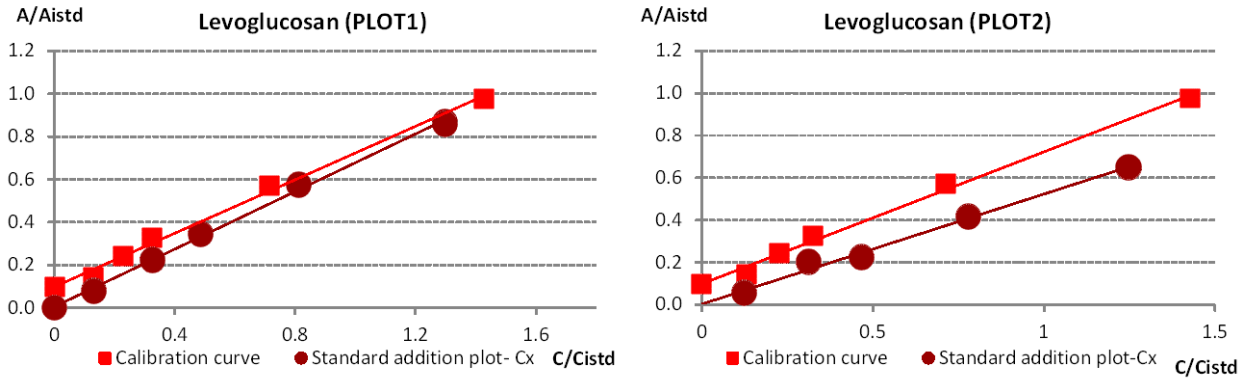

A B

Figure 4.1.2.4.b.: Comparison of the standard calibration curve and the standard addition plots-Cx for levoglucosan. A calibration curve vs PLOT1; B calibration curve vs PLOT2. A/Aistd is the ratio of the areas of the analyte to that of the internal standard; C/Cistd is the ratio of their concentrations.

4.1.2.5. Consistency of the results obtained for Levoglucosan

Levoglucosan mass concentration in SRM 1649a samples was already measured and published by other authors by using different methods of extraction and analysis [Harrison et. al 2012; Kuo et al. 2008; Larsen et al. 2006; Louchouarn et al. 2009; Orasche et al. 2011]. In Kuo, Larsen and Louchouarn studies the samples were extracted via pressurized fluid extraction (PFE) with an accelerated solvent extractor (Dionex ASE 200), the first one using a mixture of methylene chloride (DCM) – methanol (90:10), the other two ethyl acetate and both mixtures. Soxhlet extraction was also used by Larsen with a mixture of DCM : acetone (80:20). In Harrison and Orasche the sample extraction was carried out in an ultrasonic bath with respectively DCM and DCM/methanol (1:1, v/v). In all the studies reported the derivatization process was carried out using BSTFA containing 1% TMCS. Only Harrison used a second silylation mixture containing 99% of N-methyl-N-trimethylsilyltrifluoroacetamide (MSTFA) and 1% TMCS. The analysis of samples extracted was carried out in GC/MS o GC/MS-MS, except in Orasche study in which it was carried out with IDTD-GC-TOFMS.

In the present work, levoglucosan concentrations obtained (173.3 ± 27.7 μg g^{-1} and 160.3 ± 16.2 μg g^{-1}) agreed with those reported by Larsen et al. (2006) (162 ± 8 μg g^{-1}, freezer-stored samples-(b)), Kuo et al. (2008) (163.9 ± 11.8 μg g^{-1}), Orasche et al. (2011) (165.0 ± 0.8 μg g^{-1}), and Louchouarn et al. (2009) (160.5 ± 4.7 μg g^{-1}) who also analyzed SRM 1649b samples (160.5 ± 5.0 μg g^{-1}) (Fig. 4.1.2.5.a.). SRM

1649b is a recertification of SRM 1649a recently performed after sieving through a 63 μm sieve. Higher standard deviations observed in the present study can be considered acceptable since the method of standard additions is an extrapolation method, and it is generally less precise than interpolation technique that was used by all the other authors [Miller and Miller, 1993].

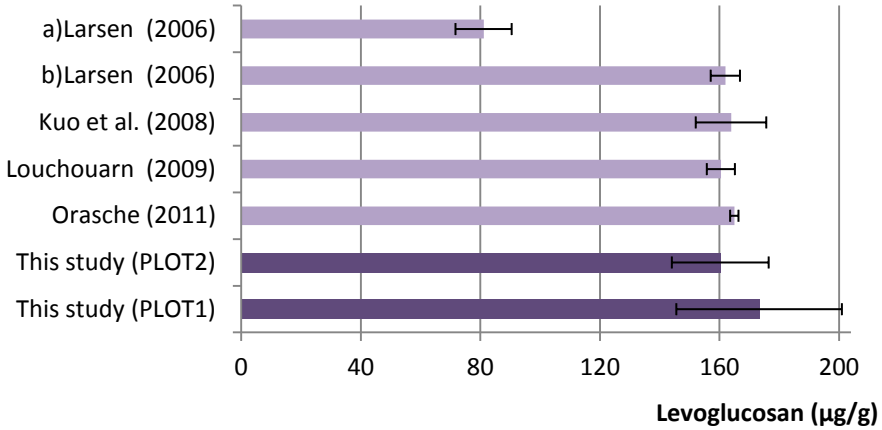

Figure 4.1.2.5.a.: Comparison among levoglucosan mass concentrations in SRM 1649a obtained in this and in other studies (Larsen 2006 (a) refers to a sample stored at room temperature; Larsen 2006 (b) to sample freezer stored)

Results obtained from 2006 to today suggest that levoglucosan can be reproducibly extracted from particulate matter samples under different laboratory conditions and encourage the potential use of SRM 1649a and SRM 1649b as working standards for levoglucosan analysis with an updated reference value of 163.6 ± 4.6 μg g^{-1}, obtained as average between the five comparable studies (see Fig. 4.1.2.5.a.), including Larsen et al. (2006) (for the freezer-stored sample).

Lastly, standard addition curves, shifted to the origin, for the quantitation of unknown samples were suggested for all the analytes except for arabitol.

Accordingly we applied the present method to PM samples collected in Rome during four seasonal sampling campaigns and compared the ratios between annual analyte concentrations in PM_{10} samples with those measured in SRM 1649a.

4.1.3. Aerosol sampling

Outdoor particulate matter PM_{10} was collected in a mixed sub-urban/rural area, fifteen kilometers South-East from the city center of Rome [Latitude 41°50'22"N; Longitude 12°38'50"E], with the dual channel sampler and in downtown Rome, 2.6 kilometers East from the very city center [Latitude 41°54'5"N; Longitude 12°30'50"E], with the low pressure multistage impactor [Di Filippo et al., 2013].

As regard the dual channel sampler, the sampling time for each PM_{10} sample was 24 hours, with a final volume of sampled air equal to about 55 Nm^3.

As regard the multistage impactor, for each urban campaign, the sampling time was about ten days, with a final volume of sampled air equal to about 140 Nm^3, necessary to collect on each of the thirteen filters enough amount of sample to reach the detection threshold of the chemical analysis [Di Filippo et al., 2010]. The sum of the results from the thirteen size fractions was calculated to obtain PM_{10} concentrations. They were compared with the daily results of the dual channel sampler, averaged for an entire seasonal sampling period.

The comparison between the results obtained from the two different samplers was believed feasible after a PM collection carried out in parallel with both of them. In only one sampling campaign (April 13–22) a second dual channel sampler was run simultaneously with the multistage impactor in downtown Rome (Fig. 4.1.3.a.), and the comparison between results showed good agreement.

Figure 4.1.3.a.: HYDRA-Dual Sampler *and DLPI- Dekati in parallel in the sampling campaign of April, in downtown Rome*

Four seasonal sampling campaigns on July-August (sampling days 31 July and 1-2-3-7-11 August), December (from 4th to 11th); April (from 13th to 20th), October (from 20th to 27th) were performed at the suburban/rural site and four seasonal sampling campaigns were carried out at the urban site with two partly time-overlapped campaigns in April and October: 13–22 April, 14–27 October, 27 December–10 January, and 25 July–4 August.

During all the sampling periods, the filter housing temperature was maintained at 15 °C by a cooling system and the filters were protected from sunlight, to avoid any possible degradation.

Both the samplers were equipped with PTFE filters (respectively 47 and 25 mm of diameter and 0.2 and 0.45 μm of porosity). The sampled filters were stored in aluminium foils in refrigerator. A total of thirty-six and fifty-two filters were respectively processed for the sub-urban/rural and urban outdoor sites. They were weighed before and after the collection, after conditioning for twenty-four hours in a chamber maintained at 40% relative humidity and 20 degrees Celsius.

4.1.4. Aerosol analysis

Following the method described above, all the eighty-eight samples were analyzed for ergosterol, arabitol and mannitol. The size-segregated samples were also analyzed for levoglucosan and xylitol, as tracers for biomass burning.

4.1.5. Biomarkers concentrations in particulate samples

PM_{10}-associated ergosterol, arabitol and mannitol concentrations obtained in April campaign from the average of nine samples collected with the dual channel sampler and the sum of the thirteen size fraction samples, collected in parallel with the low pressure multistage impactor in downtown Rome, were compared. The results were respectively 25.4 and 24.5 ng m^{-3} for arabitol, 16.3 and 15.1 ng m^{-3} for mannitol, and 0.09 and 0.08 ng m^{-3} for ergosterol. Although this test cannot be considered exhaustive and it is not a formal intercomparison, it does seem to exclude the hypothesis of any loss due to a longer sampling time of a sampler with respect to the other. In addition, as far as uncertainties regarding potential losses of ergosterol due to longer measurements are concerned, Mille-Lindblom [2004] reported the persistence of ergosterol in eventually 'not survived' fungi.

The results from all measurement campaigns (Tab. 4.1.5.α. and 4.1.5.β.) showed that biomarker concentrations at the suburban/rural site (Tab. 4.1.5.α.) ranged: arabitol from 1.7 to 39.2 ng m^{-3}; mannitol from 6.3 to 42.1 ng m^{-3}; and ergosterol from 0.07 to 1.54 ng m^{-3}. Lau, Bauer and Burshtein reported comparable values respectively in Hong Kong, Austria and Israel [Lau et al., 2006; Bauer et al., 2008a; Burshtein et al., 2011]. PM_{10} biomarker concentrations at the urban site (Tab. 4.1.5.β.) ranged: arabitol between 4.9 and 48.8 ng m^{-3}, mannitol between 13.5 and 49 ng m^{-3}, ergosterol between 0.08 and 0.26 ng m^{-3}. Unlike the other authors, at this site we observed higher values of arabitol concentrations compared to mannitol concentrations, and very low concentrations of ergosterol.

As far as the size-segregated results at the urban site are concerned, the two polyol concentrations and trends were similar, as shown in table 4.1.5.β. Both showed a unimodal trend in July-August and a trimodal trend in the other seasons, with two small peaks in the fine fraction (particles with aerodynamic diameter less than 1 μm) and one in the coarse one (particles with aerodynamic diameter higher than 1 μm). Even if the concentrations were always higher in the coarse mode except for mannitol in December–January, they also distributed in fine fraction.

On the contrary, for ergosterol, not only were its concentrations much lower but the trend was different in all the seasons and the main peaks were always shifted toward the previous stage with respect to the two sugar polyols, that is 2.5 μm in April, October and December–January and 4.4 μm in July–August. In addition, it never distributed in fine fraction except for the stages 0.4–1 μm in October.

Sub-urban/ rural site	ng /m^3 (Mannitol)	ng /m^3 (Arabitol)	ng /m^3 (Ergosterol)	μgPM_{10}/m^3
		July-August		
31-Jul	12.13	6.80	0.07	32
1-Aug	15.17	10.04	0.13	27
2-Aug	11.26	6.85	0.16	29
3-Aug	11.36	8.37	0.11	31
7-Aug	n.d.	n.d.	0.20	26
11-Aug	11.61	9.30	0.15	30
mean	12.31	8.27	0.14	29
		December		
4-Dec	22.01	39.22	0.73	17
5-Dec	30.95	31.46	0.58	37
6-Dec	32.13	20.99	0.72	70
7-Dec	42.08	17.11	0.48	73
8-Dec	25.52	22.16	0.55	38
9-Dec	15.54	10.00	0.40	28
10-Dec	36.13	10.15	0.33	34
mean	29.19	21.59	0.54	42
		April		
13-Apr	20.81	9.18	0.23	25
14-Apr	20.19	11.05	0.25	27
15-Apr	6.28	1.72	0.29	35
16-Apr	12.56	4.33	0.18	35
17-Apr	28.28	8.79	0.21	39
18-Apr	23.51	15.42	0.27	40
19-Apr	22.31	20.88	0.44	29
mean	19.13	10.20	0.27	33
		October		
20-Oct	24.70	8.16	0.32	34
21-Oct	30.67	15.77	0.53	45
22-Oct	23.54	12.13	0.49	39
23-Oct	27.74	14.93	0.53	36
24-Oct	23.06	21.71	0.83	21
25-Oct	30.52	38.93	1.54	21
26-Oct	20.21	14.40	1.09	31
mean	25.78	18.01	0.76	32

Table 4.1.5.α.: PM_{10} and fungal biomarker concentrations in samples collected at sub-urban/rural site, in July-August and December, April and October. The standard deviations never exceed 1.5%

April														
d50%	0.03	0.06	0.10	0.17	0.24	0.40	0.65	1.0	1.6	2.5	4.4	6.8	10.0	PM_{10}
µg PM/m^3	0.16	0.47	0.66	1.25	1.97	4.16	2.71	1.29	1.51	2.57	3.15	3.33	1.92	25.15
ng /m^3 (mannitol)	n.d.	0.02	1.52	0.38	0.69	0.76	0.55	0.53	0.80	1.97	3.72	1.47	2.71	15.14
ng /m^3 (arabitol)	n.d.	n.d.	n.d.	0.01	0.28	0.32	0.53	0.48	5.76	6.44	6.83	2.27	1.58	24.49
ng /m^3 (ergosterol)	n.d.	n.d.	n.d.	n.d.	n.d.	n.d.	n.d.	0.01	0.01	0.01	0.01	0.02	0.01	0.08
October														
d50%	0.03	0.06	0.10	0.17	0.24	0.40	0.65	1.0	1.6	2.5	4.4	6.8	10.0	PM_{10}
µg PM/m^3	0.17	0.44	0.76	0.81	0.97	2.43	1.91	1.38	1.58	2.51	3.23	3.19	3.07	22.45
ng /m^3 (mannitol)	n.d.	n.d.	1.13	0.59	0.65	0.80	0.85	1.06	1.69	4.55	5.75	3.31	2.02	22.40
ng /m^3 (arabitol)	n.d.	n.d.	0.31	0.07	0.09	0.21	0.46	0.29	2.00	4.79	8.24	2.86	1.51	20.83
ng /m^3 (ergosterol)	n.d.	n.d.	n.d.	n.d.	n.d.	0.009	0.009	0.005	0.011	0.014	0.012	0.011	0.012	0.08
Dec-Jan														
d50%	0.03	0.06	0.10	0.17	0.24	0.40	0.65	1.0	1.6	2.5	4.4	6.8	10.0	PM_{10}
µg PM/m^3	0.47	1.34	1.56	4.95	3.93	6.21	4.27	2.07	1.64	1.88	1.93	0.86	0.56	31.67
ng /m^3 (mannitol)	0.25	0.39	0.46	1.28	1.41	2.46	2.18	0.55	0.91	1.09	1.26	0.92	0.32	13.47
ng /m^3 (arabitol)	0.03	0.11	0.02	n.d.	0.12	0.50	0.30	0.04	0.79	1.16	1.52	0.21	0.08	4.89
ng /m^3 (ergosterol)	n.d.	n.d.	n.d.	n.d.	n.d.	n.d.	n.d.	0.03	0.05	0.07	0.06	0.05	0.01	0.26
July-August														
d50%	0.03	0.06	0.10	0.17	0.24	0.40	0.65	1.0	1.6	2.5	4.4	6.8	10.0	PM_{10}
µg PM/m^3	0.25	0.74	1.17	1.76	0.88	2.65	1.12	1.14	1.79	3.30	4.80	7.42	6.13	33.17
ng /m^3 (mannitol)	0.86	0.70	0.73	0.75	0.78	0.80	1.02	1.24	2.38	5.99	11.86	12.44	9.44	48.99
ng /m^3 (arabitol)	n.d.	n.d.	n.d.	n.d.	0.03	0.04	0.17	0.69	2.88	10.30	15.37	15.32	3.98	48.77
ng /m^3 (ergosterol)	n.d.	n.d.	n.d.	n.d.	n.d.	n.d.	n.d.	0.007	0.009	0.014	0.021	0.018	0.015	0.09

n.d. : not detected

Table 4.1.5.β.: Size segregated PM and biomarker concentrations in samples collected at urban site in April and October, December-January and July-August. The standard deviations never exceed 4.5%

Pearson correlation coefficients were also calculated between PM fraction concentrations and their marker content (Tab. 4.1.5.γ.).

April			
	mannitol	arabitol	ergosterol
PM coarse	0.4	0.0	0.6
PM fine	0.1	0.3	n.d.
October			
	mannitol	arabitol	ergosterol
PM coarse	0.5	0.4	0.1
PM fine	0.0	0.4	n.d.
December-January			
	mannitol	arabitol	ergosterol
PM coarse	0.9	1.0	0.9
PM fine	0.9	0.7	n.d.
July-August			
	mannitol	arabitol	ergosterol
PM coarse	0.9	0.5	0.7
PM fine	-0.1	-0.3	n.d.

Table 4.1.5.γ.: Pearson correlation coefficients between fungal biomarker concentrations and coarse (n=5) and fine (n=8) PM concentrations.

We couldn't correlate ergosterol and PM with diameter less than 1 μm, because ergosterol was not detected in the finest fractions. Particles in the coarse fraction and ergosterol showed a good correlation, except in October. Mannitol correlated with coarse particulate both in winter and summer; arabitol correlated with coarse particulate only in winter. Both sugar polyols also correlated with the fine particles in winter.

Figure 4.1.5.a. shows the mannitol, arabitol and ergosterol percentage in the thirteen fractions of particulate matter sampled downtown, for each measurement campaign. It is noticeable that the distribution was dependent on the compound. As it was already confirmed, mannitol and arabitol distributed in fine fraction; in addition, mannitol even showed a high distribution in the ultrafine fraction (particles with aerodynamic diameter less than 0.1 μm).

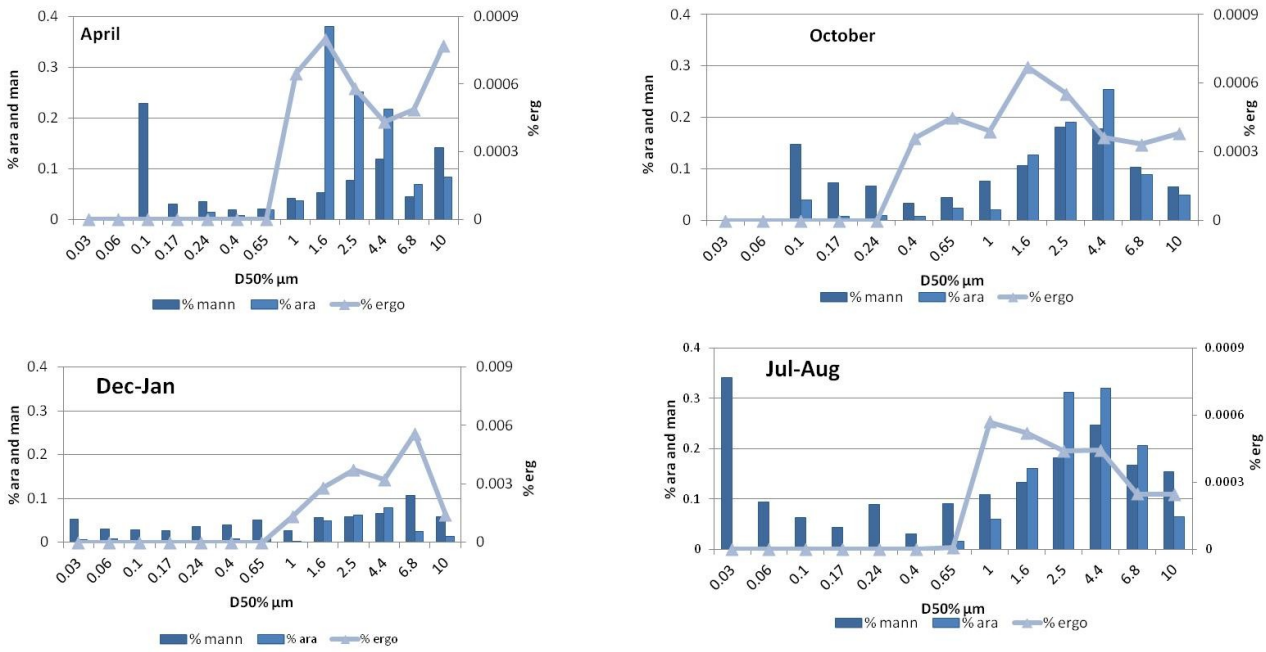

Figure 4.1.5.a.: Percentage of biomarkers in each PM size fraction, for each measurement campaign

All our observations would lead to the conclusion that the three biomarkers have different sources.

Burshtein reported that, during winter and summer in Israel, arabitol and mannitol didn't correlate with ergosterol and that arabitol and mannitol, although common in fungi, are frequently occurring sugar alcohols in plants [Graham et al., 2004; Burshtein et al., 2011]. Wan and Zhen (2007) also suggested that biomass burning and sea spray are also important sources of mannitol in PM fine fraction.

As far as the sugar alcohol emission by plants is concerned, the dominant vegetation type at our latitudes, for example the diffusive local presence of Fraxinus ornus, could explain part of the mannitol and arabitol concentrations in atmosphere.

To support the biomass burning as a further source of arabitol and mannitol, their concentrations were compared with xylitol and levoglucosan content in the same fractions of particulate (Fig. 4.1.5.b.). As expected, these last two compounds preferentially distributed into the fine fraction. In winter, when xylitol and levoglucosan showed their higher concentrations, the mannitol and arabitol percentage in the fine fraction was higher compared with the other seasons (respectively 67% and 23%). In addition, about 15% of the total amount of xylitol and levoglucosan was found in the coarse fraction, and this result might also explain part of arabitol and mannitol in the same fraction.

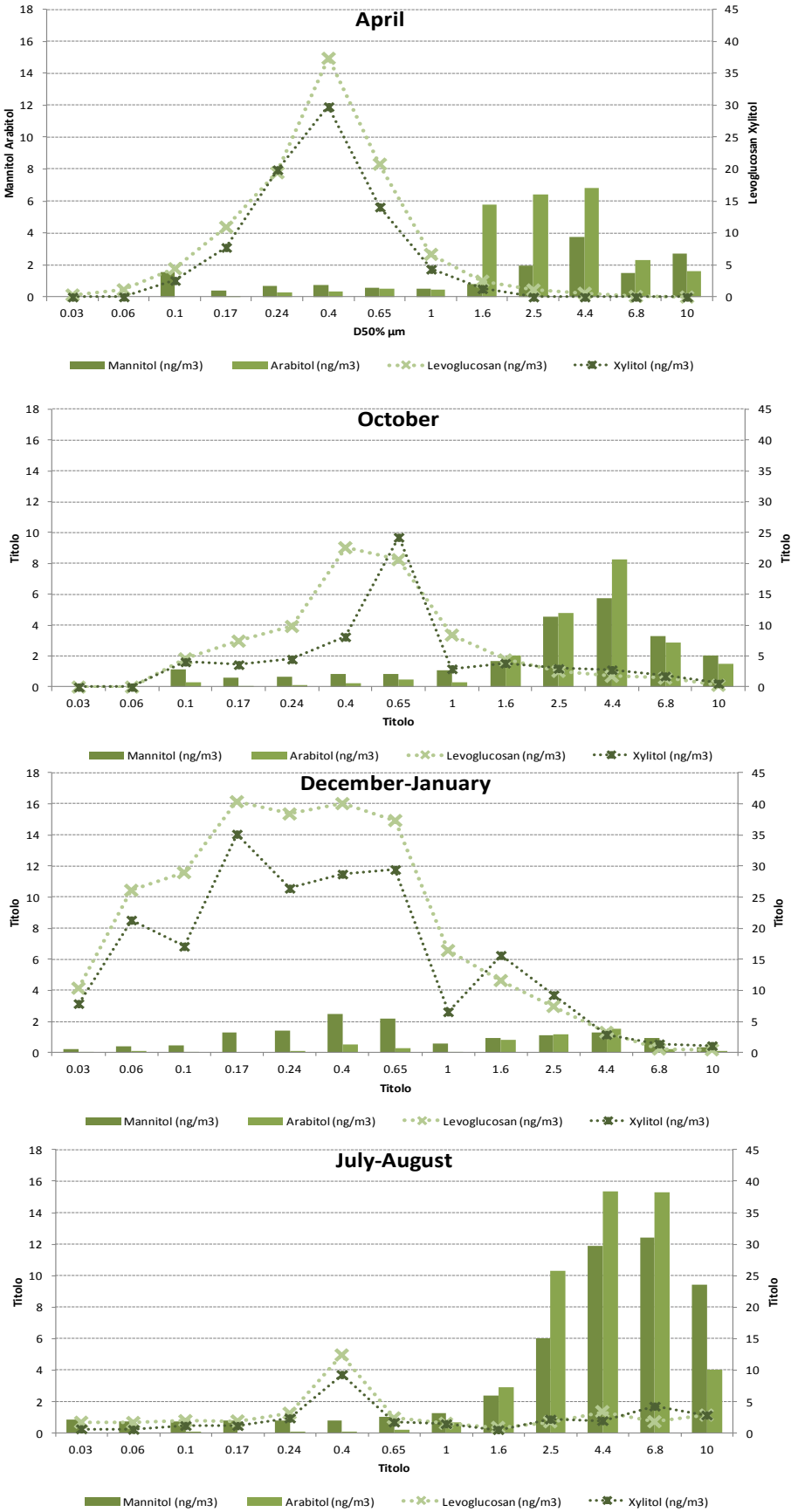

Figure 4.1.5.b.: Comparison among concentrations of arabitol, mannitol, levoglucosan and xylitol associated with size-segregated airborne particulate matter (ng m^{-3}) in four different seasons

As far as the other additional source suggested by Wan and Zhen is concerned, both the sampling sites are at less than 30 km from the sea and at the present latitudes, warm temperatures and increased solar radiation promote the development of sea breeze, causing transport of sea spray to the sampling sites. Consequently, higher arabitol and mannitol concentrations could be due to sea breeze conditions, more evident in the summer at the urban site.

4.1.6. Fungal concentrations in particulate samples

Starting from PM_{10} biomarker content, airborne fungal spore concentrations were obtained by applying, for mannitol and arabitol, Bauer conversion factors [Bauer et al., 2008b] respectively 1.7 pg of mannitol/spore and 1.2 pg of arabitol/spore and for ergosterol, Cheng conversion factor [Cheng et al., 2008a,b] 0.191 pg of ergosterol/spore. The fungal spore counts were then converted to mass, assuming an average mass of 65 pg per spore [Elbert, 2007]. The seasonal concentrations of fungal spores (μg m^{-3}) in samples collected at the sub-urban/rural and urban site are respectively summarized in tables 4.1.6.α. and 4.1.6.β.

Sub-urban/ rural site	μg spore /m^3 (Mannitol)	μg spore /m^3 (Arabitol)	μg spore /m^3 (Ergosterol)
		July-August	
31-Jul	0.46	0.37	0.02
1-Aug	0.58	0.54	0.04
2-Aug	0.43	0.37	0.05
3-Aug	0.43	0.45	0.04
7-Aug	n.d.	n.d.	0.07
11-Aug	0.44	0.50	0.05
mean	0.47	0.45	0.05
		December	
4-Dec	0.84	2.12	0.25
5-Dec	1.18	1.70	0.20
6-Dec	1.23	1.14	0.25
7-Dec	1.61	0.93	0.16
8-Dec	0.98	1.20	0.19
9-Dec	0.59	0.54	0.13
10-Dec	1.38	0.55	0.11
mean	1.12	1.17	0.18
		April	
13-Apr	0.80	0.50	0.08
14-Apr	0.77	0.60	0.08
15-Apr	0.24	0.09	0.10
16-Apr	0.48	0.23	0.06
17-Apr	1.08	0.48	0.07
18-Apr	0.90	0.84	0.09
19-Apr	0.85	1.13	0.15
mean	0.73	0.55	0.09
		October	
20-Oct	0.94	0.44	0.11
21-Oct	1.17	0.85	0.18
22-Oct	0.90	0.66	0.17
23-Oct	1.06	0.81	0.18
24-Oct	0.88	1.18	0.28
25-Oct	1.17	2.11	0.52
26-Oct	0.77	0.78	0.37
mean	0.99	0.98	0.26

Table 4.1.6.α.: Fungal concentrations from three biomarkers in PM_{10} samples collected at sub-urban/rural site, in July-August and December, April and October

Daily range data are reported for sub-urban/rural site (Tab. 4.1.6.α.) and size-resolved mass distributions, relating to nine-fourteen consecutive sampling days, are summarized for the urban site (Tab. 4.1.6.β.).

April														
d50%	0.03	0.06	0.10	0.17	0.24	0.40	0.65	1.0	1.6	2.5	4.4	6.8	10.0	PM10
μg spore/m^3 (mannitol)	0.000	0.001	0.058	0.015	0.026	0.029	0.021	0.020	0.031	0.075	0.142	0.056	0.104	0.58
μg spore/m^3 (arabitol)	n.d.	n.d.	n.d.	n.d.	0.015	0.017	0.028	0.026	0.312	0.349	0.370	0.123	0.086	1.33
μg spore/m^3 (ergosterol)	n.d.	n.d.	n.d.	n.d.	n.d.	n.d.	n.d.	0.003	0.004	0.005	0.005	0.006	0.005	0.03
October														
d50%	0.03	0.06	0.10	0.17	0.24	0.40	0.65	1.0	1.6	2.5	4.4	6.8	10.0	PM10
μg spore/m^3 (mannitol)	n.d.	n.d.	0.043	0.023	0.025	0.031	0.032	0.040	0.065	0.174	0.220	0.127	0.077	0.86
μg spore/m^3 (arabitol)	n.d.	n.d.	0.017	0.004	0.005	0.012	0.025	0.016	0.109	0.260	0.446	0.155	0.082	1.13
μg spore/m^3 (ergosterol)	n.d.	n.d.	n.d.	n.d.	n.d.	0.003	0.003	0.002	0.004	0.005	0.004	0.004	0.004	0.03
Dec-Jan														
d50%	0.03	0.06	0.10	0.17	0.24	0.40	0.65	1.0	1.6	2.5	4.4	6.8	10.0	PM10
μg spore/m^3 (mannitol)	0.009	0.015	0.018	0.049	0.054	0.094	0.083	0.021	0.035	0.041	0.048	0.035	0.012	0.52
μg spore/m^3 (arabitol)	0.002	0.006	0.001	n.d.	0.007	0.027	0.016	0.002	0.043	0.063	0.082	0.011	0.004	0.27
μg spore/m^3 (ergosterol)	n.d.	n.d.	n.d.	n.d.	n.d.	n.d.	n.d.	0.010	0.016	0.024	0.021	0.016	0.003	0.09
July-August														
d50%	0.03	0.06	0.10	0.17	0.24	0.40	0.65	1.0	1.6	2.5	4.4	6.8	10.0	PM10
μg spore/m^3 (mannitol)	0.033	0.027	0.028	0.029	0.030	0.031	0.039	0.047	0.091	0.229	0.453	0.475	0.361	1.87
μg spore/m^3 (arabitol)	n.d.	n.d.	n.d.	n.d.	0.001	0.002	0.009	0.037	0.156	0.558	0.833	0.830	0.216	2.64
μg spore/m^3 (ergosterol)	n.d.	n.d.	n.d.	n.d.	n.d.	n.d.	n.d.	0.002	0.003	0.005	0.007	0.006	0.005	0.03

n.d. : not detected

Table 4.1.6.β.: Fungal concentrations from three biomarkers in PM_{10} samples collected at urban site in April, October, December-January and July-August

At the suburban/rural sampling station, fungal amounts obtained from mannitol and arabitol through their conversion factors were better comparable in July–August, December, and October, but scarcely in April; in addition, they were higher by about one order of magnitude than those obtained from ergosterol through its conversion factor.

The Sub-urban/rural discordance between the three data sets was even more marked for urban data. Fungal spores in urban PM_{10} from arabitol concentrations showed to

be even two times higher than those obtained from mannitol concentrations, except in December–January, and fungal spores from ergosterol concentrations proved to be very low in most of the thirteen filters of each sampling campaign.
These differences may be due to the possible additional emission sources of the two polyols, but also to the difficulty of identifying conversion factors representative of fungal population characterizing the atmosphere under study.

4.1.7. Biomarkers in fungal spores

In order to exclude the possibility that conversion factors found in literature were responsible for the discordant results found, we measured mannitol, arabitol and ergosterol concentrations in the spores of five fungal species, belonging to widespread airborne genera (Aspergillus, Cladosporium, Penicillium, Trichoderma, Alternaria), kindly provided by the Department of Plant Biology, University of Rome "Sapienza". The fungal spores had been cultivated on Sabouraud maltose broth medium for three days at 25°C. Cultures had then been transferred to glass test tubes, washed with water, and freeze-dried. The dried biomass of fungal spores of each fungal specie was extracted and analyzed for arabitol, mannitol and ergosterol.
Table 4.1.7.α. shows the concentrations (ng μg^{-1}) found, and standard deviations; the data presented are the averages from triplicate extractions.

ng/µg	Arabitol	Mannitol	Ergosterol	Percentage in atmosphere
Aspergillus	32.00 ± 6.66	72.10 ± 9.09	0.94 ± 0.18	1.2%
Cladosporium	7.50 ± 1.3	14.70 ± 2.3	3.72 ± 0.55	52.0%
Penicillium	7.00 ± 0.4	57.30 ± 3.3	2.06 ± 0.65	21.1%
Trichoderma	0.05 ± 0.001	56.00 ± 8.4	3.40 ± 0.04	1%
Alternaria	1.79 ± 0.11	26.10 ± 2.24	0.94 ± 0.09	1%
weighted average	7.6 ± 2.8	28.1±0.6	3.2 ± 1.1	76.3%

Table 4.1.7.α.: Arabitol, mannitol and ergosterol concentrations in fungal spores of five fungal genera

We assumed a fungal spore percent atmospheric abundance respectively of 1.2, 52.0, 21.1, 1.0, 1.0 % for listed fungi [Flückiger et al., 2000; Cheng et al., 2008-b; Codina et al., 2008] and calculated the conversion factors as a weighted average of marker concentrations obtained by processing each fungal spore portion as a sampled filter.
Since Cladosporium and Penicillium spores are more abundant in atmosphere than the other ones: 52 and 21.1 respectively (Tab. 4.1.7.α.), we chose to calculate the average of each biomarker, assigning more influence to these two fungal spores.

Therefore the weighted average (WA) was calculated according to the following formula:

$$WA = \frac{\sum B_i p_i}{\sum p_i}$$

where B_i is the i^{th} biomarker concentration and p_i is the i^{th} percentage.

To compare the so calculated factors (ng marker μg^{-1}) with the literature ones (pg marker/spore), these last factors were divided by 65 pg (average weight of one spore) and multiplied by 1000. While mannitol and ergosterol factors showed to be comparable (respectively 28.1 and 3.2 ng μg^{-1} for calculated factors and 26.2 and 2.9 ng μg^{-1} for literature factors), arabitol factors were very different (7.6 and 18.5 ng μg^{-1} respectively for calculated factor and literature factor).

Table 4.1.7.β. shows the comparison between the contribution of fungal component to particulate matter PM_{10} obtained from the three different biomarkers calculated with literature conversion factors and with the conversion factors found in our laboratory at the two sites.

Urban site	April			October			December-January			July-August		
	µg spore/m³	µg spore/m³	µg spore/m³	µg spore/m³	µg spore/m³	µg spore/m³	µg spore/m³	µg spore/m³	µg spore/m³	µg spore/m³	µg spore/m³	µg spore/m³
	mannitol	arabitol	ergosterol	mannitol	arabitol	ergosterol	mannitol	arabitol	ergosterol	mannitol	arabitol	ergosterol
PM_{10} literature factors	0.58	1.33	0.03	1.87	2.64	0.03	0.86	1.13	0.03	0.52	0.27	0.09
PM_{10} calculated factors	0.54	3.23	0.03	1.74	6.44	0.03	0.80	2.75	0.03	0.48	0.65	0.08

Suburban-rural site	July-August			December			April			October		
	µg spore/m³	µg spore/m³	µg spore/m³	µg spore/m³	µg spore/m³	µg spore/m³	µg spore/m³	µg spore/m³	µg spore/m³	µg spore/m³	µg spore/m³	µg spore/m³
	Mannitol	Arabitol	Ergosterol	Mannitol	Arabitol	Ergosterol	Mannitol	Arabitol	Ergosterol	Mannitol	Arabitol	Ergosterol
PM_{10} literature factors	0.47	0.45	0.05	1.12	1.17	0.18	0.73	0.55	0.09	0.99	0.98	0.26
PM_{10} calculated factors	0.44	1.09	0.05	1.04	2.85	0.17	0.68	1.35	0.08	0.92	2.38	0.24

Table 4.1.7.β.: Comparison between the contribute of fungal component to particulate matter PM_{10} obtained with the three different biomarkers calculated with literature conversion factors [Bauer et al., 2008b; Cheng et al., 2008a,b] and with conversion factors found in our laboratory

As expected by the comparison of factors, the fungal component values calculated from mannitol with the two different conversion factors and from ergosterol with its own conversion factors were comparable.

Fungal spore concentrations calculated from arabitol and our conversion factor were higher and caused a difference between fungal spore calculated from mannitol and those from arabitol even in the suburban-rural site. With the new factors all the fungal spore concentrations were different and again airborne fungal spores were different depending on the marker considered.

We concluded that conversion factors found in literature were not responsible for the discordant results found and that additional and even different sources of mannitol and arabitol caused an overestimation of fungal spore concentrations in the atmosphere.

In our opinion, ergosterol still remains the only possible fungal biomarker.

Lau [Lau et al., 2006] widely described the limitation of using ergosterol-to-biomass conversion factors for both the great variability of ergosterol contents depending on physiological status of the mycelia and the variety of ecosystems causing different fungal assemblages in atmosphere.

Similarly, Cheng [Cheng et al., 2008(a, b)] demonstrated that ergosterol content varies inter- and intra- species, and it also depends on the spore or cell surface area.

However, he also demonstrated that the empirical conversion factor he had calculated was robust and relatively constant despite the variability of ergosterol concentrations.

4.1.8. Fungal mass contribution to atmospheric particulate matter

Table 4.1.8.α. reports fungal spore content in PM_{10} calculated with our conversion factor from ergosterol concentration, temperature, relative humidity, PM_{10} and OC concentrations. As expected, temperature and relative humidity are respectively inversely and directly proportional to spore concentrations.

The higher percentage of fungal content in atmospheric particulate matter was found in the suburban/rural site, where fungal spores were more abundant in autumn when the high microbial activity, soil degradation, and degradation of leaves may cause re-suspension and spreading of spores into the atmosphere. These results agree with the study conducted by Lau [Lau et al., 2006].

		µg spores/m^3	T (°C)	Relative humidity %	PM_{10} µg/m^3	OC (28-34% in PM_{10}) µg/m^3
suburban/rural ergosterol	31 Jul-11 Aug	0.04	26	60	29	9
	4-10 Dec	0.17	11	74	42	13
	13-19 Apr	0.08	14	71	33	10
	20-26 Oct	0.24	15	80	32	10
urban ergosterol	13-22 Apr	0.03	14	77	33	10
	14-27 Oct	0.03	15	77	22	7
	27 Dec-10 Jan	0.08	7.4	81	32	10
	25 Jul-4 Aug	0.03	23	72	25	8

Table 4.1.8.α.: Spore concentrations obtained by ergosterol concentrations in PM_{10} and calculated conversion factor, temperature, relative humidity, PM_{10} concentrations and putative OC concentrations at two sampling sites

Even though fungal emission may consistently occur in summer, meteorological conditions concur to maintain low concentrations of aerosol constituents [Wan and Zhen, 2007].

In the two campaigns of April and October performed almost in the same period at the two sampling sites, the fungal spore concentrations were higher at suburban/rural location, as expected as well [Bauer et al., 2008b]. In particular, the October results at the suburban/rural site are particularly high because they are relative to six days with three days of rain.

Finally, assuming an average of 28-34 % of OC in PM_{10} [Perrino et al., 2009], table 4.1.8.β. shows the percentage (w/w) of spores found in PM_{10} and in its putative OC content in the sub-urban/rural atmosphere and in the urban site. Depending on the sampling site and on the season, between 0.1 and 0.8 % of PM_{10} and between 0.3 and 2.4 % of OC was constituted by fungal spores.

	sub-urban/rural site		urban site	
	% spore in PM10	% spore in OC	% spore in PM10	% spore in OC
Jul/Aug	0.2	0.5		
December	0.4	1.3		
April	0.3	0.8	0.1	0.4
October	0.8	2.4	0.1	0.4
Dec-Jan			0.3	0.8
Jul/Aug			0.1	0.3

Table 4.1.8.β.: Percentage (w/w) of fungal spores found in PM_{10} and in its putative OC content at two sampling sites

4.2. Mycotoxin determination in bioaerosol

4.2.1. Mycotoxin analytical determination

Determination of the presence of mycotoxins in human foods and animal feeding stuffs has been the subject of numerous studies, since exposure via ingestion is recognized to cause very serious adverse health effects [Moularat and Robine, 2008]. Many different techniques have been used for the extraction of mycotoxins from food matrices and for the subsequent purification of the extracts. Mycotoxin extraction from agricultural products is mainly performed by acetonitrile/water [Scudamore et al., 1997; Berger et al., 1999; Plattner, 1999; Razzazi-Fazeli et al., 1999; Razzazi-Fazeli et al., 2002; Laganá et al., 2003; Plattner and Maragos, 2003; Razzazi-Fazeli et al., 2003; Biselli et al., 2004; Dall'Asta et al., 2004; Royer et al., 2004; Sypecka et al., 2004; Berthiller et al., 2005a; Berthiller et al., 2005b; Biselli et al., 2005; Cavaliere et al., 2005; Klötzel et al., 2005; Labuda et al., 2005; Kokkonen and Jestoi, 2009] followed by a clean-up step by MycoSep or RP-8 or carbograph columns prior to analysis by HPLC with RP18 columns [Monbaliu et al., 2010], to remove matrix interferents, and fluorescence detection or detection by mass spectrometry. Molecularly Imprinted Polymers (MIPs) have been demonstrated to be very effective tools for the selective extraction of an analyte from a complex matrix such as a food product [Wei et al., 2007; Haginaka, 2009]. Expensive immunoaffinity columns (IACs) as clean-up tool are also used [Zöllner and Mayer-Helm, 2006].

Low volatility and thermal stability make gas chromatography/mass spectrometry (GC/MS) or /electron capture detection (GC/ECD) a not suitable technique.

Moreover, screening assays based on immunochemical methods are commercially available for aflatoxins, ochratoxin and zearalenone [Zöllner and Mayer-Helm, 2006].

There are, instead, few studies about mycotoxin presence in the atmosphere; and few studies have been conducted to document the occurrence of these substances in airborne dust [Hintikka et al., 2006]. In 1999, Sorenson suggested that airborne fungal spores contributed to the health effects in damp indoor environments; and elevated risks for cancer was believed to be due to inhalation of mycotoxin even if their presence in airborne dust was not demonstrated [Sorenson, 1999]. The relationship between cancer and the inhalation of mycotoxins has however been confirmed in very contaminated environments in agriculture or industry. In 1981

Burg sampled airborne dust in a plant where peanuts and linseed were processed for their oil. Aflatoxins B_1, B_2 and G_1 were chloroform extracted and analyzed by fluorescence of the spot on a thin-layer chromatographic plates of Adsorbosil-1 [Burg et al., 1981]. In 1984 Sorenson studied aflatoxin B_1 in respirable airborne peanut dust [Sorenson et al., 1984] by thin-layer chromatography. The presence of aflatoxin B_1 in airborne dust was demonstrated in some farms during harvest, animal feeding, and bin cleaning by means of liquid extraction, thin layer chromatography, and high pressure liquid chromatography [Selim et al., 1998]. Airborne aflatoxin generated in rice and maize processing plants was assayed by an indirect competitive enzyme-linked immunosorbent assay [Ghosh et al., 1997]. Trichothecene mycotoxins in dust samples from ventilation systems of office buildings were analysed by thin-layer chromatography (TLC) [Smoragiewicz et al., 1993]. After GC-MS analysis of trimethylsilylether derivatized extract solutions, low deoxynivalenol concentrations were found in dusts sampled in a Finnish farm during milling process [Lappalainen et al., 1996]. HPLC determinations of the ochratoxin A content were performed in dust samples collected from the heating ducts in a household [Richard et al., 1999]. Ochratoxin A was extracted from Norway dairy farm airborne dusts, with a mixture of methanol, chloroform, HCl, and water, purified on immunoaffinity column, and analysed by ion-pair HPLC with fluorescence detection [Skaug et al., 2000]. Mycotoxin contamination of building dust collected from mechanical ventilation systems was demonstrated [Hintikka et al., 2009]; Sudakin studied outdoor environments [Sudakin and Fallah, 2008]; Nielsen collected and analyzed pieces of building material [Nielsen, 2003]; while Tuomi analyzed moldy interior finishes from Finnish buildings with moisture problems [Tuomi et al., 2000]. The method included extraction, sample pre-treatment and reversed-phase HPLC separation followed by tandem mass spectrometric identification and quantification using electrospray ionization on a quadrupole ion trap mass analyser. Aqueous methanol was used in the initial extraction and SPE clean-up step [Tuomi et al., 1998]. Furthermore, air samples collected from work places where cocoa, coffee and spices are processed, were extracted with methanol/water and after a clean-up step by immunoaffinity columns analyzed by HPLC with fluorescence detection with postcolumn derivatisation with pyridine-hydrobromide perbromide [Brera et al., 2002]. Finally an enzyme-linked

immunosorbent assay was used to detect mycotoxins in PM_1 collected in water-damaged buildings [Brasel et al., 2005].

4.2.2. Optimization of mycotoxin analytical method

A HPLC/MS-MS method was developed to simultaneously analyze aflatoxin B1, ochratoxin A, toxin T-2, zearalenon and sterigmatocystin in airborne particulate matter, subordinately to the presence of fungal spore in the same samples.

The development of the analytical method included:

. ESI-MS/MS experiments;

. optimization of mycotoxin separation by HPLC;

. analysis of mycotoxins by HPLC-MS/MS in the multiple reaction monitoring (MRM) mode;

. optimization of extraction, purification and pre-concentration;

. preparation of standard and matrix-matched calibration curves;

. sampling;

. application of the proposed method to the analysis of the collected samples.

4.2.2.1. ESI-MS/MS experiments

In order to achieve the highest possible sensitivity and to find the specific MS-MS transitions of the five mycotoxins, the instrument parameters, such as ion source voltage (ISV), declustering potential (DP), focusing potential (FP) and collision energy (CE) were optimized by direct continuous pump infusion of standard solutions of the analytes at 2.5 ng μL^{-1}, at a flow rate of 10 $\mu L\ min^{-1}$, in both full and product ion scan. Experiments were carried out under positive and negative polarity with different additives in order to improve ionization efficiency. The best results were obtained operating with ammonium formate 4.32 mM in positive ion mode for all compounds, except for Ochratoxin A, more efficiently ionized in negative ion mode. Ammonium $[M + NH_4]^+$ adduct was used as precursor ion for T2 toxin; $[M - H]^-$ for Ochratoxin A, and protonated $[M + H]^+$ molecular ions for all the other compounds. Full scan ESI-Q1 and their respective MS-MS spectra are shown in figures 4.2.2.1.a.b.c.d.e. Table 4.2.2.1.α. shows the mass spectrometer operating conditions found for the five analytes. The most intense product ions for each analyte were chosen for the following analysis in MRM mode.

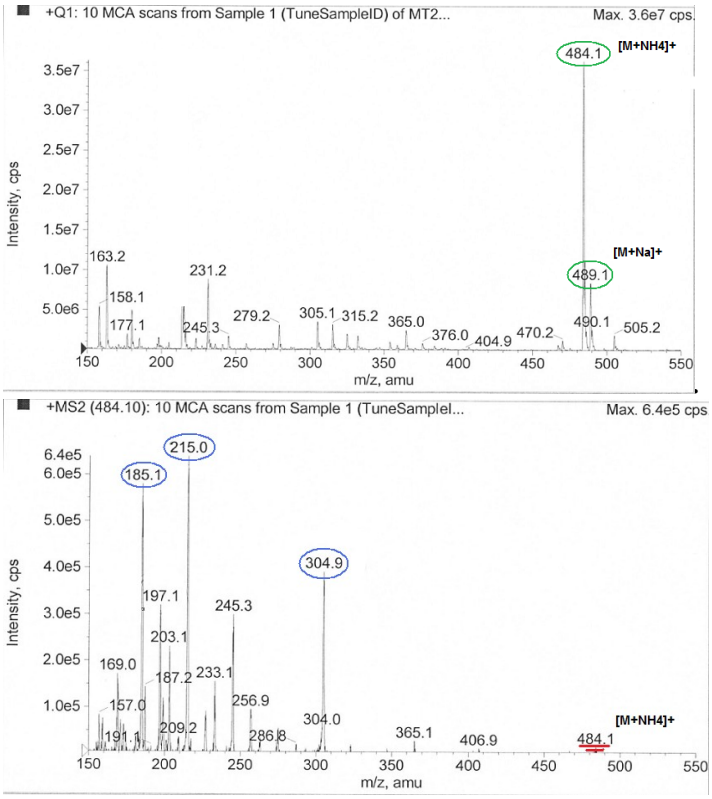

Figure 4.2.2.1.a.: Positive ESI-Q1 and MS-MS full scan spectra for T2 toxin; infusion 10 µL min^{-1} at concentration 2.5 ng µL^{-1}; parameters as in table 4.2.2.1.α.

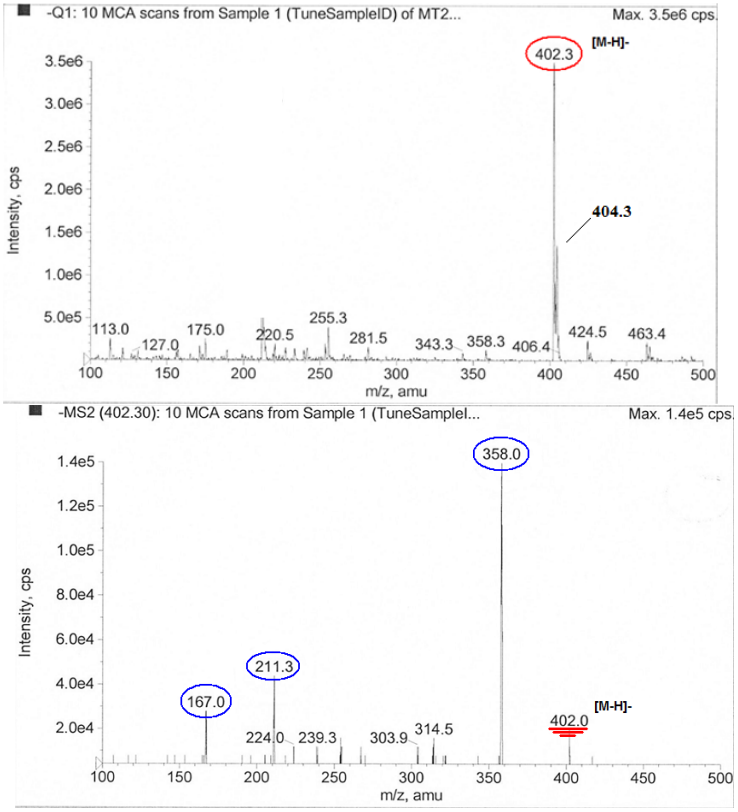

Figure 4.2.2.1.b.: Negative ESI-Q1 and MS-MS spectra for Ochratoxin A; infusion 10 µL min^{-1} at concentration 2.5 ng µL^{-1}; parameters as in table 4.2.2.1.α.

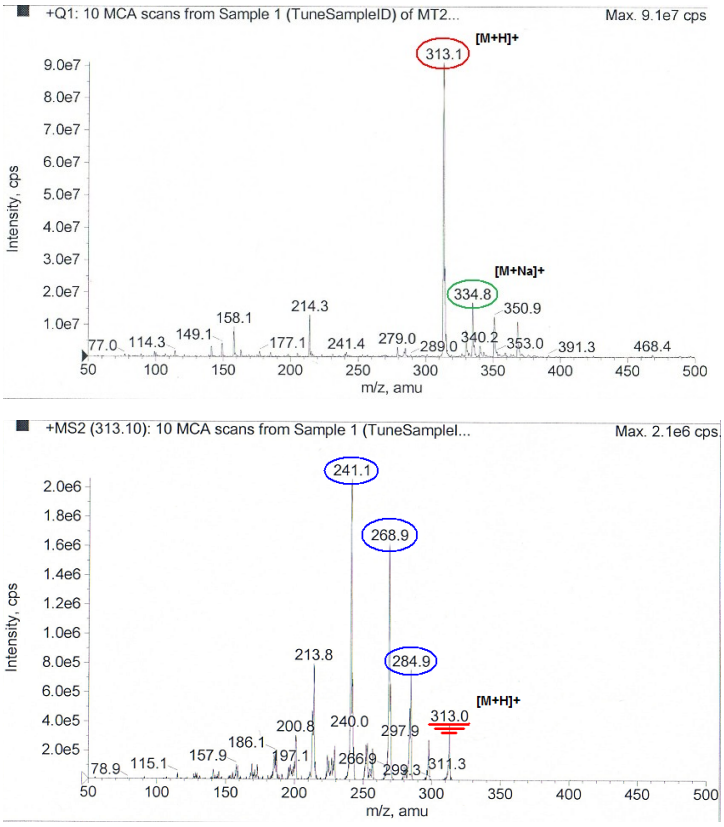

Figure 4.2.2.1.c.: Positive ESI-Q1 and MS-MS spectra for Aflatoxin B_1; infusion 10 µL min^{-1} at concentration 2.5 ng $µL^{-1}$; parameters as in table 4.2.2.1.α.

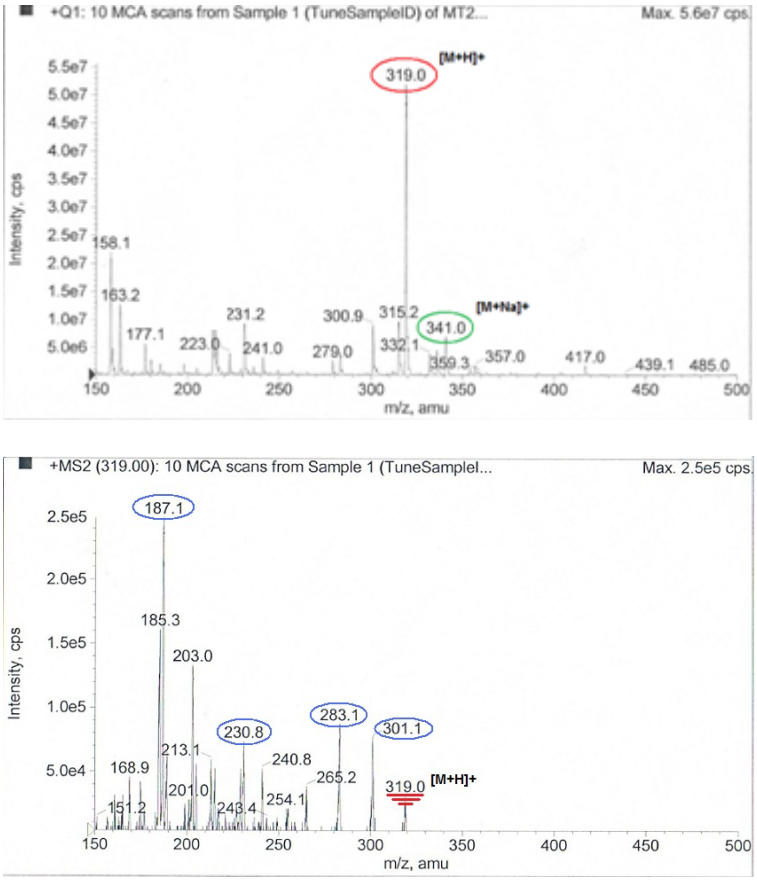

Figure 4.2.2.1.d.: Positive ESI-Q1 and MS-MS spectra for zearalenone; infusion 10 µL min^{-1} at concentration 2.5 ng µL^{-1}; parameters as in table 4.2.2.1.α.

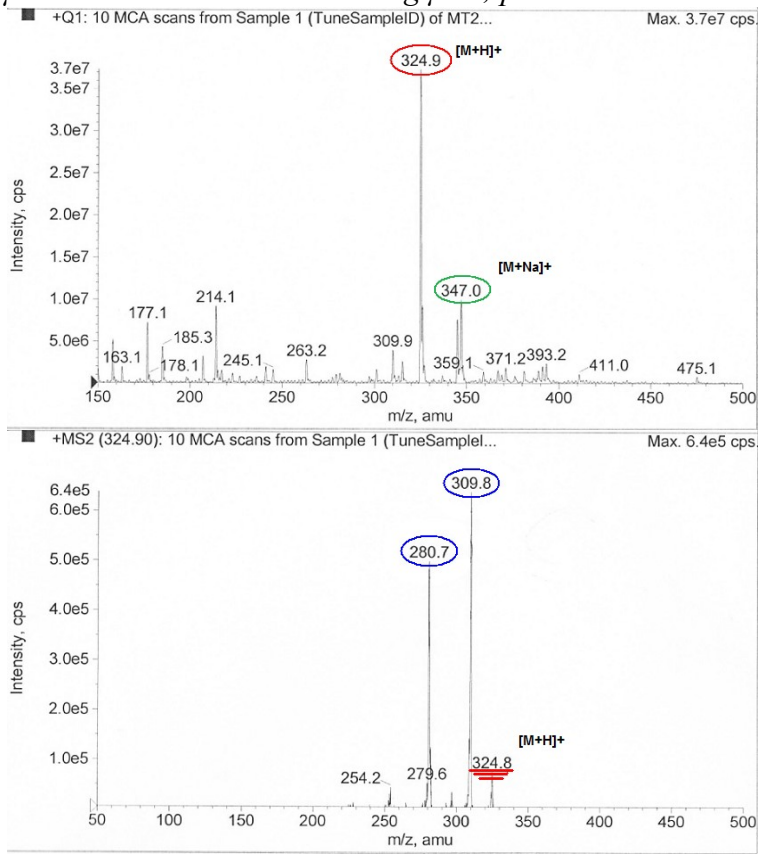

Figure 4.2.2.1.e.: Positive ESI-Q1 and MS-MS spectra for sterigmatocystin; infusion 10 µL min^{-1} at concentration 2.5 ng µL^{-1}; parameters as in table 4.2.2.1.α.

Ion Source	**Turbo Spray**				
	Aflatoxin B_1	Ochratoxin A	T2 toxin	Zearalenone	Sterigmatocystin
Curtain Gas (CUR)	15	15	30	20	20
Collision Gas (CAD)	5	3	2	2	4
IonSpray Voltage (IS)	5500	-3500	5500	5500	5300
Temperature (TEM)	400	400	400	400	400
Ion Source Gas1 (GS1)	18	26	10	10	30
Ion Source Gas2 (GS2)	20	20	20	20	20
Interface Heater (IHE)	On	On	On	On	On
Declustering Potential (DP)	50	-20	20	40	63
Focusing Potential (FP)	240	-400	400	150	370
Entrance Potential (EP)	10	-10	9	10	9
Collision Energy (CE)	45	-30	30	30	40
Collision Cell Exit Potential (CXP)	15	-15	15	15	35

Table 4.2.2.1.α.: Mass spectrometer operating conditions for the five mycotoxins

4.2.2.2. Optimization of mycotoxin separation by HPLC

Liquid chromatography was performed with a C18 Supelco Discovery (5 cm * 2.1 mm, 5 µm) fitted with its guard column. The mobile phase used was: water and methanol, both containing ammonium formate 4.32 mM. In the chromatographic run, at a flow rate of 200 µL min^{-1}, a linear gradient was applied reaching 100% methanol in 10 min, from an initial H_2O/MeOH ratio of 45:55. The analyses were carried out by LC/ESI-MS/MS in multiple reaction monitoring (MRM) mode to obtain high specificity and sensitivity. All the mycotoxins were eluted in 8 minutes.

Figure 4.2.2.2.a. shows the MRM chromatogram (TICs) of a standard solution of the five mycotoxins in the concentration of 1 µg mL^{-1}.

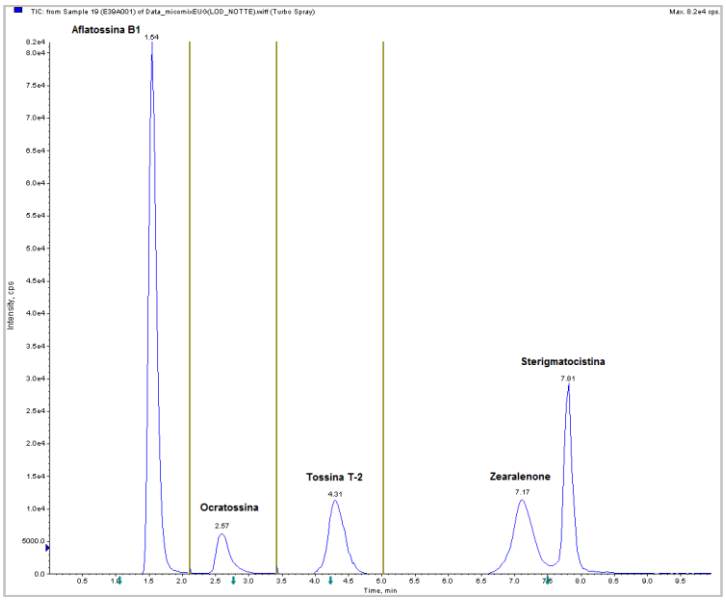

*Figure 4.2.2.2.a.: TIC HPLC-MS/MS in MRM mode of a solution of five mycotoxins at concentration of 1µg mL^{-1}. Column C18 Supelco Discovery (5 cm * 2.1 mm, 5 µm). Conditions as in tables 4.2.2.1.α. and 4.2.2.2.α.*

The most intense transitions for each mycotoxin are listed in table 4.2.2.2.α.

MYCOTOXINS	PRECURSOR ION	FRAGMENT IONS	RT
Aflatoxin B_1	313.1	284.9, 268.9, 241.1	1.5 min
Ochratoxin A	402.3	358.0, 211.3, 167.0	2.6 min
T-2 Toxin	484.1	304.9, 215.0, 185.0	4.3 min
Zearalenone	319.0	301.1, 283.1, 230.8, 187.1	7.2 min
Sterigmatocystin	324.9	309.8, 280.7	7.8 min

Table 4.2.2.2.α.: Quantifier (underlined mass fragments) and qualifier MRM transitions for each mycotoxin and their Retention Times (RT)

4.2.2.3. Standard calibration curves

Standard calibration curves were obtained by triplicate injections of 2 µL of five standard solutions containing mycotoxins at increasing concentrations from an initial concentration ranging from 1 to 130 (depending on the mycotoxin) to a final concentration of 1000 ng mL^{-1}. Good linearity was obtained in the investigated concentration range for each mycotoxin, as demonstrated by the correlation coefficients (R^2 values) between 0.994 and 0.998 of calibration curves, whose equations are given in table 4.2.2.3.α.

The external standard method was used for the quantitation.

MYCOTOXIN	Calibration curve equations	R^2
Aflatoxin B1	y = 75.7x + 834.5	0.995
Ochratoxin A	y = 2.3x - 294.8	0.994
T-2 Toxin	y = 6.0x - 16.8	0.997
Zearalenone	y = 6.4x + 84.1	0.995
Sterigmatocystin	y = 45.5x + 327.9	0.998

Table 4.2.2.3.α.: Calibration curve equations of each mycotoxin and their respective R^2 values

4.2.2.4. Extraction and recovery

In order to optimize the extraction step, sampling filters spiked with 50 ng of each analyte were subjected to ASE extraction with different solvents. The best solvent mixture for extracting all the mycotoxins was acetonitrile/water = 90:10 (ACN/H_2O = 90:10) using two static cycles of extraction at the following ASE operative conditions: Heat up Time 5'; Static Time 5'; Flush volume 60 %; Purge Time 300 sec; Cycles 2; Pressure 1500 psi; T 100 °C. The extracted solutions were evaporated, reconstituted with 100 µL of H_2O/MeOH 50:50 and analyzed in HPLC/ESI-MS/MS in MRM, as described above. The recoveries, calculated from the standard calibration curves, are summarized in table 4.2.2.4.α.

We experimentally calculated the loss due to the evaporation step, that was less than 5%.

MICOTOXIN	RECOVERIES
Aflatoxin B_1	97%
Ocratoxin A	98%
T-2 Toxin	93%
Zearalenone	96%
Sterigmatocystin	95%

Table 4.2.2.4.α.: ASE extraction recoveries with ACN/H2O= 90:10 (RSD% by 7% n=3)

4.2.2.5. Clean up step and recoveries

In order to choose an SPE cartridge for the clean-up step, 50 ng of each mycotoxin have been deposited on a Strata X, a Strata C18-E, a Strata C18-M, and an Oasis HLB columns in triplicate. After conditioning with 4 mL of MeOH, and washing with 4 mL of H_2O the analytes were eluted first with 9 mL of MeOH/H_2O 90:10 V/V and then with 4.5 mL of ACN.

The collected fractions were evaporated to dryness under nitrogen stream and finally reconstituted with 100 μL of MeOH/H_2O 50:50 V/V.

The samples were analyzed in HPLC/ESI-MS/MS in MRM, as described above, and the recoveries were calculated from the standard calibration curves.

Strata C18-M provided the best recoveries for the target analytes, between 91% (sterigmatocystin) and 94% (ochratoxin A) with a CV%, calculated on three tests in parallel, less than 8%.

The block diagram of the optimized method is shown in Table 4.2.2.5.α.

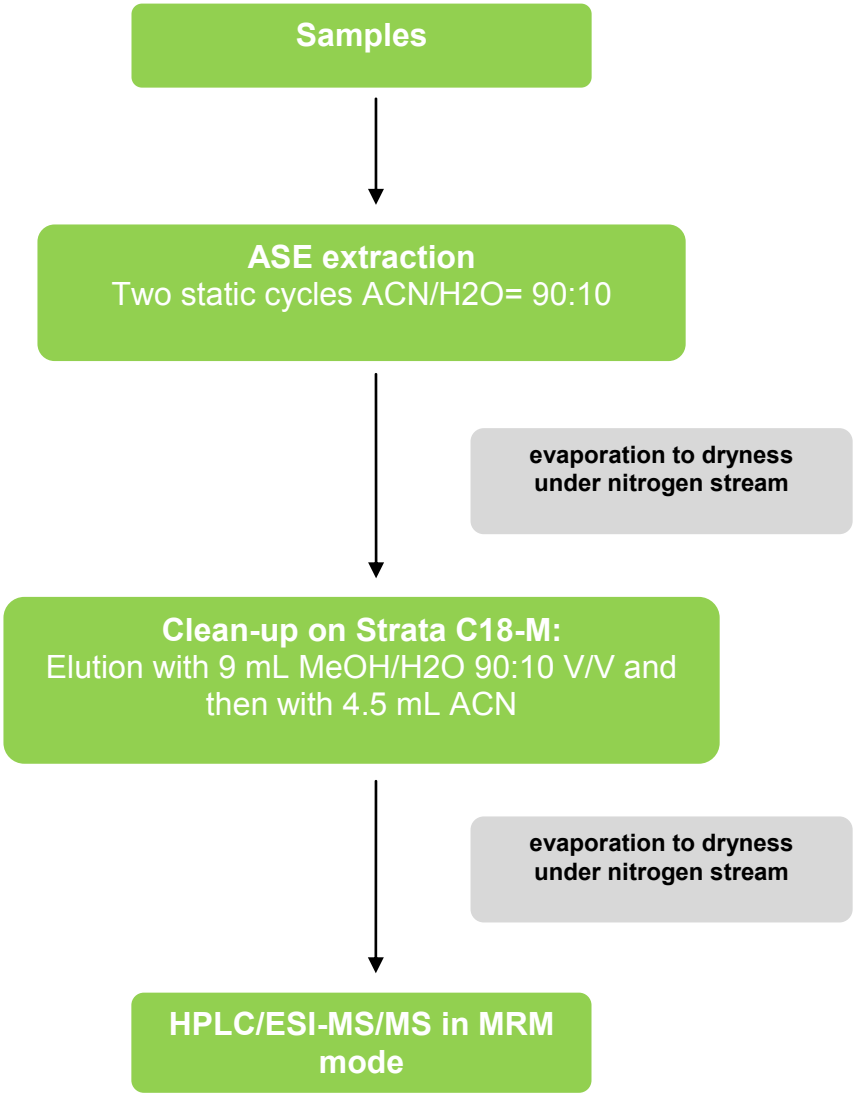

Table 4.2.2.5.α.: Block diagram of the method for extraction, purification and analysis of mycotoxins

4.2.2.6. Matrix-matched calibration curves

In order to simulate a real matrix, the Standard Reference Material NIST SRM 1649b, free of mycotoxins was chosen. This Material consists of an atmospheric particulate material collected in the Washington, DC area in 1976 and 1977. The particulate material has been collected over a period in excess of 12 months, so representing a time-integrated sample, and then passed through a 63 µm (230 mesh) sieve.

Matrix-matched calibration curves, referred to as "Post", were prepared by adding five filters with 1.5 mg of Standard Reference Material NIST SRM 1649b. After extraction, purification and evaporation, standard solutions ranging from about 1–250 to about 500–1000 ng mL^{-1} (depending on the mycotoxin), were spiked into the extracts.

The final solutions were then analyzed by HPLC/ESI-MS/MS in MRM mode. Matrix-matched calibration curve equations "Post" with the correlation coefficients (R^2 values) are shown in table 4.2.2.6.α.

In order to check interferences that may occur in the extraction and purification steps, matrix-matched calibration curves, referred to as "Ante", were also built starting from six aliquots of about 1.5 mg of SRM 1649b placed on sampling filters and spiked with standard solutions of increasing concentration of the analytes, before applying the whole procedure of Fig. 4.2.2.5.α. The first filter added with SRM aliquot was not spiked.

For all the curves, each solution was injected three times in HPLC/MS–MS and the regression model was applied to the calibration data set.

Matrix-matched calibration curve equations "Ante" with the correlation coefficients (R^2 values) are shown in table 4.2.2.6.α.

MICOTOXIN	MATRIX-MATCHED CALIBRATION CURVE EQUATIONS (post)	R^2	MATRIX-MATCHED CALIBRATION CURVE EQUATIONS (ante)	R^2
Aflatoxin B_1	y = 58.2x - 550.3	0.995	y = 21.6x + 921.1	0.987
Ochratoxin A	y = 1.9x - 188.9	0.993	y = 1.50x – 500.0	0.966
T-2 Toxin	y = 6.2x + 135.9	0.990	y = 4.5x + 265.6	0.988
Zearalenone	y = 6.1x - 14.1	0.990	y = 5x – 121.0	0.989
Sterigmatocystin	y = 50.7x - 766.9	0.995	y = 26.9x - 800.1	0.995

Table 4.2.2.6.α.: Matrix-matched calibration curve equations with the correlation coefficients (R^2 values)

The matrix effect was studied by comparing the different calibration curves (see figure 4.2.2.6 a).

Except for aflatoxin B_1, solution and matrix-matched calibration curve equations "Post" have a comparable slope for all mycotoxins. Therefore, it is reasonable to assume that no ion suppression occurs in the source of the mass spectrometer, possibly due to interfering compounds in the matrix.

All matrix-matched calibration curves "Ante" show a matrix effect, proportional to the increase of the concentration.

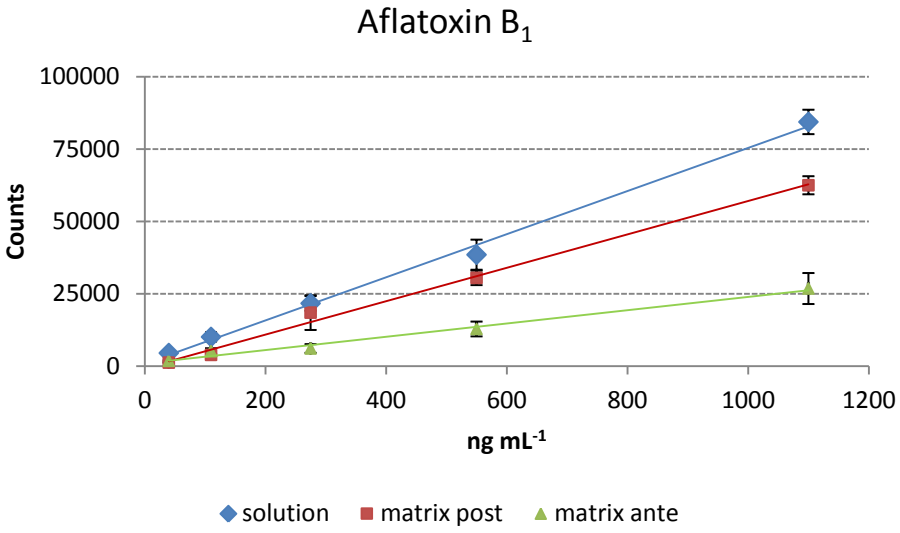

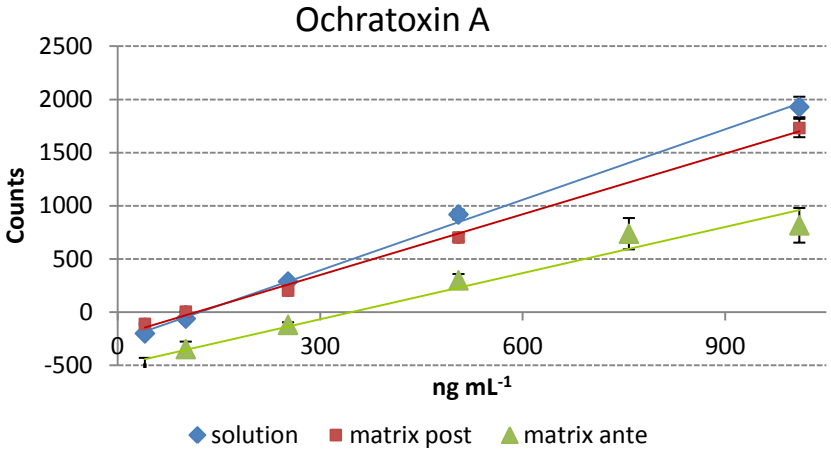

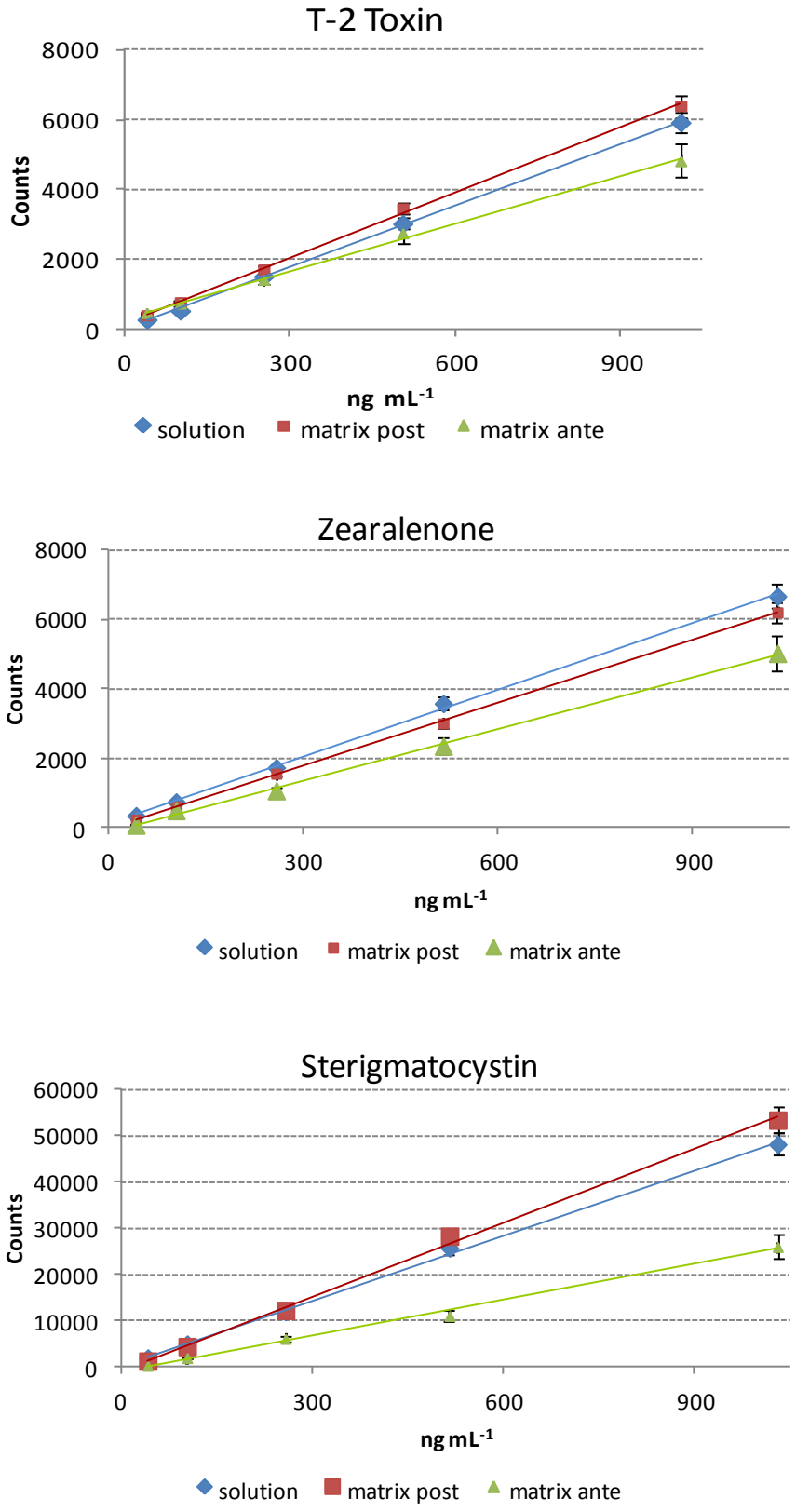

Figure 4.2.2.6.a.: comparison among solution and matrix-matched curves for the five mycotoxins.

4.2.2.7. Whole method recovery

Analytical method recovery in matrix was assessed by applying the whole procedure to three filters samples added with about 1.5 mg of SRM 1649b and fortified with 50 ng of each analyte. The samples were reconstituted with 100 µL of MeOH/H_2O 50:50 V/V. The total recoveries (extraction and purification) calculated after analysis by HPLC/ESI-MS/MS in MRM mode, from the matrix matched calibration curves "post", ranged between 40 and 80% (lower for aflatoxin B_1, ochratoxin A and sterigmatocystin and higher for T2 toxin and zearalenone), with a RSD% below 20%. Since analysis and recoveries of the simulated real samples were shown to be satisfactory, the optimized method was applied to analyze environmental samples.

4.2.2.8. LOD

The instrumental LODs are the lowest concentration of analyte which provides a signal significantly different from the background noise.

Instrumental detection limits, defined as the concentration of analyte injected producing a peak with a signal-to-noise ratio (S/N) of 3, ranged from 1 (aflatoxin) to 40 (ochratoxin A) ng mL^{-1} (Table 4.2.2.7.α). These values were extrapolated from the S/N of the respective peaks following an injection of the lowest standard concentration.

The limits of detection (LODs) in the matrix were calculated from the 99% confidence interval of the calibration curves and ranged from 6 ng mL^{-1} (T2 toxin) to 339 ng mL^{-1} (ochratoxin A) (Table 4.2.2.7.α).

MICOTOXIN	LOD in solution (ng μL^{-1})	LOD IN MATRIX (ng μL^{-1})
Aflatoxin B_1	0.001	0.009
Ochratoxin A	0.129	0.339
T-2 Toxin	0.003	0.006
Zearalenone	0.006	0.029
Sterigmatocystin	0.003	0.031

Table 4.2.2.7.α.: LOD values in ng μL^{-1} for mycotoxins in solution and in matrix

4.2.3. Mycotoxins in samples of atmospheric particulate matter

4.2.3.1. Aerosol sampling and analysis

Atmospheric particulate matter was sampled in four different sites: a wet indoor environment, two workplaces that had experienced flooding, finally an outdoor environment where fungal spores had been detected. A particle mass of about 1 mg was collected on each filter in indoor sites and 2.5 mg in the outdoor site.

Low volume Universal XR Pumps were used in the indoor environments at a flow rate of 2.5 L min^{-1}; the dual channel sampler was used in the outdoor environment at a flow rate of 2.3 m^3 h^{-1} (38.3 L min^{-1}). The sampled filters were stored in aluminum foils in refrigerator, then weighed, after conditioning for twenty-four hours in a chamber maintained at 50% relative humidity and 20 °C. Particulate matter amounts on each filter ranged from 0.6 to 2.8 mg and the sampled volumes raged between 14 m^3 in indoor samplings to 110 m^3 for outdoor samples.

Sampled filters from all the four different sites were processed following the procedure illustrated in figure 4.2.2.5.α., and all mycotoxins studied showed values below LODs (Tab. 4.2.3.1.α.).

	indoor	outdoor
MICOTOXIN	ng/mg	ng/mg
Aflatoxin B1	< 0.9	< 0.36
Ochratoxin A	< 33.9	< 13.56
T-2 Toxin	< 0.64	< 0.26
Zearalenone	< 2.9	< 1.16
Sterigmatocystin	< 3.1	< 1.24

Table 4.2.3.1.α.: Mycotoxin concentrations in atmospheric particles collected from indoor and outdoor sites. Notice that all values are below the LODs.

4.3. Free and combined amino acids determination in bioaerosol

4.3.1. Free amino acid analytical determination

As for amino acid analytical determination, the high polarity of these compounds, their low volatility and the lack of strong chromophore groups (except for tyrosine, tryptophan, phenylalanine) make their separation and determination difficult. In order to solve these problems, pre- and post-column derivatization reactions have been developed, for either increasing the volatility of the analytes for analysis by gas chromatography [Mandalakis et al., 2010; Mandalakis et al., 2011], or introducing chromophore/fluorophores groups in their structure for analysis by liquid chromatography with UV or fluorescence.

In most studies [Gorzelska et al., 1992; Zhang and Anastasio, 2001; Zhang et al., 2002; Zhang and Anastasio, 2003; Matsumoto and Uematsu, 2005], the identification and quantitation of amino acids in particulate matter were performed by HPLC analysis with a fluorescence detector, after derivatization of compounds with o-phthalaldehyde/mercaptoethanol (OPA).

In addition, in the same studies, the extraction of amino acids from aerosols was performed in an ultrasonic bath by hydroalcoholic solutions, and, after centrifugation and filtration, the samples were directly analyzed [Zhang and Anastasio, 2003; Barbaro et al., 2011] by chromatography.

All of the existing derivatization methods present various analytical problems: derivative instability, reagent interference, long preparation times, inability to derivatize the secondary amino groups and difficulties in derivatization toward specific amino acids [Petritis et al., 2002]. Therefore the ability to investigate amino acids, without derivatization, by liquid chromatography-tandem mass spectrometry (HPLC/MS-MS), reduces sample preparation times and eliminates reagent associated interferences and the possible side reactions that may occur by performing derivatization in complex sample matrix [Samy et al, 2011].

4.3.2. Optimization of amino acid analytical method

We optimized a method for the detection of underivatized amino acids by high resolution liquid chromatography coupled to tandem mass spectrometry (HPLC-MS/MS) in multiple reaction monitoring (MRM) mode on a triple quadrupole.

Stock standard solutions of all analytes were prepared by dissolving each compound in water/methanol 50:50 (1 mg mL^{-1}) and storing them at -20°C. Working solutions were prepared by successive dilution of the stock standard solutions.

After ESI-MS/MS experiments, we optimized amino acids separation by HPLC.

Three different columns were evaluated. Column 1 was a C_{18} (250 mm x 2.1 mm) slurry packed in our lab with size particles of 5 µm (Spherisorb, Deeside Ind. Est., Queensferry, UK); column 2 was a LUNA HILIC 50 mm x 2.0 mm I.D, 3 µm (Phenomenex, Castel Maggiore, Bologna, Italy); column 3 was an Acclaim® Trinity™ Analytical P1 2.1 mm x 100 mm I.D, 3µm (Thermo Scientific, Rodano, Milan, Italy).

Analyses of amino acids by HPLC-MS/MS in the multiple reaction monitoring (MRM) mode were carried out, in order to build standard and matrix-matched calibration curves and then to optimize the extraction and purification steps.

Since we needed to focus on the detection of amino acids in atmospheric particulate matter, and there are no urban dusts with certified and reference values for amino acids, we optimized their extraction, purification and analysis in a standard reference material (SRM) from National Institute of Standards and Technology (NIST), SRM 1649a-Urban Dust.

SRM 1649a was ASE extracted using H_2O/MeOH 80:20, at a temperature of 100°C and a pressure of 1500 psi.

As regards extract purification, two subsequent solid phase extractions were performed prior to analysis by HPLC-MS/MS.

The ASE extracts (about 12 mL) were evaporated to 6 mL, using a nitrogen flow at a temperature of 80°C and loaded onto the first cartridges, Strata-X SPE, linked to a vacuum system. Strata-X cartridges were previously conditioned with 6 mL of MeOH and equilibrated with 6 mL of H_2O. The amino acids and polar compounds were not retained, whereas non-polar and low-polar interferences were held by the stationary phase. The solutions containing polar compounds were evaporated to dryness and redissolved in a diluent solution (DIL) prepared as follows: 5% 5mM CH_3COONH_4 solution, adjusted to pH 4 with HCOOH and 95% mixed solution of 90% ACN, 10% H_2O acidified with 0.1% HCOOH, i.e. at a pH suitable to convert all the amino acids into cationic form. The solutions were then loaded on the Alltech SCX cartridges (a strong cation-exchange column) previously conditioned with 3 mL of 0.25 M HCOOH (pH ~2).

Six mL of 5 mM HCOOH/MeOH 95:5 were used as washing solution. Finally, amino acids were eluted with 20 mL of 0.5 M NH_3 solution (pH ~ 11) containing 50% ACN.

The samples were evaporated to dryness, in order to concentrate amino acids as well as to volatilize NH_3, and the residues were redissolved in 500 µL of the diluent solution DIL prior to HPLC/MS-MS analysis.

The whole procedure is illustrated in figure 4.3.2.a.

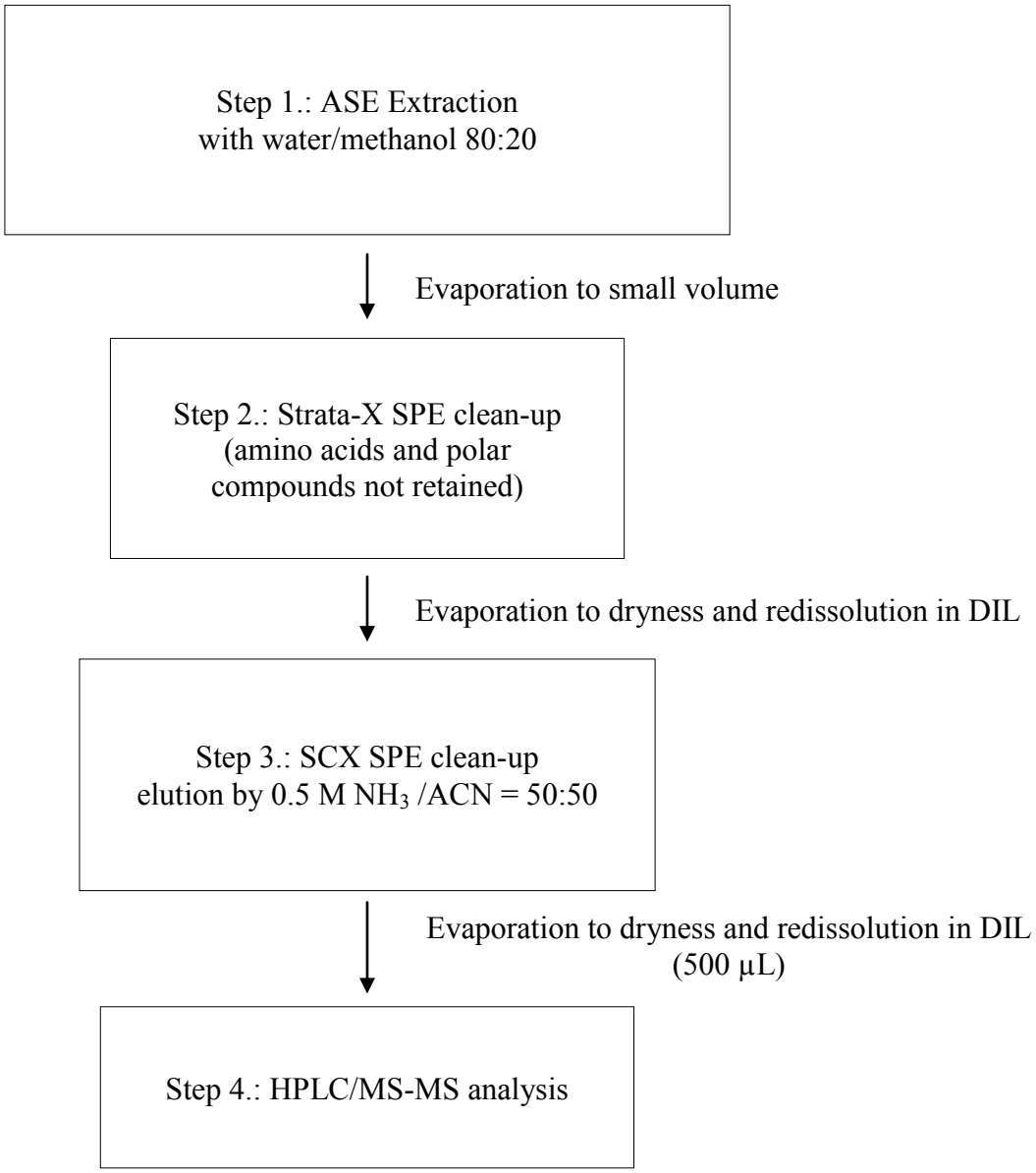

Figure 4.3.2.a.: Block diagram of the complete procedure for amino acid analyses

4.3.2.1. ESI-MS/MS experiments

In order to achieve the highest possible sensitivity and to find the specific MS-MS transitions, the instrument parameters, such as ion source voltage (ISV), declustering potential (DP), focusing potential (FP) and collision energy (CE) were optimized through the steady infusion of each solution of the analytes at 10 ng μL^{-1}, using a syringe pump at a flow rate of 10 $\mu L\ min^{-1}$, in both full and product ion scan.

Experiments were carried out under positive and negative polarity with different additives to improve ionization efficiency. The best results were obtained operating in positive ion mode using formic acid for all compounds. All amino acid spectra showed an abundant $[M+H]^+$ ion on Q1, which was then chosen as precursor ion for MS–MS analysis. Full scan Q1 spectra of some analytes are shown in figure 4.3.2.1.a.

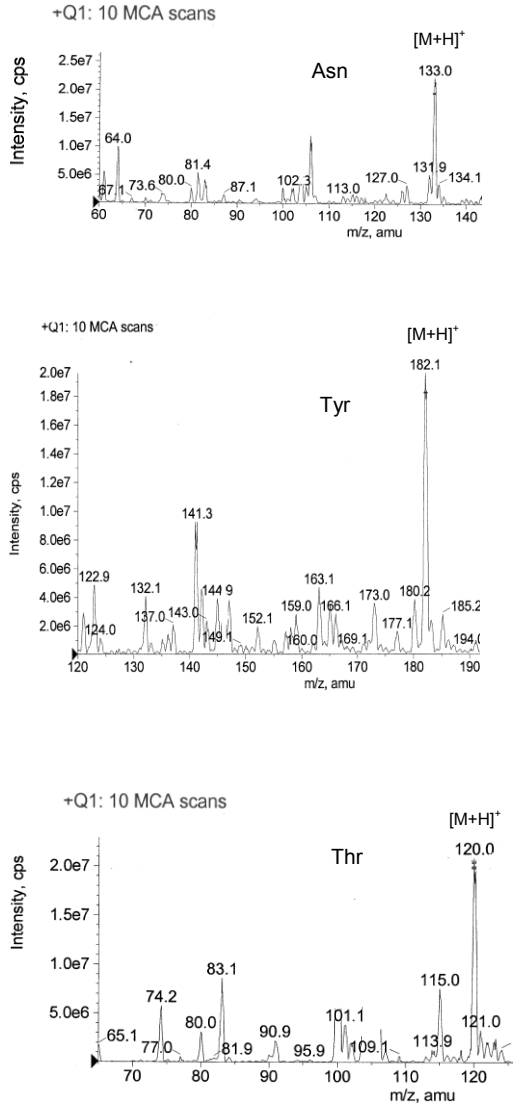

Figure 4.3.2.1.a.: Full scan Q1 spectra from Asn, Tyr, and Thr. Infusion at 10 ng mL^{-1}, 10 $\mu L\ min^{-1}$, conditions as in table 4.3.2.1.α.

Table 4.3.2.1.α. shows ISV, DP, FP and CE parameters for each amino acid.

Compound	Ion Source Voltage (ISV)	Declustering Potential (DP)	Focusing Potential (FP)	Collision Energy (CE)
Phe	5500	20	400	30
Trp	5500	10	400	20
Leu	5500	10	400	15
Ile	5500	10	400	15
Tyr	5500	15	380	20
Met	5500	20	400	20
Pro	5500	20	400	20
Val	5500	15	400	15
Thr	5500	20	400	20
Ala	5500	15	350	20
Ser	5500	10	400	20
Gly	5500	20	400	20
Gln	5500	20	400	30
Asn	5500	15	400	20

Table 4.3.2.1.α.: Optimized values of ISV, DP, FP and CE parameters for each amino acid

The most prominent fragmentation of amino acids was the loss of HCOOH leading to abundant immonium ions $[R–CH=NH_2]^+$, where R is the residue of the amino acid. Asn preferably formed the immonium ion $[HO_2C\text{-}CH=NH_2]^+$ (m/z 74) after elimination of acetamide. The contemporaneous loss of formic acid and ammonia was characteristic of Gln. Some amino acids also showed other characteristic fragmentations resulting from the loss of ammonia (Tyr m/z 165; Met m/z 133) and from the loss of H_2O (Thr m/z 102; and Ser m/z 88). The ^2H-labeled amino acids showed the same ionizations and losses than their corresponding compounds.

MS–MS spectra of some amino acids, chosen as representative according to their characteristic fragmentations, are shown in figure 4.3.2.1.b.

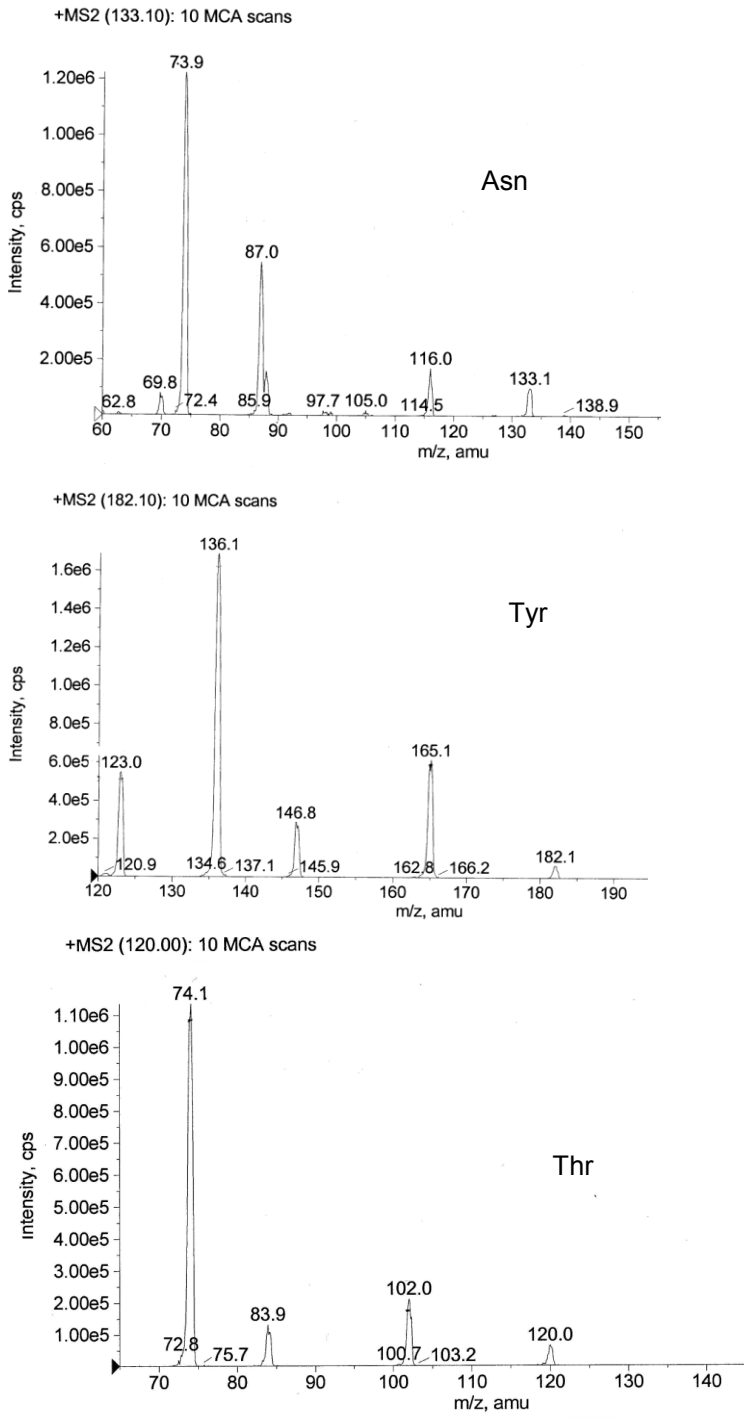

Figure 4.3.2.1.b.: MS–MS spectra of Asn, Tyr and Thr chosen as representative according to their characteristic fragmentations (Asn m/z 74 and m/z 87; Tyr m/z 136 and m/z 165; Thr m/z 74 and m/z 102). Conditions as in figure 4.3.2.1.a.

A summary of the transitions monitored for each amino acid is given in table 4.3.2.1.β.

Compound	Q1 (m/z)	Q3 (m/z)
Phe	166	120
Trp	205	146 – 188
Leu	132	86
Ile	132	86
Tyr	182	136 – 165
Met	150	104 – 133
Pro	116	70
Val	118	72
Thr	120	74 – 102
Ala	90	44
Ser	106	60 – 88
Gly	76	30
Gln	147	84
Asn	133	74 – 87
$^{2}H_{8}$ - Trp	213	196
$^{2}H_{3}$ - Ser	109	63
$^{2}H_{2}$ - Thr	122	76
$^{2}H_{1}$- Ile	133	87
$^{2}H_{7}$ - Pro	123	77

Table 4.3.2.1.β.: Monitored precursor (Q1) and product (Q3) ions for each amino acid and IS

4.3.2.2. Chromatographic conditions

Preliminary experiments were performed to find the most suitable column for the separation of amino acids. Columns 1 and 2 (See Para # 4.3.2.), with different compositions of mobile phase (H_2O/MeOH and H_2O/ACN), added by HCOOH, CH_3COOH or CH_3COONH_4 and $HCOONH_4$ (in order to increase chromatographic separation) did not give satisfactory results due to poor retention or tailed peaks.

In order to solve these problems, we used an Acclaim® Trinity™ Analytical P1 column, based on Nanopolymer Silica Hybrid (NSH) technology, that provides multiple retention mechanisms including reversed-phase, anion-exchange and cation-

exchange. In order to improve chromatographic separations and optimize the selectivity, different parameters, such as ionic strength of mobile phase, pH and content of organic solvent, were changed. Amino acid chromatographic runs were carried out under different conditions, both individually and in mixture, injecting a volume of 20 μL.

The best separation and chromatographic run-time results were obtained by eluting amino acids in isocratic condition with 15% phase A (5 mM CH_3COONH_4, adjusted to pH 4 with HCOOH), and 85% phase B (ACN/H_2O acidified with 0.1% HCOOH, 90:10). All the compounds and IS were eluted in less than 5 min. Table 4.3.2.2.α. shows retention times for each amino acid.

Compound	Retention time (min)	Compound	Retention time (min)
Phenylalanine (Phe)	2.40	**Tyrosine (Tyr)**	2.87
Proline (Pro)	2.42	**Alanine (Ala)**	3.38
Leucine (Leu)	2.54	**Threonine (Thr)**	3.47
Isoleucine (Ile)	2.54	**Glutamine (Gln)**	3.65
Methionine (Met)	2.62	**Glycine (Gly)**	3.85
Valine (Val)	2.75	**Serine (Ser)**	3.93
Tryptophan (Trp)	2.80	**Asparagine (Asn)**	4.03

Table 4.3.2.2.α.: Retention times of amino acids in HPLC by Acclaim® TrinityTM Analytical P1 column under isocratic condition with
Pump A: 15% (mobile phase A: 5mM CH3COONH4, adjusted to pH 4 with HCOOH)
Pump B: 85% (mobile phase B: ACN/H2O acidified with 0.1% HCOOH=90:10).
Flow 0.250 mL/min

Finally multi-standard analyses were carried out by LC/MS/MS in multiple reaction monitoring (MRM) mode, according to table 4.3.2.1.β., to obtain high specificity and sensitivity. Figure 4.3.2.2.a. shows the MRM chromatogram (extracted ion currents XICs) of a standard mixture. The XICs refer to the most intense chosen transitions for each amino acid.

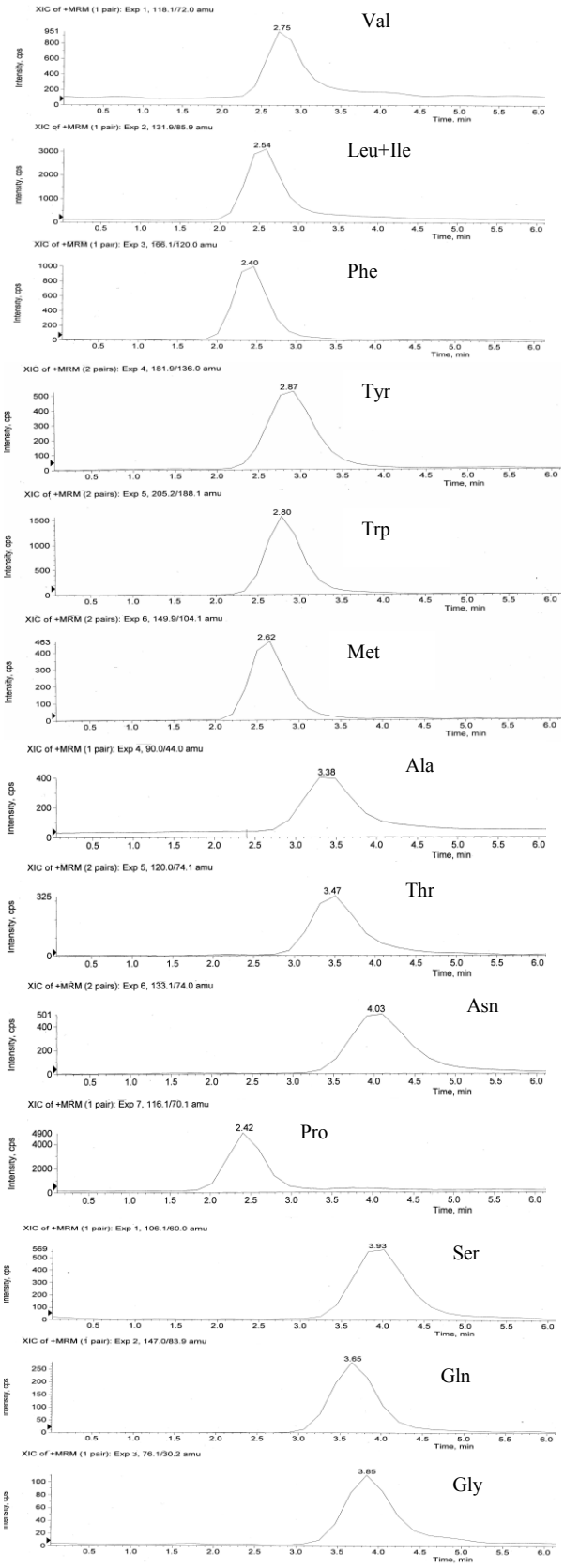

Figure 4.3.2.2.a.: MRM chromatogram (extracted ion currents XICs) of a standard mixture. The XICs refer to the most intense chosen transitions for each amino acid

4.3.2.3. Solvent calibration curves (type "A")

Solvent calibration curves (type "A") consisted of six standard solutions with increasing analyte concentrations, including zero (blank), and constant concentrations of the ^{2}H-labeled amino acids added as internal standard (IS).

The multistandard solutions contained amino acids at different concentrations depending on instrument sensitivity. Thus, for example, tyrosine concentration ranged from 44.5 to 430.1 ng mL^{-1}, while glycine concentration ranged from 495 to 940.5 ng mL^{-1}. Working standard solutions are shown in table 4.3.2.3.α.

Compound	I ng/mL	II ng/mL	III ng/mL	IV ng/mL	V ng/mL	VI ng/mL
Val	0	56.4	94.1	188.2	282.3	470.5
Leu	0	58.2	97.0	194.0	291.0	485.0
Ile	0	55.2	92.1	184.2	276.4	460.7
Phe	0	49.5	89.1	178.2	277.2	475.2
Tyr	0	44.8	80.6	161.2	250.9	430.1
Trp	0	59.4	99.0	198.0	297.0	495.0
Met	0	65.5	102.9	234.0	327.6	514.8
Pro	0	57.6	96.0	192.0	288.0	480.0
Ser	0	460.5	506.5	598.6	690.8	874.9
Gln	0	94.8	142.2	284.4	379.2	568.8
Gly	0	495.0	544.5	643.5	742.5	940.5
Ala	0	69.2	108.7	247.1	346.0	543.7
Thr	0	99.0	148.5	297.0	396.0	594.0
Asn	0	97.2	145.8	291.6	388.8	583.2

Compound	VII ng/mL
$^{2}H_8$ - Trp	158.4
$^{2}H_3$ - Ser	611.2
$^{2}H_2$ - Thr	235.0
$^{2}H_1$- Ile	189.6
$^{2}H_7$ - Pro	228.3

Table 4.3.2.3.α.: Multistandard solutions used to build calibration curves

For all the curves, each solution was injected three times in HPLC/MS–MS and the regression model was applied to the calibration data set.

Leu, Ile, Val, Met and Phe were quantified with $^2H_1$-Ile; Tyr and Trp with $^2H_8$-Trp; Ser, Gln, Gly and Asn with $^2H_3$-Ser; Ala and Thr with $^2H_2$-Thr and Pro with $^2H_7$-Pro.

4.3.2.4. Recovery

Amino acid recovery was determined for each step of the procedure of figure 4.3.2.a. (ASE extraction, first SPE purification, second SPE purification), adding amino acid standard solutions before the single step, and adding the IS just before HPLC injection, using the corresponding calibration curves "A".

Each sample was analyzed in triplicate by LC–MS/MS in MRM mode.

As for step 1, the amino acid standard solutions II, IV and VI of table 4.3.2.3.α. were added in ASE cells, and, after extraction, the solutions were evaporated and analyzed by HPLC/MS-MS, adding the IS just before injection. Mixtures of H_2O/MeOH at different percentages were tried to check the ASE extraction efficiency and the best results were obtained using H_2O/MeOH 80:20, at a temperature of 100°C and a pressure of 1500 psi. ASE extraction gave recoveries between 70% and 103%, depending on the amino acid (the lower recovery was observed for Trp and the higher for Ser and Ala).

As for step 2, the same multistandard solutions were loaded on Strata-X cartridges. Each analyte showed a recovery higher than 95%.

As for step 3, three types of strong cation exchange cartridges were tested: Phenomenex Strata, on both silica and styrene-DVB base, and Alltech SCX cartridges. The silica based sorbent, having a limited pH work range, was unsuitable to elute amino acids. Therefore, polymer based columns were selected and the best results were obtained using Alltech SCX cartridges. A first attempt to elute the total amino acids was carried out with 10 mL of a mixture 0.5M NH_3 (pH~11)/ACN, 90:10 but the amino acid recoveries were low. Therefore the percentage of the organic solvent was increased from 10% to 50%. Since results were still unsatisfactory, we doubled the volume of eluent (20 mL), improving the results, and obtaining recoveries of over 70% with an average of 85%. Table 4.3.2.4.α. summarizes the partial method recoveries.

Compound	ASE recovery ± RSD	SPE SCX recovery ± RSD
Phe	79 ± 8	75 ± 15
Trp	70 ± 6	82 ± 16
Leu	89 ± 1	91 ± 11
Ile	89 ± 1	91 ± 11
Tyr	102 ± 10	72 ± 10
Met	71 ± 5	77 ± 9
Pro	83 ± 5	102 ± 4
Val	92 ± 4	93 ± 13
Thr	102 ± 6	81 ± 7
Ala	103 ± 12	84 ± 11
Ser	103 ± 13	98 ± 11
Gly	73 ± 4	79 ± 16
Gln	71 ± 11	78 ± 12
Asn	101 ± 9	81 ± 9

Table 4.3.2.4.α.: Average recovery (over three concentrations) for ASE extraction, and second clean-up (SPE SCX) steps. The relative standard deviation (RSD) are also shown

4.3.2.5. Calibration curves (type "B" and "C")

Two other sets of calibration curves ("B" and "C") were prepared in order to evaluate the method linearity, estimate the matrix effect, determine amino acid concentrations in SRM-urban dust and quantify amino acids in environmental samples. In order to build "B" curves, six aliquots of about 0.2 mg of SRM 1649a each, subjected to steps 1–3 of figure 4.3.2.a., were spiked with the same standard solutions of curve "A" (Tab. 4.3.2.3.α.), immediately prior to LC injection.

The standard addition method was applied to build curve "C". Six aliquots of about 0.2 mg of SRM 1649a were spiked with the standard solutions I, II, III, IV,V, VI, VII of table 4.3.2.3.α., before applying the whole procedure of figure 4.3.2.a. The amino acid concentrations in solution I were 0 and the first SRM aliquot was only spiked with IS. A linear plot of the peak area ratios (ordinate) against the amount of standard added (abscissa) estimated the analyte concentrations in SRM 1649a by extrapolating the regression line to y=0; the negative intercept on the x-axis

corresponded to the amount of the amino acid in SRM 1649a. After translation to 0, curve "C" can also be used to determine amino acid concentrations in environmental atmospheric samples.

4.3.2.6. Linearity

A good linearity for each calibration curve was demonstrated by R^2 values between 0.980 and 0.999. Equations of calibration curves "A", "B", and "C", and their R^2 values are reported in table 4.3.2.6.α.

Compound	Equations of calibration curve type "A"	R^2	Equations of calibration curve type "B"	R^2	Equations of calibration curve type "C"	R^2
Phe	Y = 0.408X + 0.041	0.993	Y = 0.329X + 0.078	0.993	Y = 0.206X + 0.092	0.988
Trp	Y = 0.586X - 0.021	0.994	Y = 0.393X + 0.041	0.998	Y = 0.046X + 0.019	0.992
Leu+Ile	Y = 0.585X + 0.676	0.996	Y = 0.802X + 0.373	0.998	Y = 0.637X + 0.862	0.993
Tyr	Y = 0.259X + 0.025	0.994	Y = 0.293X + 0.042	0.995	Y = 0.166X + 0.091	0.996
Met	Y = 0.168X + 0.015	0.992	Y = 0.175X + 0.009	0.997	Y = 0.114X – 0.006	0.993
Pro	Y = 1.670X + 0.021	0.997	Y = 1.479X + 0.143	0.999	Y = 1.580X + 0.476	0.999
Val	Y = 0.566X - 0.011	0.999	Y = 0.485X + 0.112	0.994	Y = 0.431X + 0.308	0.995
Thr	Y = 1.341X + 0.043	0.994	Y = 1.187X + 0.111	0.994	Y = 1.088X + 0.474	0.980
Ala	Y = 1.758X + 0.080	0.993	Y = 1.481X + 0.486	0.998	Y = 0.943X + 2.150	0.992
Ser	Y = 0.804X + 0.008	0.997	Y = 0.769X + 0.227	0.995	Y = 0.352X + 0.609	0.999
Gly	Y = 0.126X - 0.001	0.994	Y = 0.129X + 0.002	0.997	Y = 0.198X + 0.005	0.998
Gln	Y = 0.576X - 0.007	0.992	Y = 0.591X – 0.020	0.992	Y = 0.587X – 0.016	0.996
Asn	Y = 1.424X + 0.039	0.995	Y = 1.369X + 0.132	0.996	Y = 1.502X + 0.015	0.999

Table 4.3.2.6.α.: Equations and R^2 of the three calibration curves ("A", "B", "C") for each amino acid

4.3.2.7. LODs

We calculated the LODs of the analytical procedure as three times signal-to-noise ratios, by injecting gradually more dilute SRM1649a extracts spiked with standard solutions, and adding internal standard just prior to the injection. LODs were found to range between 9.5 ng mL^{-1} for Tyr up to 26 ng mL^{-1} for Thr.

4.3.2.8. Whole procedure recovery

Total recovery was calculated on SRM 1649a spiked with different amounts of amino acids before the extraction and adding the IS prior to LC-MS/MS analysis, using calibration curves "B".

In order to calculate total recovery at five concentration levels, the SRM 1649a was spiked with solutions II, III, IV, V and VI of Tab. 4.3.2.3.α., and submitted to the whole procedure, adding solution VII of Tab. 4.3.2.3.α prior to LC-MS/MS analysis. The recovery results ranged between 60 and 95%. Table 4.3.2.8.α. summarizes the total recoveries.

Compound	Whole Procedure recovery
Phe	70 – 79
Trp	60 – 75
Leu	62 – 95
Ile	62 – 95
Tyr	67 – 88
Met	62 – 74
Pro	64 – 83
Val	72 – 95
Thr	61 – 93
Ala	85 – 95
Ser	78 – 90
Gly	65 – 90
Gln	62 – 77
Asn	66 – 93

Table 4.3.2.8.α.: Average recovery (over five concentrations) for the whole procedure. The relative standard deviation (RSD) are also shown

4.3.2.9. Matrix effect

In order to prevent errors associated with co-eluting components, matrix effects were evaluated thanks to type "A" and type "C" curves. With this aim in view, we calculated the slope ratios of the calibration curves obtained from matrix ("C") and from standard solutions ("A"), which were then multiplied by 100 to get the enhancement or suppression in percentage.

Both positive and negative matrix effects were observed for most of the amino acids, except for five of them: Gln, Val, Thr, Asn, and Pro.

Phe, Trp, Met, Ser and Tyr showed a signal suppression in the matrix-matched calibration curve. Leu/Ile, Gly and Ala exhibited signal enhancement in the same curves. Figure 4.3.2.9.a. shows the comparison between the two calibration curves obtained for three amino acids: Gly, Phe and Gln chosen for illustrating positive (signal enhancement), negative (signal suppression), and absence of matrix effects.

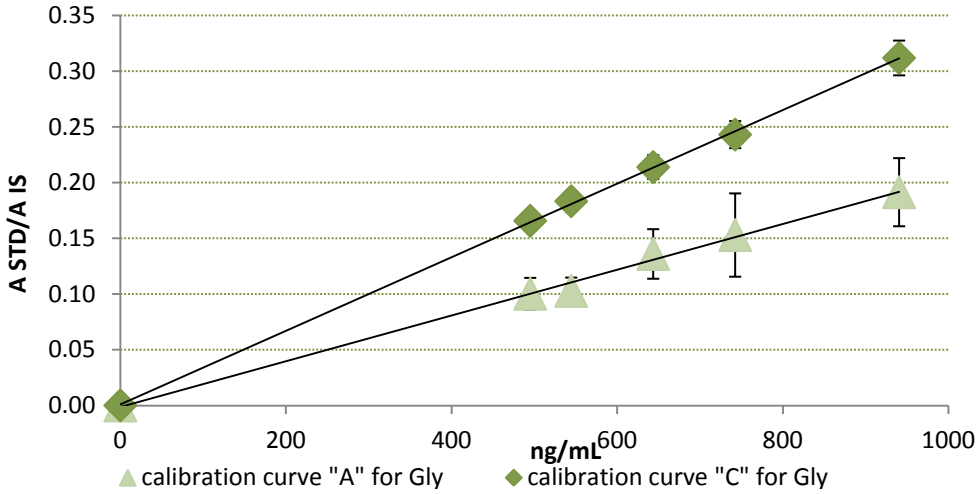

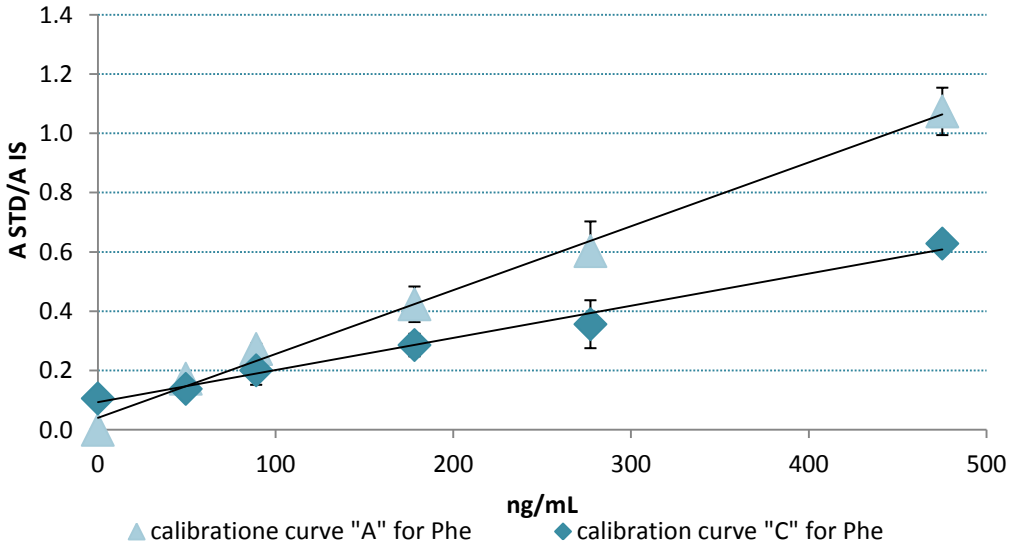

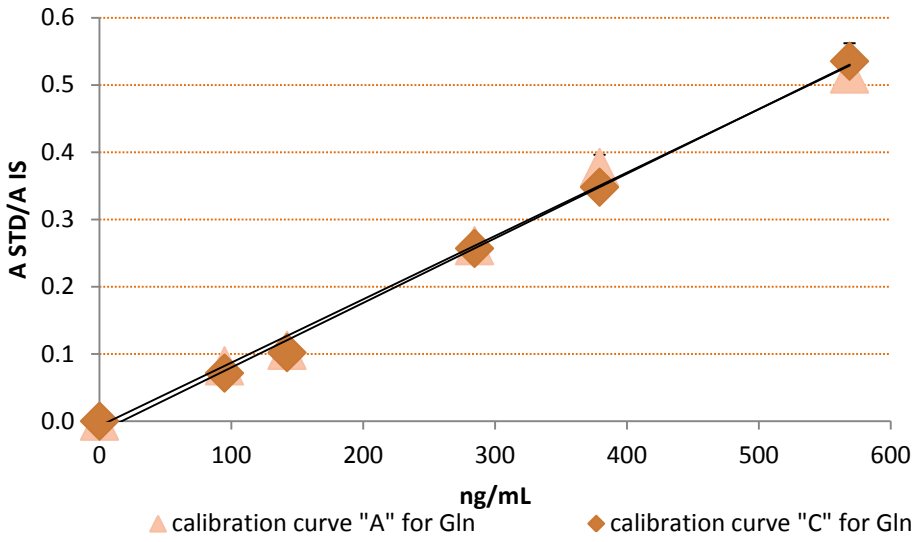

Figure 4.3.2.9.a.: Comparison between calibration curves "A" and "C" obtained for three amino acids: Gly, Phe and Gln chosen to illustrate positive (signal enhancement), negative (signal suppression), and absence of matrix effects

On the basis of the present results, possible environmental complex samples must be quantified through matrix-matched calibration curves, in order to guarantee the correct data results.

4.3.2.10. Amino acids in urban dust NIST SRM 1649a

Concentrations of amino acids in urban dust SRM 1649a were calculated using the calibration curve type "C".

The x-intercept of the standard addition plot was used to obtain amino acid content in the sample, after accounting for dilution.

In table 4.3.2.10.α. amino acid concentrations in urban dust SRM 1649a, expressed in ng of compound per mg of dust, are shown.

Serine and alanine were the most abundant amino acids according to their high natural abundance, while asparagine, methionine, and glutamine were the less abundant amino acids. Concerning to methionine trace amount, it was probably due to common atmospheric reactions causing its oxidation to methionine sulfoxide and methionine sulfone, not checked in the present work.

Amino acid content in SRM 1649a represented about 0.6% by weight of urban dust.

Compound	ng aa/mg SRM1649a		SD
Phe	213.0	±	15.5
Pro	145.5	±	2.0
Leu/Ile	641.0	±	11.0
Met	26.0	±	1.5
Val	338.5	±	7.5
Trp	190.5	±	7.0
Tyr	261.0	±	2.5
Ala	1339.5	±	33.5
Thr	256.0	±	6.5
Gln	42.5	±	2.0
Gly	293.5	±	8.0
Ser	2644.5	±	37.5
Asn	15.5	±	1.0

Table 4.3.2.10.α.: Amino acid concentrations in urban dust SRM 1649a, expressed in ng of compound per mg of dust. Each value is associated to its standard deviation (SD)

4.3.3. Combined amino acid extraction and analysis

In order to extract combined amino acids from the sample of urban atmospheric particulate, we chose to utilize three different extraction solutions in series, one following the other, performing an accelerated solvent extraction by the ASE-200.

The first solution was a NaCl 0.02 M solution, the second one was 20% (v/v) propanol, dithiothreitol (DTT) 1mM, 1% (v/v) acetic acid; the third one was a buffer tris-HCl pH=8, sodium dodecyl sulfate (SDS) 0.005%, DTT 1mM.

The different pH values and ionic force, the use of surfactants and redox agents guaranteed the extraction of combined amino acids with different solubility characteristics.

The use of DTT as reducing agent prevents the oxidation of any thiol group present in proteins, while the use of the surfactant SDS is essential for the extraction of membrane proteins [Shewry and Fido, 1996; Ersson et al., 2011].

An aliquot of the extract solutions were diluted to a final volume of 2.5 mL of NanoOrange® reagent solution, incubated in the dark for 10 minutes at a temperature between 90° and 96 °C, prior to spectrofluorimetric analysis.
The amount of combined amino acids was determined using a calibration curve constructed using a series of standard bovine serum albumin solutions (from 0 to 6 $\mu g\ mL^{-1}$).

4.3.4. Amino acids and Proteins in samples of atmospheric particulate matter

4.3.4.1. Aerosol sampling

The low-pressure impactor DLPI, Dekati was used to collect the size-segregated aerosol samples. Sampling site (downtown Rome) and procedure are described above in Para # 4.1.3. Each of the two sampling campaigns were conducted for two weeks, the first starting from 3 October, and the second from 18 October, 2012. Within the first campaign, and for only forty eight hours, in parallel, two PM_{10} samples were collected using the HYDRA Dual Sampler, at a flow rate of 2.3 $m^3\ h^{-1}$, starting from 10 October.
Thus, we had twenty-six sampled filters coming from the two DLPI sampling campaigns, each of them carrying particles of different size and whose sum represented PM_{10} particles collected for fourteen consecutive days; and two sampled filters carrying PM_{10} particles collected for forty eight hours, coming from Hydra. We also had a couple of field blanks for each sampler.
The sampled filters were stored in aluminum foils in refrigerator, after gravimetric determination of particle mass, subsequent to conditioning for twenty-four hours in a chamber maintained at 40% relative humidity and 20 °C.
Filters from DLPI first sampling campaign were processed for free amino acid analysis, filters from DLPI second sampling campaign were processed for combined amino acid content, filters from Hydra were processed one for free amino acid analysis and the other for combined amino acids.

4.3.4.2. Particulate matter concentrations

Due to the lack of two identical impactors, we had to use two subsequent sampling campaigns to have both size segregated amino acids and total protein content. From the comparison of the PM results from the two different samplings, we assumed that

the periods were very similar each other and the results could be comparable. In 3–17 October campaign, PM_{10} concentration was 23.6 µg m^{-3} (with ultrafine, fine, and coarse PM respectively 1.8, 11.2, 10.6 µg m^{-3}), while in 18 October – 5 November campaign, PM_{10} concentration was 26.6 µg m^{-3} (with ultrafine, fine, and coarse PM respectively 1.1, 13.4, 12.1 µg m^{-3}). Fig. 4.3.4.2.a. shows a comparison between size segregated mass concentration (µg m^{-3}) of ambient aerosol samples collected in the two PM samplings.

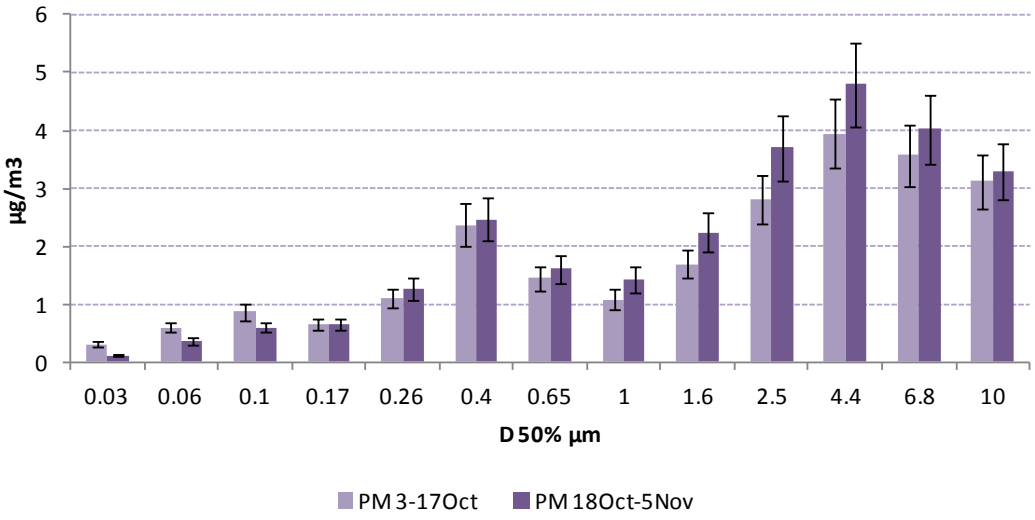

Figure 4.3.4.2.a.: Size segregated mass concentration (µg m^{-3}) of ambient aerosol samples collected in two subsequent sampling campaign from 3 October to 5 November

PM_{10} particles collected for forty eight hours, coming from Hydra, showed a concentration equal to 24.6 µg m^{-3} in the first filter and 24.7 µg m^{-3} in the second filter, concentrations comparable to that obtained by the sum of the thirteen filters sampled by the impactor.

4.3.4.3. Free Amino Acid in size segregated particles and in PM_{10}

As regards any single amino acid, Figure 4.3.4.3.a. shows respirable particle-bound amino acids in air from both PM_{10} sampled by HYDRA Dual Sampler and collected by multistage impactor DLPI, obtained as the sum of the thirteen fractions. Although the first sampler had sampled only for 48 hours within 360 hours of the multistage impactor, amino acid concentrations are comparable within experimental error.

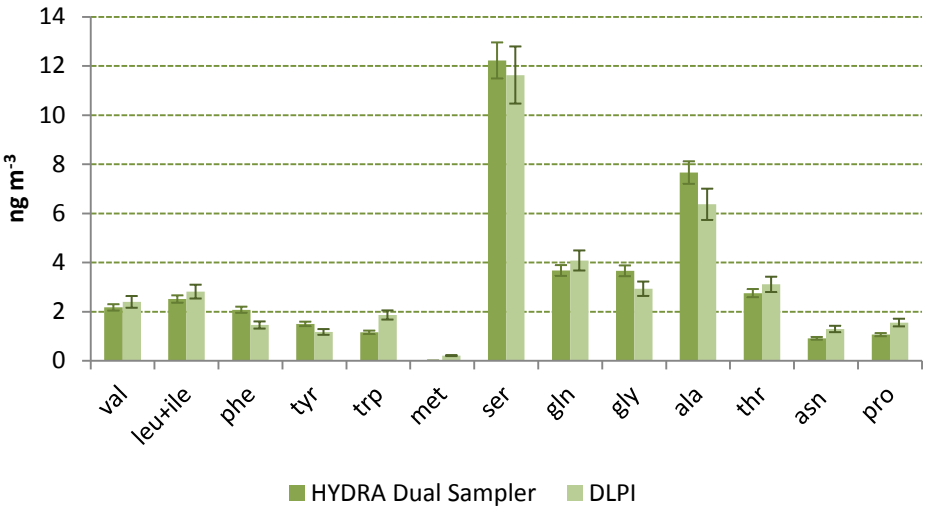

Figure 4.3.4.3.a.: Comparison between respirable particle-bound amino acids in air obtained from PM_{10} sampled by HYDRA Dual Sampler and obtained as the sum of the thirteen fractions collected by multistage impactor DLPI.(Results from two consecutive sampling campaigns from 3 October to 5 November)

Ser showed to be the most abundant, amounting to 28% of the total free amino acids, Ala and Gln respectively accounted for 6 and 4%, while Thr, Gly, Leu and Val percentages were between 2 and 4%; finally Trp, Pro, Phe, Asn, and Tyr were under 2% of total amino acids. These results agree with those reported by other authors. According to literature [Zhang and Anastasio, 2003; Barbaro et al., 2011; Mandalakis et al., 2011], Ser, Ala, Gln, Thr and Gly are the most abundant amino acids in atmosphere. Zhang and Anastasio [2003], who analyzed free amino acids in $PM_{2.5}$, found that Gly and Thr were the most abundant compounds, with an average combined contribution of 26% to the total free amino acids. Ser and Ala also contributed significantly, accounting for an average of 13% and 6%, respectively. Barbaro et al. [2011] showed that Gly was the dominant compound, accounting for about 23% of the total free amino acids, followed by Gln that accounted for 17%. Furthermore, Mandalakis et al. [2011] also observed a substantial contribution of glycine that accounted for, on average, 61% of the total free amino acids in aerosol; Gln, Ala and Ser were the next most abundant compounds, accounting for 3.5-8% of total free amino acids.

In support of these results, it is appropriate to give some general remarks on the abundance of natural amino acids. Ser, Ala and Gly are some of the most frequent amino acids in the proteins [Voet et al., 2008]. Ala is one of the most versatile and abundant in nature because of its small size and its neutral character. The same

considerations can be made for Gly, a fundamental component of collagen, the most abundant protein in nature. Ser and Thr, having a hydroxyl group in the side chain, are very hydrophilic and therefore the water-soluble proteins, such as albumin, widely distributed in the animal and plant kingdom, contain many of those amino acids. Gln is the most abundant free amino acid in the blood and one of the most abundant amino acids of prolamines, proteins extremely widespread in nature. In addition, Gly, Ser, Gln, Ala and Thr are abundant in barley and in cereals in general [Thiele et al., 2008], and legumes [Odunfa, 1979].

As for total particle-bound amino acids collected by HYDRA Dual Sampler, the concentration found was 42.9 ng m^{-3} and PM_{10} concentration was 24.6 µg/m^3; as regards amino acids sampled by multistage impactor, found as the sum of the thirteen fractions, the concentration was 40.9 ng m^{-3} in 23.6 µg m^{-3} of PM_{10}. In both cases amino acids represented about 0.2% by weight of respirable urban particulate matter. Amino acid concentrations found in atmosphere were comparable regardless of the sampler used and the sampling duration. Therefore, it does seem to exclude the hypothesis of any sampling artifact due to degradation of proteins or peptides, on filters, by airborne enzymes [Baur, 2005; Sehgal et al., 2005; Gunawan et al., 2008] that might be present in the sampled particulate matter.

As for size segregated amino acid content, figure 4.3.4.3.b. shows the distribution of total amino acids, expressed as ng m^{-3}, in the thirteen size fractions of particulate matter sampled by multistage impactor, whose mass concentration (µg m^{-3}) is also shown.

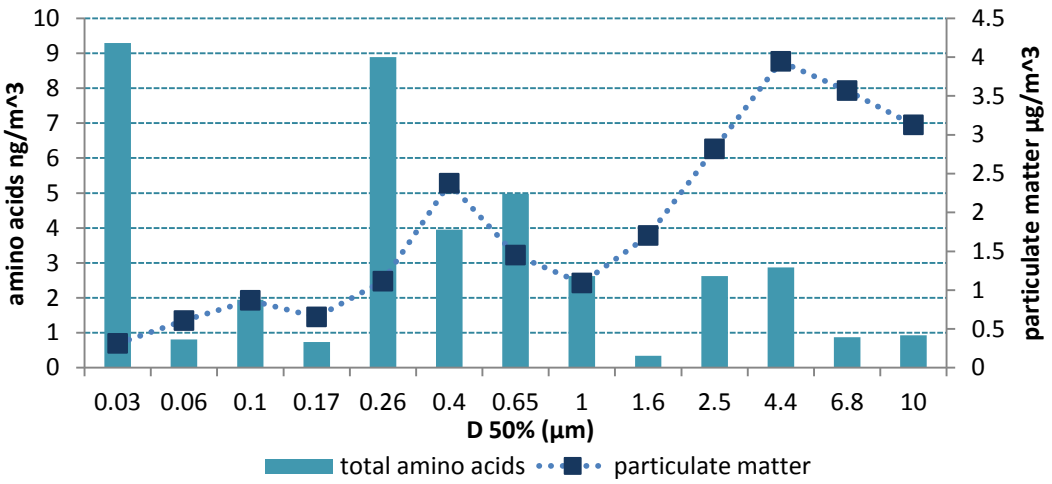

Figure 4.3.4.3.b.: Atmospheric concentration of total amino acids (ng m^{-3}), distributed in thirteen size fractions of airborne particulate matter, and particle mass concentration (µg m^{-3})

The highest concentration of total amino acids is observed within the ultrafine fraction, namely in the stage 0.03 µm; similarly high concentration is also observed within the fine fraction, namely in the stage 0.26 µm. Figure 4.3.4.3.c. shows the concentration of total amino acids, 12.0, 24.1 and 4.7 ng m^{-3}, in the ultrafine, fine, and coarse PM fractions, at atmospheric concentrations respectively equal to 1.8, 11.2, and 10.6 µg m^{-3} (also shown in figure 4.3.4.3.c.).

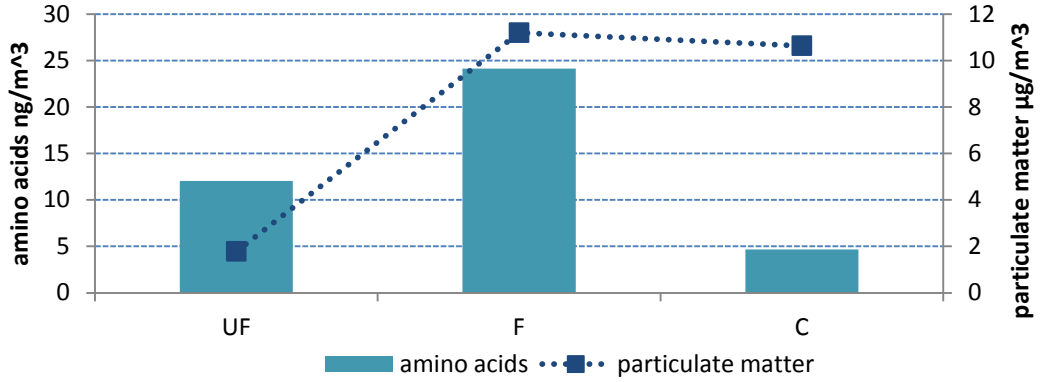

Figure 4.3.4.3.c.: Atmospheric concentration of total amino acids (ng m^{-3}), distributed in ultrafine (aerodynamic diameter < 0.1 µm), fine (aerodynamic diameter 0.1-2.5 µm), and coarse (aerodynamic diameter 2.5-10 µm) urban air pollution particles and particle mass concentration (µg m^{-3})

Amino acids in the fine fraction show a concentration of about two times greater than in the ultrafine fraction; on the contrary, there is a poor distribution in the coarse fraction.

From the study of the percentage by weight of the amino acids compared to the particulate matter (Fig. 4.3.4.3.d.), it is evident that 0.67% of the weight of ultrafine, 0.22% of fine, and only 0.04% of coarse particles is due to amino acids.

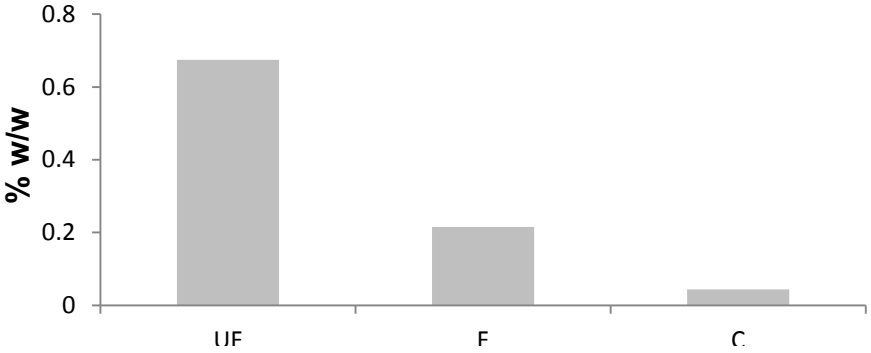

Figure 4.3.4.3.d.: Percentage distribution (by weight) of total amino acids in ultrafine, fine, and coarse urban air pollution particles

4.3.4.4. Combined Amino Acid in size segregated particles and in PM_{10}

We found 1.67 µg m^{-3} of particle-associated combined amino acids (CAA) in atmosphere. As regard the size-resolved mass distributions derived from the thirteen stage impactor, figure 4.3.4.4.a. shows both atmospheric concentration of combined amino acids (µg m^{-3}), distributed in the thirteen size fractions of airborne particulate matter PM_{10}, and the relative particle mass concentration (µg m^{-3}).

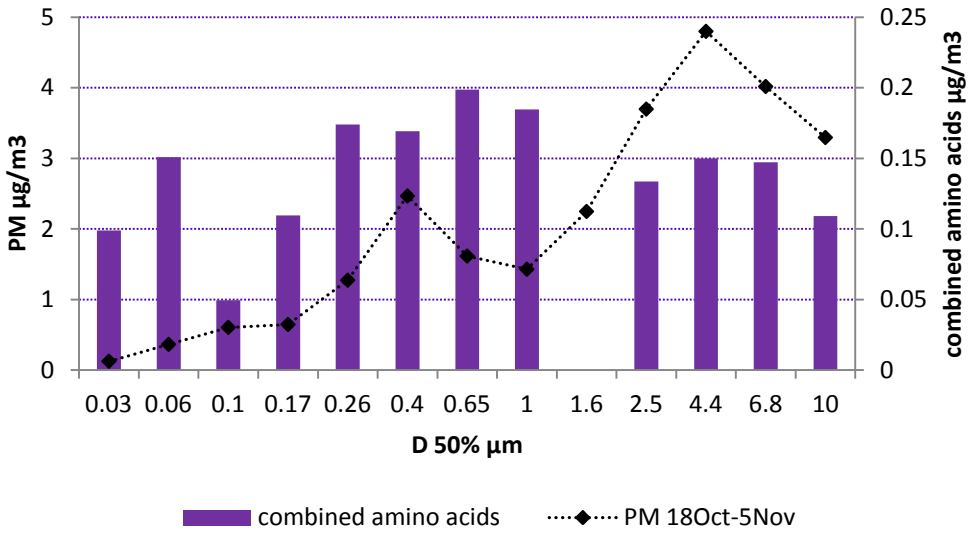

Figure 4.3.4.4.a.: Atmospheric concentration of combined amino acids (ng m^{-3}), distributed in thirteen size fractions of airborne particulate matter, and the relative particle mass concentration (µg m^{-3})

Combined amino acids in the different stages range from 0.05 to 0.2 µg m^{-3}. Similarly to amino acids, in the stage 1.6 µm, combined amino acids fell under the limit of detection, even if they are more uniformly distributed into the other fractions on respect free amino acids.

Figure 4.3.4.4.b. shows the concentration of combined amino acids in the ultrafine, fine, and coarse PM fractions. 0.30, 0.97, and 0.41 µg m^{-3} of combined amino acids were respectively found in 1.09, 13.37, and 12.11 µg m^{-3} of ultrafine, fine and coarse airborne particles.

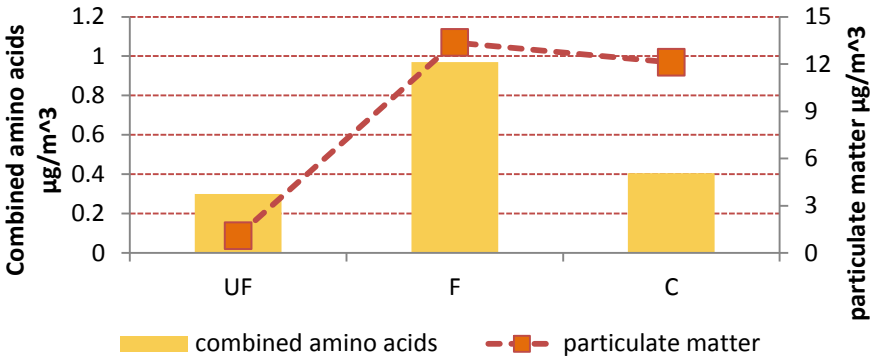

Figure 4.3.4.4.b.: Atmospheric concentration of combined amino acids (µg m^{-3}), distributed in ultrafine (aerodynamic diameter < 0.1 µm), fine (aerodynamic diameter 0.1-2.5 µm), and coarse (aerodynamic diameter 2.5-10 µm) urban air pollution particles and particle mass concentration (µg m^{-3})

Therefore the combined amino acids are at higher concentration in the fine fraction, but if we analyze the data on respect the percentage weight/weight (Figure 4.3.4.4.c.), the ultrafine fraction is characterized by a major content in combined amino acids, as well as in the case of free amino acids. In particular 27% of the weight of ultrafine (77.6 µg of CAA in 283.4 µg of UF PM); 7% of fine (251.3 µg of CAA in 3466.6 µg of UF PM); and only 3% of coarse particles is due to combined amino acids. (105.3 µg of CAA in 3139.6 µg of UF PM).

More generally, in a total of 6.9 mg of sampled particles, we found 0.434 mg of combined amino acids, i.e. 6% w/w of PM_{10} was constituted of combined amino acids

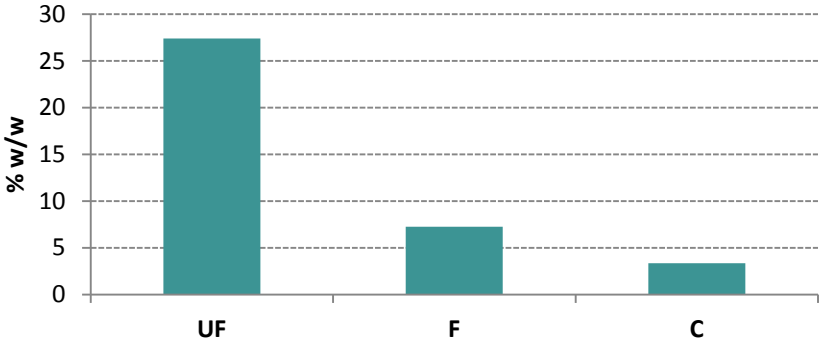

Figure 4.3.4.4.c.: Percentage distribution (by weight) of combined amino acids in ultrafine, fine, and coarse urban air pollution particles

Hence, both in the case of free and combined amino acids, the percentage of organic content in the ultrafine fraction is higher on respect the other fractions, albeit with two and a half orders of magnitude higher for combined amino acids (see figure 4.3.4.4.d.).

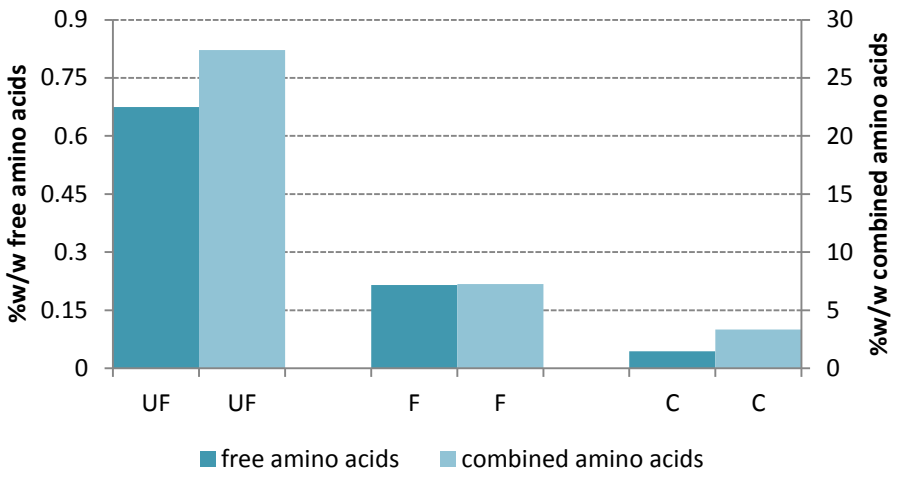

Figure 4.3.4.4.d.: Comparison between the percentage distribution (by weight) of free and combined amino acids in ultrafine (UF) fine (F),and coarse(C) particles

Table 4.3.4.4.α. reports the amounts in µg of combined amino acids and particles found in each stage of impactor.

Menetrez, in 2009 [Menetrez et al., 2009], showed that the peak protein quantity was 40.85 µg, at the 1 µm aerodynamic diameter size stage. We found a very similar amount at the same stage (47.9 µg), even if the particulate quantity was higher (370 µg), and similar amounts at aerodynamic diameter size stages 0.26, 0.4, 0.65 µm. In fact, we have a constant amount of protein in all the fine fractions regardless of the amount of particulate material. There are currently no literature data to compare ultrafine particle protein content.

D50 % µm	PM (µg)	Combined amino acids (µg)
0.03	32.3	25.7
0.06	94.3	39.1
0.1	156.8	12.8
0.17	167.5	28.4
0.26	330	45.1
0.4	639.3	43.8
0.65	418.7	51.5
1	370.3	47.9
1.6	582.5	0
2.5	958.3	34.6
4.4	1244	38.9
6.8	1041.5	38.1
10	854.1	28.3

Table 4.3.4.4.α.: Amounts in µg of combined amino acids and particles found in each stage of the thirteen-stage cascade impactor, DLPI

The second sample of PM_{10}, sampled by HYDRA Dual Sampler in parallel with the sample used for amino acid analysis, was studied for its combined amino acid content. The result was equal to 1.2 µg m^{-3} of total protein in PM_{10} (24.7 µg m^{-3}) and represented about 5% by weight, according to the literature [Rosas et al., 1995; Franze et al., 2005; Menetrez et al., 2007]. The lower value could be due to a less efficient extraction caused by a bulkier sample: for ELPI, the dust amount on the filters ranged between 0.03 – 1.2 mg; while particles on Hydra filter amounted to 2.7 mg.

4.3.4.5. Toxicity

Being the average volume of air that one person breathes in a hour 0.36 m^3 (corresponding to 500 mL of air which enters the lungs with each breath and considering 12 breaths per minute at rest), we can say that, in hourly exposed individuals, of the 0.603 µg of proteins in the thoracic fraction transported through the respiratory epithelium into the respiratory system and the inner tissues of the body [Nemmar et al., 2012], 511 ng can penetrate beyond the conducting airways to the pulmonary region of the lung and of these 511 ng, 108 ng can even penetrate from the lungs into the bloodstream. Table 4.3.4.5.α shows thoracic, respirable and ultrafine combined amino acids present in 0.36 m^3 of air, in the October sampling campaign.

	ng
thoracic particle-bound combined amino acids in 0.36 m^3	603
respirable particle-bound combined amino acids in 0.36 m^3	511
ultrafine particle-bound combined amino acids in 0.36 m^3	108

Table 4.3.4.5.α: Thoracic, respirable and ultrafine combined amino acids in 0.36 m^3 of air, sampled in Rome, in October 2012

Although we can not distinguish potential pathogen proteins from innocuous ones, nevertheless all of them have direct access into the cells where they may greatly express their toxic potential [Geiser et al., 2005].

5. CONCLUSIONS

In order to extend the knowledge about organic compounds in atmospheric particulate matter causing mucous membrane irritation, bronchitis and obstructive pulmonary disease, allergic rhinitis and asthma, allergic alveolitis (granulomatous pneumonitis) or organic dust toxic syndrome (inhalation fever or toxic pneumonitis), bioaerosol components were studied.

In particular, we applied an analytical method to detect fungal spores, and optimized analytical methods to study mycotoxins, and free and combined amino acids in samples of particulate matter. We applied those methods to environmental samples, after aerosol sampling campaigns performed at different sites and seasons. It should be noted that ultrafine particles were also collected and analyzed.

As for the fungal component of aerosol in outdoor environments, PM_{10} and size-segregated atmospheric aerosols were respectively collected from suburban/rural and urban locations, in different seasons. Particles sampled on filters were extracted and analyzed for arabitol, mannitol and ergosterol as fungal biomarkers and their concentrations were correlated to the airborne fungal spores through conversion factors.

The three markers were differently distributed among aerosol size fractions, showing to have different sources. Ergosterol proved to be the only reliable biomarker at our latitudes, probably because the low concentration of fungal spores makes significant the occurrence of other local sources of mannitol and arabitol. It's known that biomass burning and sea spray are also important sources of arabitol and mannitol in PM and they often occur in plants. At our latitude, which is in our meteorological condition, and dominant vegetation type, arabitol and mannitol major primary emission sources are different from fungi. Therefore we calculated the fungal spore concentrations at the two sampling sites by using ergosterol as biomarker. The concentrations found were respectively inversely and directly proportional to temperature and relative humidity and were more abundant in autumn at the suburban/rural site and in winter at the urban site. Depending on the sampling site and on the season, between 0.1 and 0.8 % of PM_{10} and between 0.3 and 2.4 % of OC was constituted by fungal spores.

As for mycotoxins, secondary fungal spore metabolites, an analytical method for the simultaneous determination of aflatoxin B_1, ochratoxin A, T-2 toxin, zearalenone

and sterigmatocystin in indoor and outdoor particulate samples was developed, using HPLC-MS/MS.

For this purpose, we proceeded with the study of fragmentation in mass spectrometry and of chromatographic separation; we optimized also the extraction procedure and the purification on SPE cartridge. Then, we calculated the recoveries of the whole analytical method, and the LODs which showed to be sufficiently low for all mycotoxins.

The developed method was applied to both outdoor and indoor particulate samples where the presence of fungal spores was confirmed, and all samples provided negative results.

Finally, proteins are one of the most abundant and different classes of allergens whom the immune system can respond to. Their presence in the atmosphere, as well as that of free amino acids, can be an index both of allergenic activity of the atmospheric aerosol and of biological material dispersed.

A method for the analysis of amino acids, present in trace amounts in environmental matrices, was developed. The present method also allowed the determination of this class of compounds in an urban dust standard reference material NIST SRM 1649a. An extraction at high pressure and temperature with H_2O/MeOH 80:20, a clean-up using two SPE cartridges in series, and the analysis in HPLC/MS-MS in MRM mode provided good results for the determination of underivatized amino acids in a complex matrix such as that of urban particulate. The present method, suitable to a SRM-Urban Dust, was applied to environmental samples. Free amino acids concentrations in ultrafine, fine, and coarse airborne particulate matter was respectively 12.05, 21.18, and 7.64 ng m^{-3} with a total concentration in PM_{10} of 40.9 ng m^{-3}. Free amino acid percentage content in atmospheric ultrafine, fine, and coarse particulate matter respectively resulted 0.67%, 0.22%, and 0.04%., representing about 0.2% by weight of urban particulate matter PM_{10}.

Serine, alanine, glutamine, threonine and glycine were the most abundant amino acids in atmosphere. In particular serine was the most abundant, amounting to 28% of the total free amino acids.

The amino acids sampled by a multistage impactor and those sampled by the HYDRA Dual Sampler were fully comparable, demonstrating that the duration of the sampling did not produce any degradation of proteins or peptides on filters by enzymes that might be present in the sampled particulate matter.

The extraction method of combined amino acids in samples of airborne particulate matter involved three solutions in series: the first one was a NaCl 0.02 M solution, the second one was a 20% (v/v) propanol, dithiothreitol (DTT) 1mM, 1% (v/v) acetic acid water solution; the third one was a buffer tris-HCl pH=8, sodium dodecyl sulfate (SDS) 0.005%, DTT 1mM. The different pH values and ionic force, the use of surfactants and redox agents guaranteed the extraction of combined amino acids with different solubility characteristics. The use of DTT as reducing agent prevented the oxidation of any thiol group present in proteins, while the use of the surfactant SDS was essential for the extraction of membrane proteins.

The extracted solutions were analyzed by spectrofluorimetry using the NanoOrange® reagent. Airborne protein concentration was 1.6 μg m^{-3}, representing 6% w/w of $PM_{10.}$ We found a percentage content w/w of combined amino acids equal to 21% for ultrafine, 7% for fine, and 3% for coarse fractions.

Free and combined amino acid size-segregated distribution demonstrated a higher percentage w/w in the ultrafine fraction of particulate matter of both the classes of compounds. Therefore amino acids and proteins are capable of reaching the alveolar regions of exchange and penetrating into the cardiovascular system, some of them possibly causing adverse effects on human health.

In conclusion, particularly interesting is the study of the ultrafine fraction of the particulate material. With the exception of the fungal spores, which are not detected in this portion, free and combined amino acids constitute more than 22% of the total UF atmospheric quantity. Since these particles largely escape the surveillance of alveolar macrophages thus granting their access to the pulmonary interstices, the components of which they are composed can reach via the blood, target tissues like the cardiovascular system, the spleen, the liver, the brain where they can cause adverse chemical reactions and therefore exert their harmful effects.

Therefore, the sampling and analysis of the chemical composition of the ultrafine particles are considered essential for understanding their prevalence, the potential damage to the environment and their impact on human health, also in order to improve the current legislation.

REFERENCES

Adhikari A., Reponen T., Grinshpun S.A., Martuzevicius D., LeMasters G., 2006. Correlation of ambient inhalable bioaerosols with particulate matter and ozone: A two-year study. Environmental Pollution 140, 16–28.

Barbaro E., Zangrando R., Moret I., Barbante C., Cescon P., Gambaro A., 2011. Free amino acids in atmospheric particulate matter of Venice, Italy. Atmospheric Environment 45, 5050–5057.

Bauer H., Kasper-Giebl A.. Zibuschka F., Hitzenberger R., Kraus G.F., Puxbaum H., 2002. Determination of the Carbon Content of Airborne Fungal Spores. Analytical Chemistry 74, 91–95.

Bauer H., Claeys M., Vermeylen R., Schueller E., Weinke G., Berger A., Puxbaum, H., 2008a. Arabitol and mannitol as tracers for the quantification of airborne fungal spores. Atmospheric Environment 3, 42, 588–593.

Bauer H., Schueller E., Weinke G., Berger A., Hitzenberger R., Marr I. L. Puxbaum, H., 2008b. Significant contributions of fungal spores to the organic carbon and to the aerosol mass balance of the urban atmospheric aerosol. Atmospheric Environment 22, 42, 5542–5549.

Baur X., 2005. Enzymes as occupational and environmental respiratory sensitisers. International Archives of Occupational and Environmental Health 78, 279–286.

Bennett, J.W., 1987. Mycotoxins, mycotoxicoses, mycotoxicology and mycopathology. Mycopathlogia 100, 3–5.

Berger U., Oehme M., Kuhn F., 1999. Quantitative Determination and Structure Elucidation of Type A- and B-Trichothecenes by HPLC/Ion Trap Multiple Mass Spectrometry. Journal of Agricultural and Food Chemistry 47, 10, 4240–4245.

Berthiller F., Dall'Asta C., Schuhmacher R., Lemmens M., Adam G., Krska R., 2005a. Masked Mycotoxins: Determination of a Deoxynivalenol Glucoside in Artificially and Naturally Contaminated Wheat by Liquid Chromatography−Tandem Mass Spectrometry. Journal of Agricultural and Food Chemistry 53, 9, 3421–3425.

Berthiller F., Schuhmacher R., Buttinger G., Krska R., 2005b. Rapid simultaneous determination of major type A- and B-trichothecenes as well as zearalenone in maize by high performance liquid chromatography–tandem mass spectrometry. Journal of Chromatography A 1062, 2, 209–216.

Biselli S., Hartig L., Wegner H., Hummert C., 2004. Analysis of Fusarium Toxins using LC/MS–MS: Application to Various Food and Feed Matrices. Recent Applications in LC-MS LC-GC Europe 17, 25 2–7.

Biselli S., Hartig L., Wegner H., Hummert C., 2005. Analysis of fusarium toxins using LC–MS-MS: application to various food and feed matrices. Spectroscopy 20, 20–31.

Brasel T.L., Douglas D.R., Wilson S.C., Straus D.C., 2005. Detection of Airborne Stachybotrys chartarum Macrocyclic Trichothecene Mycotoxins on Particulates Smaller than Conidia. Applied and environmental microbiology 71, 1, 114–122.

Brera C., Caputi R., Miraglia M., Iavicoli I., Salerno A., Carelli G., 2002. Exposure assessment to mycotoxins in workplaces: aflatoxins and ochratoxin A occurrence in airborne dusts and human sera. Microchemical Journal 73, 167–173.

Buiarelli F., Canepari S., Di Filippo P., Perrino C., Pomata D., Riccardi C., Speziale R., 2013a. Extraction and analysis of fungal spore biomarkers in atmospheric bioaerosol by HPLC-MS-MS and GC-MS. Talanta 15,105, 142–151.

Buiarelli F., Gallo V., Di Filippo P., Pomata D., Riccardi C., 2013b. Development of a method for the analysis of underivatized amino acids by liquid chromatography/tandem mass spectrometry: application on Standard Reference Material 1649a (urban dust). Talanta 115, 966–972.

Bünger J., Antlauf-Lammers M., Schulz T.G., Westphal G.A., Müller M.M., Ruhnau P., Hallier E., 2000. Health complaints and immunological markers of exposure to bioaerosols among biowaste collectors and compost workers. Occupational and Environmental Medicine 57, 7, 458–464.

Burg W.R., Shotwell O.L., Saltzman B.E., 1981. Measurements of airborne aflatoxins during the handling of contaminated corn. American Industrial Hygienist Association Journal 42, 1–11.

Burshtein N., Lang-Yona N., and Rudich Y., 2011. Ergosterol, arabitol and mannitol as tracers for biogenic aerosols in the eastern Mediterranean. Atmospheric Chemistry and Physics 11, 829–839.

Busse W.W., Reed C.E., Hoehne J.H., 1972. Where is the allergic reaction in ragweed asthma? II. Demonstration of ragweed antigen in airborne particles smaller than pollen. Journal of Allergy and Clinical Immunology 50, 5, 289–293.

Carvalho A., Pio C. , Santos C. , 2003. Water-soluble hydroylated organic compounds in German and Finnish aerosols. Atmospheric Environment 37, 1775–1783.

Cavaliere C., D'Ascenzo G., Foglia P., Pastorini E., Samperi R., Laganà A., 2005. Determination of type B trichothecenes and macrocyclic lactone mycotoxins in field contaminated maize. Food Chemistry 92, 559–568.

Chan M.N., Choi M.Y., Ng N.L., Chan C.K., 2005. Hygroscopicity of water-soluble organic compounds in atmospheric aerosols: amino acids and biomass burning derived organic species. Environmental Science and Technology 39, 1555–1562.

Chen Q., Hildemann L.M., 2009. Size-Resolved concentrations of particulate matter and bioaerosols inside versus outside of homes. Aerosol Science and Technology 43, 699–713.

Cheng J.Y.W., Lau A.P.S., Fang M., 2008a. Assessment of the atmospheric fungal prevalence through field ergosterol measurement I—Determination of the specific ergosterol content in common ambient fungal spores and yeast cells. Atmospheric Environment 42, 5526–5533.

Cheng J.Y.W., Lau A.P.S., Fang M., 2008b. Assessment of the atmospheric fungal prevalence through field ergosterol measurement II: Establishing the conversion factor. Atmospheric Environment 42, 5534–5541.

Codina R., Fox R.W., Lockey R.F., DeMarco, P., Bagg A., 2008. Typical levels of airborne fungal spores in houses without obvious moisture problems during a rainy season in Florida, USA. Journal of Investigational Allergology and Clinical Immunology 18, 3, 156–162

Czerwieniec G.A., Russell S.C., Tobias H.J., Pitesky M.E., Fergenson D.P., Steele P., Srivastava A., Horn J.M., Frank M., Gard E.E., Lebrilla C.B, 2005. Stable isotope labeling of entire bacillus atrophaeus spores and vegetative cells using bioaerosol mass spectrometry. Analytical Chemistry 77, 1081–1087.

Dall'Asta C., Sforza S., Galaverna G., Dossena A., Marchelli R., 2004. Simultaneous detection of type A and type B trichothecenes in cereals by liquid chromatography–electrospray ionization mass spectrometry using NaCl as cationization agent. Journal of Chromatography A 1054, 1–2, 389–395.

Deguillaume L., Leriche M., Amato P., Ariya P. A., Delort A.-M., Poschl U., Chaumerliac N., Bauer H., Flossmann A. I., Morris C.E., 2008. Microbiology and atmospheric processes: chemical interactions of primary biological aerosols. Biogeosciences 5, 1073–1084.

Deguillaume L., Leriche M., Amato P., Ariya P.A., Delort A.M., Pöschl U., Chaumerliac N., Bauer H., Eduard W., 2009. Fungal spores: A critical review of the toxicological and epidemiological evidence as a basis for occupational exposure limit setting. Critical Reviews in Toxicology 39, 10, 799–864.

Després V. R., Huffman J. A., Burrows S. M., Hoose C., Safatov A., Buryak G., Fröhlich-Nowoisky J., Elbert W., Andreae M., Poschl U., Jaenicke R., 2012. Primary biological aerosol particles in the atmosphere, a review. Tellus B, North America, 64, feb. 2012. Available at: http://www.tellusb.net/index.php/tellusb/article/view/15598.

Di Filippo P., Riccardi C., Pomata D., Buiarelli F., 2010. Concentrations of PAHs, and nitro- and methyl-derivatives associated with a size-segregated urban aerosol. Atmospheric Environment 44, 23, 2742–2749.

Di Filippo P., Pomata D., Riccardi C., Buiarelli F., Perrino C., 2013. Fungal contribution to size-segregated aerosol measured through biomarkers. Atmospheric Environment 64, 132–140.

Donaldson K., Tran L., Jimenez L.A., Duffin R., Newby D.E., Mills N., MacNee W., Stone V., 2005. Review. Combustion-derived nanoparticles: A review of their toxicology following inhalation exposure Particle and Fibre Toxicology 2005, 2:10 doi:10.1186/1743-8977-2-10 http://www.particleandfibretoxicology.com/content/2/1/10.

Douwes J., Thorne P., Pearce N., Heederik D., 2003. Review. Bioaerosol Health Effects and Exposure Assessment: Progress and Prospects. The Annals of Occupational Hygiene 47, 3, 187–200.

Elbert W., Taylor P.E., Andreae M.O., Poschl, U., 2007. Contribution of fungi to primary biogenic aerosols in the atmosphere: wet and dry discharged spores, carbohydrates, and inorganic ions. Atmospheric Chemistry and Physics 7, 4569–4588.

Elias, V.O., Simoneit, B.R.T., Cordeiro, R.C., Turcq, B., 2001. Evaluating levoglucosan as an indicator of biomass burning in Carajas, Amazonia: a comparison to the charcoal record. Geochimica et Cosmochimica Acta 65, 2, 267–272.

Ersson B., Rydén L., Janson J.C., 2011. Protein Purification 54, III ed., cap.1; Janson J.C. (Wiley), New Jersey.

Fairs A., Wardlaw A.J., Thompson J.R., Pashley C.H., 2010. Guidelines on ambient intramural airborne fungal spores. Journal of Investigational Allergology and Clinical Immunology 20, 6, 490–498.

Flückiger B., Koller T., & Monn C., 2000. Comparison of airborne spore concentrations and fungal allergen content. Aerobiologia 16, 393–396.

Franze T., Weller M.G., Niessner R., Pöschl U., 2005. Protein nitration by polluted air. Environmental Science and Technology 39, 1673–1678.

Fraser M.P., Yuea Z.W., Tropp R.J., Kohl S.D., Chow J.C., 2002. Molecular composition of organic fine particulate matter in Houston, TX. Atmospheric Environment 36, 5751–5758.

Georgakopoulos D.G., Desprées V., Fröhlich-Nowoisky J., Psenner R., Ariya P.A., Pósfai M., Ahern H.E., Moffett B.F., Hill T.C.J., 2009. Microbiology and atmospheric processes: biological, physical and chemical characterization of aerosol particles. Biogeosciences 6, 721–737

Gessner M.O., Chauvet E., 1993. Ergosterol-to-biomass conversion factors for aquatic hyphomycetes. Applied and Environmental Microbiology 59, 502–507.

Ghosh S.K., Desai M.R., Pandya G.L., Venkaiah K., 1997. Airborne aflatoxin in the grain processing industries in India. American Industrial Hygiene Association Journal 58, 583–586.

Gorzelska K., Galloway J.N., Watterson K., Keene W.C., 1992. Water-soluble primary amine compounds in rural continental precipitation. Atmospheric Environment 26A, 6, 1005–1018.

Graham B., Guyon P., Taylor P.E., Artaxo P., Maenhaut W., Glovsky M.M., Flagan R.C., Andreae M.O., 2003. Organic compounds present in the natural Amazonian aerosol: characterization by gas chromatography—mass spectrometry. Journal of Geophysical Research 108, D24, 4766.

Graham B., Falkovich A.H., Rudich Y., Maenhaut W., Guyona P., Andreae M.O., 2004. Local and regional contributions to the atmospheric aerosol over Tel Aviv, Israel: a case study using elemental, ionic and organic tracers. Atmospheric Environment 38, 1593–1604.

Gunawan H., Takai T., Ikeda S., Okumura K., Ogawa H., 2008. Protease Activity of Allergenic Pollen of Cedar, Cypress, Juniper, Birch and Ragweed. Allergology International 57, 83–91.

Haan D.O., Corrigan A.L., Smith K.W., Stroik D.R., Turley J.J., Lee F.E., Tolbert M.A., Jimenez J.L., Cordova K.E., Ferrell G.R., 2009. Secondary Organic Aerosol-Forming Reactions of Glyoxal with Amino Acids. Environmental Science and Technology 43, 2818–2824.

Haginaka, J., 2009. Molecularly imprinted polymers as affinity-based separation media for sample preparation. Journal of Separation Science 32, 10, 1548–1565.

Harrison, R.M., Beddows, D.C.S., Hu, L., Yin, J., 2012. Comparison of methods for evaluation of wood smoke and estimation of UK ambient concentrations. Atmospheric Chemistry and Physics 12, 8271–8283.

Heal M.R., Naysmith P., Cook G.T., Xu S., Duran T.R., Harrison R.M., 2011. Application of 14C analyses to source apportionment of carbonaceous PM2.5 in the UK. Atmospheric Environment 45, 2341–2348.

Hintikka E.-L., Johnsson T., Tuomi T., Reijula K., 2006. Aerosol mycotoxins: Animal and human health effects. The Mycotoxin Factbook: Food & Feed Topics [World Mycotoxin Forum, Netherlands, 2005] edited by D. Barug, D. Bhatnagar, H.P. van Egmond, J.W. van der Kamp, W.A. van Osenbruggen, A. Visconti. Wageningen Academic Publishers The Netherland. 107–120.

Hintikka E.L., Holopainen R., Asola A., Jestoi M., Peitzsch M., Kalso S., Larsson L., Reijula K., Tuomi T., 2009. Mycotoxins in the ventilation systems of four schools in Finland. World Mycotoxin Journal 4, 369–379.

Hippelein M., Rügamer, M., 2004. Ergosterol as an indicator of mould growth on building materials. International Journal of Hygiene and Environmental Health 207, 4, 379–385.

Ho H.M., Rao C.Y., Hsu H.H., Chiu Y.H., Liu C.M., Chao H.J., 2005. Characteristics and determinants of ambient fungal spores in Hualien. Taiwan. Atmospheric Environment 39, 5839–5850.

Jaenicke R., 2005. Abundance of Cellular Material and Proteins in the Atmosphere. Science 308, 73.

Kang H., Xie Z., Hu Q., 2012. Ambient protein concentration in PM10 in Hefei, central China. Atmospheric Environment 54, 73–79.

Kanakidou M., Seinfel J. H., Pandis S. N., Barnes I., Dentener F. J., Facchini M. C., Van Dingenen R., Ervens B., Nenes A., Nielsen C.J., Swietlicki E., Putaud J.P., Balkanski Y., Fuzzi S., Horth J., Moortgat G. K., Winterhalter R., Myhre C.E.L., Tsigaridis, Vignati E., Stephanou E.G., Wilson J., 2005. Organic aerosol and global climate modelling: a review Atmospheric Chemistry and Physics 5, 1053–1123.

Kim S., Shen S., Sioutas C., Zhu Y., Hinds W.C., 2002. Size distribution and diurnal and seasonal trends of ultrafine particles in source and receptor sites of the Los Angeles basin. Journal of the Air & Waste Management Association 52, 297–307.

Klötzel M., Gutsche B., Lauber U., Humpf H.-U., 2005. Determination of 12 Type A and B Trichothecenes in Cereals by Liquid Chromatography−Electrospray Ionization Tandem Mass Spectrometry. Journal of Agricultural and Food Chemistry 53, 23, 8904–8910.

Kokkonen M.K., Jestoi M.N., 2009. A Multi-compound LC-MS/MS Method for the Screening of Mycotoxins in Grains. Food Analytical Methods 2, 128–140.

Kuo, L.J., Herbert, B.E., Louchouarn, P., 2008. Can levoglucosan be used to characterize and quantify char/charcoal black carbon in environmental media? Organic Geochemistry 39, 1466–1478.

Labuda R., Parich A., Berthiller F., D. Tančinová, 2005. Incidence of trichothecenes and zearalenone in poultry feed mixtures from Slovakia. International Journal of Food Microbiology 105, 1, 19–25.

Lacey J., Dutkiewicz J., 1994. Bioaerosols and occupational lung disease. Journal of Aerosol Science 25, 8, 1371–1404.

Laganá A., Curini R., D'Ascenzo G., De Leva I., Faberi A., Pastorini E., 2003. Liquid chromatography/tandem mass spectrometry for the identification and determination of trichothecenes in maize. Rapid Communications In Mass Spectrometry 17, 1037–1043.

Lappalainen S., Nikulin M., Berg S., Parikka P., Hintikka E.-L., Pasanen A.-L., 1996. Fusarium toxins and fungi associated with handling of grain on eight Finnish farms. Atmospheric Environment 30, 17, 3059–3065.

Larsen, R.K., Schantz, M.M., Wise, S.A., 2006. Determination of Levoglucosan in Particulate Matter Reference Materials. Aerosol Science and Technology 40, 781–787.

Lau A.P.S., Lee A.K.Y., Chan C.K., Fang M., 2006. Ergosterol as a biomarker for the quantification of the fungal biomass in atmospheric aerosols. Atmospheric Environment 40, 2, 249–259.

Lee C., Howarth R.W., Howes B.L., 1980. Sterols in decomposing Spartina alterniflora and the use of ergosterol in estimating the contribution of fungi to detrital nitrogen. Limnology and Oceanography 25, 290–303.

Lee T., Grinshpun S.A., Martuzevicius D., Adhikari A., Crawford C.M., Reponen T., 2006a. Culturability and concentration of indoor and outdoor airborne fungi in six single-family homes. Atmospheric Environment 40, 2902–2910.

Lee T., Grinshpuna S.A, Martuzevicius D., Adhikaria A., Crawford C.M., Reponen T., 2006b. Culturability and concentration of indoor and outdoor airborne fungi in six single-family homes. Atmospheric Environment 40, 2902–2910.

Li N., Sioutas C., Cho A., Schmitz D., Misra C., Sempf J., Wang M., Oberley T., Froines J., Nel A., 2003. Ultrafine particulate pollutants induce oxidative stress and mitochondrial damage. Environmental Health Perspectives 111, 4, 455–460.

Lobert J.M., Warnatz J., 1993. Emissions from the combustion process in vegetation. Fire in the environment: the ecological, atmospheric, and climate importance of vegetation fires. Edited by P.J. Crutzen and J.G. Goldammer. John Wiley & Sons LTD.

Louchouarn, P., Kuo, L.J., Wade, T.L., Schantz, M., 2009. Determination of levoglucosan and its isomers in size fractions of aerosol standard reference materials. Atmospheric Environment 43, 5630–5636.

Mandalakis M., Apostolaki M., Stephanou E.G., 2010. Trace analysis of free and combined amino acids in atmospheric aerosols by gas chromatography–mass spectrometry. Journal of Chromatography A 1217, 143–150.

Mandalakis M., Apostolaki M., Tziaras Y., Polymenakou P., Stephanou E.G., 2011. Free and combined amino acids in marine background atmospheric aerosols over the Eastern Mediterranean. Atmospheric Environment 45, 1003–1009.

Mauderly J.L., Chow J.C., 2008. Health effects of organic aerosols. Inhalation Toxicology 20, 257–288.

Matsumoto K., Uematsu M., 2005. Free amino acids in marine aerosols over the western North Pacific Ocean. Atmospheric Environment 39, 2163–2170.

Menetrez M.Y., Foarde K.K., Dean T.R., Betancourt D.A., Moore S.A., 2007. An evaluation of the protein mass of particulate matter. Atmospheric Environment 41, 8264–8274

Menetrez M.Y., Foarde K.K., Esch R.K., Dean T.R., Betancourt D.A., Moore S.A., Svendsen, E.R., Yeatts K., 2007. The Measurement of Ambient Bioaerosol Exposure. Aerosol Science and Technology 41, 884–893.

Menetrez M.Y., Foarde K.K., Esch R.K., Schwartz T.D, Dean T.R., Hays M.D., Cho S.H., Betancourt D.A., Moore S.A., 2009. An evaluation of indoor and outdoor biological particulate matter. Atmospheric Environment 43, 5476–5483.

McGregor K.G., Anastasio C., 2001. Chemistry of fog waters in California's Central Valley: 2. Photochemical transformations of amino acids and alkyl amines. Atmospheric Environment 35, 6, 1091–1104.

Melillo J.M., Aber J.D., Linkins A.E., Ricca A., Fry B, Nadelhoffer K.J., 1989. Carbon and nitrogen dynamics along the decay continuum: Plant litter to soil organic matter. Plant and Soil 115, 189–198.

Miguel A.G., Cass G.R., Weiss J., Glovsky M.M., 1996. Latex allergens in tire dust and airborne particles. Environmental Health Perspectives 104, 11, 1180–1186.

Miguel A.G., Cass G.R., Glovsky M.M., Weiss J., 1999. Allergens in Paved Road Dust and Airborne Particles. Environmental Science and Technologies 33, 4159–4168.

Mille-Lindblom C., Wachenfeld E., Tranvik L.J., 2004. Ergosterol as a measure of living fungal biomass: persistence in environmental samples after fungal death. Journal of Microbiological Methods 59, 253–262.

Miller, J. C., and Miller, J. N., 1993. Errors in instrumental analysis; regression and correlation (Ch.5; Sec-5.8) in: Statistics for analytical chemistry (3rd edition), by Ellis Horwood Limited, Chichester, England, pp.117-120.

Miller J.D., Young J.C., 1997. The Use of Ergosterol to Measure Exposure to Fungal Propagules in Indoor Air. American Industrial Hygiene Association Journal 58, 1, 39–43.

Milne P.J., Zika R.G., 1993. Amino acid nitrogen in atmospheric aerosols: Occurrence, sources and photochemical modification. Journal of Atmospheric Chemistry 16, 361–398.

Monbaliu S., Van Poucke K., Heungens K., Van Peteghem C., De Saeger S., 2010. Production and Migration of Mycotoxins in Sweet Pepper Analyzed by Multimycotoxin LC-MS/MS. Journal of Agricultural and Food Chemistry 58, 10475–10479.

Mondal A.K., Parui S., Mandal S., 1998. Biochemical analysis of four species of Cassia L. pollen. Aerobiologia 14, 45–50.

Moularat S., Robine E., 2008. A method to determine the transfer of mycotoxins from materials to air. Clean - Soil, Air, Water 36, 7, 578–583.

Na K., Sawant A.A., Song C., Cocker III D.R., 2004. Primary and secondary carbonaceous species in the atmosphere of Western Riverside County, California. Atmospheric Environment 38, 1345–1355.

Nel A., Xia T., Mädler L., Li N., 2005. Toxic potential of materials at the nanolevel. Science 311, 622–627.

Nemmar A., Zia S., Subramaniyan D. Al-Amri I., Al Kindi M.A., Ali B.H., 2012. Interaction of Diesel Exhaust Particles with Human, Rat and Mouse Erythrocytes in Vitro. Physiology and Biochemistry 29, 163–170.

Nielsen K.F., 2003. Review. Mycotoxin production by indoor molds. Fungal Genetics and Biology 39, 103–117.

Oberdörster G., 2001. Pulmonary effects of inhaled ultrafine effects. International Archives of Occupational and Environmental Health 74, 1–8.

Oberdörster G., Oberdörster E., Oberdörster J., 2005. Nanotoxicology: An emerging discipline evolving from studies of ultrafine particles. Environmental Health Perspectives 113, 823–839.

Odunfa A.V.S., 1979. Free amino acids in the seed and root exudates in relation to the nitrogen requirements of rhizosphere soil fusaria. Plant and Soil 52, 491–499.

O'Gorman C.M., Fuller H.T., 2008. Prevalence of culturable airborne spores of selected allergenic and pathogenic fungi in outdoor air. Atmospheric Environment 42, 4355–4368.

Ong E.K., Singh M.B., Knox R.B., 1995. Seasonal distribution of pollen in the atmosphere of Melbourne: an airborne pollen calendar. Aerobiologia 11, 1, 51–55.

Orasche, J., Schnelle-Kreis, J., Abbaszade, G., Zimmermann, R., 2011. Technical Note: In-situ derivatization thermal desorption GC-TOFMS for direct analysis of particle-bound non-polar and polar organic species. Atmospheric Chemistry and Physics 11, 8977–8993.

Pasanen A.L., Pietila K.Y., Pasanen P., Kalliokoski P., Tarhanen J., 1999. Ergosterol content in various fungal species and biocontaminated building materials. Applied and Environmental Microbiology 65, 138–142.

Peña R., Alcaraz M.C., Arce L., Rios A., Valcarel M., 2002. Screening of aflatoxins in feed samples using a flow system coupled to capillary electrophoresis. Journal of Chromatography A 967, 303–314.

Penn A., Murphy G., Barker S., Henk W., Penn L., 2005. Combustion-Derived Ultrafine Particles Transport Organic Toxicants to Target Respiratory Cells. Environmental Health Perspectives 113, 8, 956–963.

Perrino C., Canepari S., Catrambone M., Dalla Torre S., Rantica E., Sargolini T., 2009. Influence of natural events on the concentration and composition of atmospheric particulate matter. Atmospheric Environment 43, 4766–4779.

Pio C.A, Alves C.A, Duarte A.C., 2001. Identification, abundance and origin of atmospheric organic particulate matter in a Portuguese rural area. Atmospheric Environment 35, 8, 1365–1375.

Pizzuti, I.R., de Kok, A., Cardoso, C.D., Reichert, B., de Kroon, M., Wind, W., Righi, L.W., da Silva, R.C., 2012. A multi-residue method for pesticides analysis in green coffee beans using gas chromatography–negative chemical ionization mass spectrometry in selective ion monitoring mode. Journal of Chromatography A 1251, 16–26.

Plattner R.D., 1999. HPLC/MS analysis of Fusarium mycotoxins, fumonisins and deoxynivalenol. Natural Toxins 7, 6, 365–370.

Plattner R.D., Maragos C.M., 2003. Determination of Deoxynivalenol and Nivalenol in Corn and Wheat by Liquid Chromatography with Electrospray Mass Spectrometry. Journal of AOAC International 86, 1, 61–65.

Pomata D., 2012. Measurement of primary biological aerosol responsible for the onset of respiratory diseases. PhD in "Environmental and Industrial Hygiene" - XXIV Cycle – University of Rome "Sapienza".

Pomata D., Di Filippo P., Riccardi C., Buiarelli F., Gallo V., 2014. Determination of non-certified levoglucosan, sugar polyols and ergosterol in NIST Standard Reference Material 1649a. Atmospheric Environment, DOI: 10.1016/j.atmosenv.2013.11.069.

Poole, C.F., 2007. Matrix-induced response enhancement in pesticide residue analysis by gas chromatography. Journal of Chromatography A 1158, 241–250.

Poruthoor S.K., Dasgupta P.K., Genfa Z., 1998. Indoor air pollution and sick building syndrome. monitoring aerosol protein as a measure of bioaerosols. Environmental Science and Technologies 32, 1147–1152.

Rahmani A., Jinap S., Soleimany F., Khatib A., Tan C.P., 2011. Sample preparation optimization for the simultaneous determination of mycotoxins in cereals. European Food Research and Technology 232, 4, 723–735.

Razzazi-Fazeli E., Böhm J., Luf W., 1999. Determination of nivalenol and deoxynivalenol in wheat using liquid chromatography–mass spectrometry with negative ion atmospheric pressure chemical ionization Journal of Chromatography A 854, 1–2, 45–55.

Razzazi-Fazeli E., Rabus B., Cecon B., Böhm J., 2002. Simultaneous quantification of A-trichothecene mycotoxins in grains using liquid chromatography–atmospheric pressure chemical ionisation mass spectrometry. Journal of Chromatography A 968, 1–2, 129–142.

Razzazi-Fazeli E., Böhm J., Jarukamjorn K., Zentek J., 2003. Simultaneous determination of major B-trichothecenes and the de-epoxy-metabolite of deoxynivalenol in pig urine and maize using high-performance liquid chromatography–mass spectrometry. Journal of Chromatography B 796, 21–33.

Richard J.L., Plattner R.D., May J., Liska S.L., 1999. The occurrence of ochratoxin A in dust collected from a problem household. Mycopathologia 146, 99–103.

Romero-González R., Martínez Vidal J.L., Aguilera-Luiz M.M., Garrido Frenich A., 2009. Application of Conventional Solid-Phase Extraction for Multimycotoxin Analysis in Beers by Ultrahigh-Performance Liquid Chromatography−Tandem Mass Spectrometry, Journal of Agricultural and Food Chemistry 57, 9385–9392.

Royer D., Humpf H.-U., Guy P.A., 2004. Quantitative analysis of Fusarium mycotoxins in maize using accelerated solvent extraction before liquid chromatography/atmospheric pressure chemical ionization tandem mass spectrometry. Food Additives and Contaminants 21, 7, 678–692.

Samy S., Robinson J., Hays D.M., 2011. An advanced LC-MS (Q-TOF) technique for the detection of amino acids in atmospheric aerosols. Analytical and Bioanalytical Chemistry 401, 3103-3113.

Saxena P., Hildemann L.M., 1996. Water-Soluble Organics in Atmospheric Particles: A Critical Review of the Literature and Application of Thermodynamics to Identify Candidate Compounds. Journal of Atmospheric Chemistry 24, 57–109.

Scott P.M., 1995. Mycotoxin methodology. Food Additives & Contaminants 12, 3, 395–403.

Scudamore, K.A., Hetmanski M.T., Nawaz S., 1997. Determination of mycotoxins in pet foods sold for domestic pets and wild birds using linked-column immunoassay clean-up and HPLC. Journal of Food Additives & Contaminants 14, 2, 175–186.

Seinfeld J.H., Pankow J.F., 2003.Organic atmospheric particulate material. Annual Reviews of Physical Chemistry 54, 121–140.

Schauer J.J., Rogge W.F., Hildemann L.M., Mazurek M.A., Cass G.R., Simoneit B.R.T., 1996. Source apportionment of airborne particulate matter using organic compounds as tracers. Atmospheric Environment 30, 22, 3837–3855.

Sehgal N., Custovic A., Woodcock A., 2005. Potential Roles in Rhinitis for Protease and Other Enzymatic Activities of Allergens. Current Allergy and Asthma Reports 5, 221–226.

Seitz L.M., Mohr H.E., Burroughs R., Sauer D. B., 1977. Ergosterol as an indicator of fungal invasion in grains. Cereal Chemistry 54, 1207–1217.

Seitz L. M., Sauer D. B., Burroughs R., Mohr H.E., Hubbard J.D., 1979. Ergosterol as a measure of fungal growth. Phytopathology 69, 1202–1203.

Selim M.I., Juchems A.M., Popendorf W., 1998. Assessing airborne aflatoxin B_1 during on-farm grain handling activities. American Industrial Hygiene Association Journal 59, 4, 252–256.

Shewry P.R., Fido R.J., 1996. Protein purification protocols 59, cap.3; Doonan S. (Humana Press), New Jersey.

Shimada A., Kawamura N., Okajima M., Kaewamatawong T., Inoue H., Morita T., 2006. Translocation Pathway of the Intratracheally Instilled Ultrafine Particles from the Lung into the Blood Circulation in the Mouse. Toxicologic Pathology 34, 949–957.

Sioutas C., Delfino R.J., Singh M., 2005. Exposure assessment for atmospheric ultrafine particles (UFPs) and implications in epidemiologic research. Environmental Health Perspectives 113, 8, 947–955.

Skaug M.A., Eduard W., Størmer F.C., 2000. Ochratoxin A in airborne dust and fungal conidia. Mycopathologia 151, 93–98.

Smoragiewicz W., Cossette B., Boutard A., Krzystyniak K., 1993. Trichothecene mycotoxins in the dust of ventilation systems in office buildings. International Archives of Occupational and Environmental Health 65, 2 113–7.

Sorenson W.G., Jones W., Simpson J., Davidson J.I., 1984. Aflatoxin in respirable airborne peanut dust. Journal of Toxicology and Environmental Health 14, 525–533.

Sorenson W.G., Lewis D.M., 1996. Organic Dust Toxic Syndrome. Human and Animal Relationships. The Mycota 6, 159–172.

Sorenson W.G., 1999. Fungal Spores: Hazardous to Health? Environmental Health Perspectives Supplements 107, S3, 469–472.

Srikanth P., Sudharsanam S., Steinberg R., 2008. Bio-aerosols in indoor environment: composition. health effects and analysis, Indian Journal of Medical Microbiology 26, 4, 302–12.

Sudakin D., Fallah P., 2008. Toxigenic fungi and mycotoxins in outdoor, recreational environments. Clinical Toxicology 46, 738–744.

Sun J., Ariya P.A., 2006. Atmospheric organic and bio-aerosols as cloud condensation nuclei (CCN): A review. Atmospheric Environment 40, 795–820.

Sypecka Z., Kelly M., Brereton P., 2004. Deoxynivalenol and Zearalenone Residues in Eggs of Laying Hens Fed with a Naturally Contaminated Diet: Effects on Egg Production and Estimation of Transmission Rates from Feed to Eggs. Journal of Agricultural and Food Chemistry 52, 17, 5463–5471.

Thiele B., Füllner K., Stein N., Oldiges M., Kuhn A.J., Hofmann D., 2008. Analysis of amino acids without derivatization in barley extracts by LC-MS-MS. Analytical and Bioanalytical Chemistry 391, 2663–2672.

Tuomi T., Saarinen L., Reijula K.,1998. Detection of polar and macrocyclic trichothecene mycotoxins from indoor environments. Analyst 123, 9, 1835–41.

Tuomi T., Reijula K., Johnsson T., Hemminki K., Hintikka E.-L., Lindroos O., Kalso S., Koukila-Kähkölä P. , Mussalo-Rauhamaa H., Haahtela T., 2000. Mycotoxins in Crude Building Materials from Water-Damaged Buildings. Applied and Environmental Microbiology 66, 5, 1899–1904.

Turner N.W., Subrahmanyam S., Piletsky S.A., 2009. Analytical methods for determination of mycotoxins: a review. Analytical Chimica Acta 632, 168–180.

Turpin B.J., Saxena P., Andrews E., 2000. Measuring and simulating particulate organics in the atmosphere: problems and prospects. Atmospheric Environment 34, 2983–3013.

Van Egmond H. P. and Paulsch W.E., 1986. Determination of mycotoxins. Pure and Applied Chemistry 58, 2, 315–326.

Voet D., Voet, J.G., Pratt C.W., 2008. Principles of Biochemistry. 3rd edition, Wiley.

Volker E.J., Dilella D., Terneus K., Baldwin C., Volker I., 2000. The Determination of Ergosterol in Environmental Samples. Journal of Chemical Education 77, 12, 1621–1623.

Ye B., Ji X., Yang H., Yao X., Chan C.K., Cadle S.H., Chan T., Mulawa P.A., 2003. Concentration and chemical composition of PM2.5 in Shanghai for a 1-year period. Atmospheric Environment 37, 499–510.

Vélëz H., Glassbrook N.J., Daub M.E., 2007. Mannitol metabolism in the phytopathogenic fungus Alternaria Alternata. Fungal Genetics and Biology 44, 258–268.

Wan E.H., Zhen Y.J., 2007. Analysis of Sugars and Sugar Polyols in Atmospheric Aerosols by Chloride Attachment in Liquid Chromatography/Negative Ion Electrospray Mass Spectrometry. Environmental Science & Technology 41, 2459–2466.

Wei Y., Qiu L., Yu J.C.C., 2007. Molecularly imprinted solid phase extraction in a syringe needle packed with polypyrrole-encapsulated carbon nanotubes for determination of ochratoxin A in red wine. Food Science and Technology International 13, 5, 375–380.

Womiloju T.O., Miller J.D., Mayer P.M., Brook J.R., 2003. Methods to determine the biological composition of particulate matter collected from outdoor air. Atmospheric Environment 37, 4335–4344.

Zhang Q., Anastasio C., 2001. Chemistry of fog waters in California's Central Valley-Part 3: concentrations and speciation of organic and inorganic nitrogen. Atmospheric Environment 35, 5629–5643.

Zhang Q., Anastasio C., Jimenez-Cruz M., 2002. Water-soluble organic nitrogen in atmospheric fine particles (PM2.5) from northern California. Journal of Geophysical Research 107, D11, AAC 3 – 1 - AAC 3 - 9.

Zhang Q., Anastasio C., 2003. Free and combined amino compounds in atmospheric fine particles (PM2.5) and fog waters from Northern California. Atmospheric Environment 37, 2247–2258.

Zhang T., Engling G., Chan C.Y., Zhang Y.N., Zhang Z.S., Lin M., Sang X.F., Li Y.D., Li Y.S., 2010. Contribution of fungal spores to particulate matter in a tropical rainforest. Environmental Research Letters 5, 2, 024010.

Zhao Z., Sebastian A., Larsson L., Wang Z., Zhang Z., Norback D., 2008. Asthmatic symptoms among pupils in relation to microbial dust exposure in schools in Taiyuan. China. Pediatric Allergy Immunology 19, 455–465.

Zöllner P., Mayer-Helm B., 2006. Review. Trace mycotoxin analysis in complex biological and food matrices by liquid chromatography–atmospheric pressure ionisation mass spectrometry. Journal of Chromatography A 1136, 123–169.